



**Titre:** Doped fiber external cavity laser for radio over fiber applications  
Title:

**Auteur:** Run nan Liu  
Author:

**Date:** 2008

**Type:** Mémoire ou thèse / Dissertation or Thesis

**Référence:** Liu, R. (2008). Doped fiber external cavity laser for radio over fiber applications  
Citation: [Thèse de doctorat, École Polytechnique de Montréal]. PolyPublie.  
<https://publications.polymtl.ca/8126/>

 **Document en libre accès dans PolyPublie**  
Open Access document in PolyPublie

**URL de PolyPublie:** <https://publications.polymtl.ca/8126/>  
PolyPublie URL:

**Directeurs de  
recherche:**  
Advisors:

**Programme:** Non spécifié  
Program:

**UNIVERSITÉ DE MONTRÉAL**

**DOPED FIBER EXTERNAL CAVITY LASER FOR RADIO OVER FIBER  
APPLICATIONS**

**RUN NAN LIU**

**DÉPARTMENT DE GÉNIE ÉLECTRIQUE  
ÉCOLE POLYTECHNIQUE DE MONTRÉAL**

**THÈSE PRÉSENTÉE EN VUE DE L'OBTENTION  
DU DIPLÔME DE PHILOSOPHIAE DOCTOR (Ph.D.)  
(GÉNIE ÉLECTRIQUE)  
FÉVRIER 2008**

**© Run nan Liu, 2008**



Library and  
Archives Canada

Published Heritage  
Branch

395 Wellington Street  
Ottawa ON K1A 0N4  
Canada

Bibliothèque et  
Archives Canada

Direction du  
Patrimoine de l'édition

395, rue Wellington  
Ottawa ON K1A 0N4  
Canada

*Your file    Votre référence*

*ISBN: 978-0-494-41753-9*

*Our file    Notre référence*

*ISBN: 978-0-494-41753-9*

#### NOTICE:

The author has granted a non-exclusive license allowing Library and Archives Canada to reproduce, publish, archive, preserve, conserve, communicate to the public by telecommunication or on the Internet, loan, distribute and sell theses worldwide, for commercial or non-commercial purposes, in microform, paper, electronic and/or any other formats.

The author retains copyright ownership and moral rights in this thesis. Neither the thesis nor substantial extracts from it may be printed or otherwise reproduced without the author's permission.

#### AVIS:

L'auteur a accordé une licence non exclusive permettant à la Bibliothèque et Archives Canada de reproduire, publier, archiver, sauvegarder, conserver, transmettre au public par télécommunication ou par l'Internet, prêter, distribuer et vendre des thèses partout dans le monde, à des fins commerciales ou autres, sur support microforme, papier, électronique et/ou autres formats.

L'auteur conserve la propriété du droit d'auteur et des droits moraux qui protègent cette thèse. Ni la thèse ni des extraits substantiels de celle-ci ne doivent être imprimés ou autrement reproduits sans son autorisation.

---

In compliance with the Canadian Privacy Act some supporting forms may have been removed from this thesis.

Conformément à la loi canadienne sur la protection de la vie privée, quelques formulaires secondaires ont été enlevés de cette thèse.

While these forms may be included in the document page count, their removal does not represent any loss of content from the thesis.

Bien que ces formulaires aient inclus dans la pagination, il n'y aura aucun contenu manquant.

UNIVERSITÉ DE MONTRÉAL

ÉCOLE POLYTECHNIQUE DE MONTRÉAL

Cette thèse est intitulée

DOPED FIBER EXTERNAL CAVITY LASER FOR RADIO OVER FIBER  
APPLICATIONS

**Présentée par: LIU, Runnan**

**En vue de l'obtention du diplôme de : Philosophiae Doctor  
a été dûment acceptée par le jury d'examen constitué de :**

**M. CALOZ, Christophe, Ph.D., président**

**M. KASHYAP, Raman, Ph.D., membre et directeur de recherche**

**M. WU, Ke, Ph.D., membre et co-directeur de recherche**

**M. MACIEJKO, Romain, Ph.D., membre**

**M. CARTLEDGE, John, Ph.D., membre externe**

**To my wife, my parents, my son**

## ACKNOWLEDGEMENTS

Like all theses, this task has been a difficult and challenging one. This work would not have been possible to finish without generous support, co-operation, and understanding of many people.

I am deeply indebted to my supervisor, Prof. Raman Kashyap, Ph.D., for his enthusiasm, inspiration, invaluable instruction and strong supervision. Without him, I could not imagine that I could have kept on working in this field, and finish this hard work.

I would like to record my sincere thanks to my co-supervisor, Prof. Ke Wu, Ph.D., for his constant encouragement and guidance; without him, I could not have finished my study in this school and could not have had a chance to have all the wonderful results.

I would like to express my deep gratitude to Dr. Irina Kostko, the former post doctoral fellow in Advanced Photonics Concept Lab (APCL), for her great help, and co-work in this challenging project, especially in simulation and theoretical analysis.

I would like to thank Prof. Jean Jacques Laurin, Ph.D., for his encouraging and helpful suggestion for my project proposal.

I would also like to thank Prof. Jianping Yao, Ph.D., from Microwave Photonics Research Lab, University of Ottawa, for his very helpful discussions on my project.

I would like to thank Mr. Joe Seregelyi, P. Eng., from Communication Research Center Canada (CRC), for his helpful discussions and suggestions for this project and continuous work, and Mr. Howard Rideout, from CRC, for his help in the experiment of the fully erbium doped fiber external cavity laser.

I would like to thank Prof. Sophie Larochelle, from the Center for Optic Photonic and Laser (COPL), Laval University, for her valuable suggestion on application and co-operation in OFDM experiments, and thank Mr. Mohammad Ebrahim Mousa Pasandi, from COPL, Laval University, for his discussions on the application, and co-work in OFDM experiments.

I would also like thank my colleagues in Advanced Photonics Concept Laboratory (APCL). They are Dr. Vincent Tréanton, Lütfü Çelebi Özcan, Francis Guay, Jerome Poulin, Mathieu Gagne, etc. for useful discussions, help and friendship.

I would like thank all the colleagues in Poly-Grames Research Center, for their help and friendship.

I would like thank all my friends and family for having faith in me. All their encouragement and help are appreciated.

Lastly, I should say thanks to my dear wife Ling, who constantly supported me during all my studies. And thanks to my lovely son Yuming, who is always happy to know my progress, and believes that I can finish my work. And thanks to my parents, Prof. Zhen-tian Liu and Prof. Shi-ou Wang, as they always placed their trust in their son, and always wished me success.

## RÉSUMÉ

La technologie de radio sur fibre (ROF) ou plus généralement la photonique microondes est une méthode hybride de transmission de l'information. À l'aide d'un système ROF les signaux électromagnétiques peuvent être transmis par fibres optiques vers des endroits reculés sans pertes notoires et dégradation du signal. Le système ROF présente ensuite l'avantage de la communication sans-fil, la mobilité.

L'architecture classique d'un système ROF comprend habituellement des stations centrales de modulation, un réseau de fibres optiques et des stations éloignées. Le signal RF module l'onde optique transmise dans la fibre. À la station éloignée, le signal optique est démodulé. Dans les stations centrales, la taille et la consommation énergétique des dispositifs ne sont pas cruciales. On préfère installer des appareils qui permettent de transmettre des signaux de très bonne qualité. Quant à elles, les stations éloignées peuvent potentiellement être construites partout dans le pays. Vu leur grand nombre, ces stations doivent être équipées de dispositifs de petites tailles et très abordables. Le réseau de fibres optiques déjà en place peut servir de vecteur pour la transmission ROF. En ce sens, c'est un avantage.

Des lasers de fine largeur d'émission et très stables en longueurs d'onde ont déjà été utilisés pour des applications ROF. Récemment des études ont montré la pertinence d'utiliser des lasers à cavités externes à fibre dopée (DFECL) pour ce genre d'applications. Une analyse détaillée des principes et des expériences encourues ne sont pas présentées ici.

Cette thèse propose plutôt s'attarder sur le design, la fabrication et la caractérisation d'un nouveau type de DFECL ultra-long principalement orienté vers des applications ROF.



En premier lieu, on étudie les caractéristiques de la fibre dopée comme partie prenante de la cavité. Bien que ces fibre aient été étudiées pour des applications d'amplifications, la situation ici est très différente. On présente les observations et la caractérisation empirique de deux phénomènes : l'auto-blanchiment de l'absorption (self-pump absorption bleaching) ainsi que l'absorption large bande dans le régime de pompage intra bande (whole-band absorption bleaching in the in-band pump regime). La modulation de l'absorption et le blanchiment de l'absorption peuvent se traduire par l'induction d'une modification de l'indice de réfraction le long de la fibre dopée. Ce phénomène est utilisé pour inscrire un réseau périodique et dynamique le long de la fibre dopée permettant, en bout de ligne, de réduire la largeur de la raie d'émission en plus d'augmenter la stabilité en longueur d'onde.

Un nouveau design de DFECL a été proposé lors de ces travaux. Le laser opère à 1490 nm, la frontière de la bande d'absorption de la fibre dopée à l'Erbium. Ce laser est testé sous plusieurs angles dont la stabilité en puissance et fréquentielle ainsi que sa réponse à une modulation directe du courant aux bornes de la diode laser à semi-conducteurs.

Le nouveau laser présente une des fluctuations mineures de puissances ( $\pm 0,25$  dBm) et en longueur d'onde ( $\pm 2,5$  pm). A l'aide de méthodes de battement hétérodynes, la largeur de raie d'émission des lasers a été évalué à quelques kHz avec un facteur de suppression des modes secondaires de l'ordre de 15-20 dB. Le dernier DFECL a été conçu avec une cavité presque exclusivement constituée de fibre dopée à l'Erbium. Ce laser opérant à 1530 nm présente des meilleures performances en ce qui a trait au taux de suppression des modes secondaires (45 dB), à la stabilité en longueur d'onde ( $\pm 1$  pm) ainsi qu'à la largeur de la raie d'émission ( $< 350$  kHz).

D'autres études montrent que les DFECL fabriqués possèdent une accordabilité fréquentielle de l'ordre de 50 MHz/mA lorsque l'on varie le courant d'injection aux bornes de la diode laser.

L'absorbant saturable se trouvant à l'intérieur de la cavité permet de moduler directement le DFECL avec une porteuse RF de haute fréquence. La fréquence de modulation peut être plus élevée que le 22ième multiple de la fréquence de résonance de la cavité résonante du laser. Des signaux FM et OFDM de bandes passante de plus de 20 MHz ont ainsi été transmis. Des signaux de haute qualité 64-QAM IEEE 802.11a/g ont été transmis sans erreurs notoires. Le tout ayant été validé à travers la magnitude du vecteur d'erreur (EVM) qui se situait à -40 dB.

## ABSTRACT

Radio over fiber is an optical-microwave hybrid technique. With a radio over fiber system, the microwave or radio frequency waves can be generated and transmitted over the fiber optic communication systems to remote locations. The radio over fiber system has the advantages of wireless communications, which are convenience and mobility. Also it has the advantages of fiber optic communications, which are the long distance low loss and high capacity transmission.

A radio over fiber system is generally structured with the center stations, the fiber optic communication system and the remote base stations. The microwave or radio waves modulate the light wave and are transmitted on the fiber optic system by optical transmitters. Laser sources are the key optical devices for optical microwave transmission. The stability and noise figure of the laser sources can affect the signal transmission performance for all the radio over fiber systems.

Narrow line-width and stable wavelength laser has been studied for radio over fiber communication and fiber optic communication for a long time. Recent studies have shown that Doped Fiber External Cavity Laser (DFECL) has very good performance in line-width and wavelength in its free running state. It is a potential laser source for radio over fiber applications. The detailed analysis of the principle and the experimental studies of the application have not reported before.

This thesis is focused on analysis, design and demonstration of a novel ultra long DFECL, for the purposes of radio over fiber communication applications.

This thesis starts with the study of doped fiber characteristics for an external cavity laser. Although the doped fiber has been extensively studied for applications in fiber amplifiers, the situation has been different for external cavity lasers. This study presents the phenomenon of self-pumped absorption-bleaching and whole-band absorption-

bleaching in the in-band pumping regime. The absorption modulation and absorption bleaching can induce a refractive index modulation in the doped fiber. This forms a dynamic grating in the doped fiber inside the external cavity, which has an additional effect for line-width narrowing and wavelength stability.

The DFECL is structured with a normal semiconductor laser, a piece of doped fiber and a fiber Bragg grating (FBG). Novel DFECLs have been built in this project. The new DFECLs operated at 1490 nm wavelength, where it is at the edge of erbium doped fiber absorption band. This new laser is studied in depth for its short and long term stability, tunability and modulation capability.

The new laser presented long term stability with fluctuations of only  $\pm 2.5$  pm in wavelength and  $\pm 0.025$  dBm in power. With self-beating and heterodyne beating methods, the line-width of the laser has been shown to be in the order of kHz, with the side-mode suppression of between 15-20 dB. The DFECL's good stability at 1490 nm indicated that a DFECL could be built anywhere within the absorption band of the doped fiber. The latest DFECL was designed with almost fully doped fiber in the external cavity. The laser light was directly coupled to the fiber lens made on the erbium doped fiber (EDF), which is splicing very close to a FBG. The DFECL operating at  $\sim 1530$  nm presented even better performance; the side mode suppression ratio was better than 45 dB, with wavelength stability better than  $\pm 1$  pm, and line-width narrower than 350 kHz.

Further studies have pointed out that the DFECL can have either wide or fine tunability. The slow response of the dynamic grating in doped fiber can eliminate fast wavelength fluctuations and stabilize the laser. By slowly and constantly tuning the drive current or temperature of the laser diode, the DFECL wavelength can also be tuned within the bandwidth of the external fiber Bragg grating. The precise tuning rate was 50 MHz/mA, which is very attractive for radio over fiber applications.

Applications of the DFECL have been demonstrated in the thesis for the first time. Due to the saturable absorber inside the external cavity, the DFECL can be directly modulated at high RF carrier frequency; the modulating microwave frequency can be more than the 22<sup>nd</sup> multiple of its cavity resonant frequency. The experimental results had shown that the direct modulation transmission signal was clean, and can be easily identified. Up to 20 MHz bandwidth FM and OFDM signals have been demonstrated in this thesis. The measured high quality 64-QAM IEEE802.11a/g OFDM signal transmissions achieved an error vector magnitude (EVM) for the OFDM transmission as low as -40 dB, which is even lower than for most externally modulated transmission systems.

## CONDENSÉ EN FRANÇAIS

### 1. Introduction

La technologie de radio sur fibre (ROF) ou plus généralement la photonique microondes est une méthode hybride de transmission de l'information. À l'aide d'un système ROF les signaux électromagnétiques peuvent être transmis par fibres optiques vers des endroits reculés sans pertes notables et dégradation du signal. Le système ROF présente ensuite l'avantage de la communication sans-fil, la mobilité.

L'architecture classique d'un système ROF comprend habituellement des stations centrales de modulation, un réseau de fibres optiques et des stations éloignées. Le signal RF module l'onde optique transmise dans la fibre. À la station éloignée, le signal optique est démodulé. Dans les stations centrales, la taille et la consommation énergétique des dispositifs ne sont pas cruciales. On préfère installer des appareils qui permettent de transmettre des signaux de très bonne qualité. Quant à elles, les stations éloignées peuvent potentiellement être construites partout dans le pays. Vu leur grand nombre, ces stations doivent être équipées de dispositifs de petites tailles et très abordables. Le réseau de fibres optiques déjà en place peut servir de vecteur pour la transmission ROF. En ce sens, c'est un avantage.

La transmission de signaux micro-ondes sur la porteuse optique est réalisée en appliquant le signal micro-onde directement aux bornes de la diode laser ou à travers l'intermédiaire d'un modulateur externe. Trois approches sont habituellement considérées pour transmettre le signal micro-ondes sur le lien optique : la modulation directe, la modulation externe et la génération sans fil. La modulation directe présente un coût d'implémentation très bas mais ses performances dépendent largement des caractéristiques fondamentales de la source laser utilisée.

## 2. Sources laser

Comme mentionné, la composante la plus importante d'un système ROF est la source laser. Une source stable, de très fine largeur spectrale et présentant un faible bruit est recherchée pour les applications ROF.

Les lasers à semi-conducteurs (LSC) offrent deux avantages notoires : ils sont très compacts et offrent la possibilité d'être modulés directement à travers une variation du courant d'injection aux fréquences micro-ondes.

La majorité des LSC dont la cavité est de type Fabry-Perot (FP) ne possèdent pas les caractéristiques nécessaires à leur utilisation dans les réseaux standards de télécommunications fonctionnant sous le paradigme du multiplexage dense en longueur d'onde (DWDM) en vertu de fait qu'ils sont instables, que leur largeur de bande d'émission est trop grande et que la suppression des lobes secondaires d'émission n'est pas assez élevée. Toutefois, en utilisant une rétroaction optique, on peut contrôler de manière plus efficace ces dispositifs. L'utilisation d'un réflecteur externe permet d'améliorer la stabilité et de réduire la largeur de bande des cavités FP sans toutefois conférer le statut monomode au dispositif. Il est pourtant d'opérer dans ce régime puisqu'une multitude modes longitudinaux équivaut à un élargissement spectral de la source. Donc, il faut trouver un moyen d'obtenir un réflecteur externe sélectif en longueur d'onde afin de sélectionner la longueur d'onde qui lasera, celle qui atteindra le seuil en premier.

Le laser à cavité externe (ECL) fibrés opérant une réflexion sélective en longueur d'onde grâce à un réseau de Bragg (FBG) permettent de contourner les problèmes d'alignement. Les FBG sont des dispositifs intra-fibre qui réfléchissent une gamme bien précise de longueur d'onde se propageant dans le guide d'onde.

Les lasers à cavité externe assistés par réseaux de Bragg (FGECL) sont composés d'un laser à semi-conducteur, fusionné à un morceau de fibre optique monomode (SMF)

dans lequel est inscrit un FBG. La diode laser possède un revêtement anti-reflet sur sa facette. Donc le dispositif fonctionne en fait comme un très long laser FP.

### 3. Fibre dopée aux terres rares

Lorsqu'on la dope avec des éléments de la catégorie des terres rares, la silice présente des caractéristiques lui permettant d'être un milieu de gain pour une plage bien définie de longueur d'onde. Les applications les plus intéressantes de cette propriété sont les lasers à fibre et les amplificateurs.

Il existe deux paradigmes de construction des lasers fibrés basés sur l'utilisation de fibres dopées aux terres rares. Le premier consiste à mettre en cascade linéaire le laser suivi d'un amplificateur. Dans ce cas, il est nécessaire de pomper le milieu avec une longueur d'onde plus petite que celle que l'on veut obtenir en sortie. La deuxième approche consiste à placer la fibre dopée à l'intérieur de la cavité résonnante. On peut donc fusionner la fibre dopée à la fibre monomode où le FBG est inscrit afin de réaliser une telle structure. Cette technique possède un avantage notoire : aucune pompe extérieure n'est nécessaire. Seule les longueurs d'onde émises par le laser dans le mode principal et les quelques modes d'ordres supérieurs traverse la fibre dopée. Ces modes se propage tous sur des longueurs d'ondes très près de la longueur d'onde dominante du milieu de gain, la fibre dopée.

À  $1,5\ \mu\text{m}$ , la fibre dopée à l'Erbium (EDF) peut agir comme milieu de gain en absorbant et réémettant par émission stimulée. Nos expériences montrent que l'absorption sature lorsque la puissance de la pompe excède un seuil. Ce phénomène est communément appelé *absorption bleaching*. L'expérience montre aussi qu'un pompage de très fine largeur de bande peut saturer l'absorption dans tout le spectre de gain de l'EDF. Même si la pompe opère à  $1550\ \text{nm}$ , longueur d'onde où l'absorption est très faible, on observe un blanchissement du gain vers  $1530\ \text{nm}$ .



Lorsqu'une onde stationnaire est formée dans la cavité d'un ECL comprenant un absorbant saturable tel l'EDF, la modulation des niveaux de population des ions crée le phénomène de brûlure de trous (*spatial hole burning*). Ceci entraîne une modulation périodique de l'indice de réfraction le long de l'EDF selon l'effet de Kramers-Krönig. Cette structure agit comme un FBG dynamique dont la réflectivité augmente à mesure que la puissance intra-cavité qui cause le changement d'indice. On assiste donc à une dynamique d'échange entre ces deux phénomènes.

Ce réseau dynamique est à la base de la réalisation de laser à très fine largeur de bande. À la sortie de la diode laser plusieurs longueurs d'ondes oscillent selon des modes spatiaux différents. Toutefois, la longueur d'onde présentant la plus forte absorption dans le spectre de l'EDF atteindra la saturation en premier et créera un FBG dynamique le long de celle-ci qui aura la plus forte modulation d'indice. Ce réseau agira donc comme un filtre pour les autres modes de sorties du laser. De plus, l'utilisation du *bleaching* de l'absorption sur tout le spectre contribue à augmenter le rapport d'intensité entre la longueur d'onde dominante et les autres présentes dans le spectre d'émission de la diode laser.

#### 4. Largeur de raie d'émission et stabilité des DFECL

Le DFECL opère à 1535 nm, qui est la meilleure longueur d'onde pour l'absorption et l'émission d'une EDF. Le DFECL basé sur la fibre dopée à l'Ytterbium opère quant à lui à 980 nm, longueur d'onde optimisant les performances en termes d'absorption et émission.

Analysé précédemment au pic d'absorption, la modulation d'absorption est maximale et génère un réseau de Bragg dynamique dont les performances sont elles aussi maximisées. Un nouveau design de DFECL opérant à l'extérieur de la région d'absorption de l'EDF a été tenté. Le problème est que l'absorption et l'émission sont

beaucoup plus faible à ces longueurs d'ondes. Si le laser fonctionne correctement, ceci indique que la totalité de la bande d'absorption de l'EDF peut être utilisée pour la conception d'un DFECL.

Les diodes laser utilisées lors des expériences sont des lasers de type FP dont la facette est recouverte d'une couche anti-reflet. Ces lasers émettent de 1450 à 1500 *nm*. Les FBGs utilisés présentaient une réflexion maximale vers 1490 *nm* et avec une largeur de bande de 0,2 *nm*. La réflectivité des FBGs était de 75 à 80%. Environ 30 cm de EDF fut utilisée. Les DFECLs opéraient à 1490 *nm*.

La méthode de mesure optique permet de mesurer la largeur de bande sur une plage de longueurs d'onde très grande. L'équipement doit posséder une résolution adéquate puisque ces techniques de mesures sont différentielles : on compare le signal reçu à une lumière de référence. Ce signal de référence doit posséder une largeur d'émission plus petite que le signal testé. Le problème majeur rencontré est que le signal du DFECL est si fin que les mesures optiques ne peuvent se faire avec des instruments conventionnels. On doit donc se tourner vers d'autres techniques.

En convertissant le signal optique en signal électrique à l'aide d'une photodiode, on peut indirectement mesurer la largeur de bande de l'émission LASER en utilisant le battement de deux signaux incohérents. Le spectre de ce battement est analysé avec un analyseur. Les détecteurs homodyne et hétérodyne sont le plus souvent utilisés pour mesurer la largeur de bande des sources laser fines. Le fait qu'il y a plusieurs modes de cavités la méthode d'auto-battement est une méthode simple de mesure de la largeur de bande des lasers. Le taux de suppression de ces modes secondaires peut aussi être mesuré à l'aide de cette technique.

Le DFECL présentait une bonne stabilité en longueur d'onde ainsi qu'en largeur de bande. La stabilité à long terme de la longueur d'onde était de  $\pm 2,5$  *pm* alors qu'à court terme, elle était plutôt de  $\pm 1$  *pm*. La largeur de bande des dispositifs s'est avérée plus petite que la résolution des analyseurs de spectres optiques standards. Afin de mesurer

la largeur de bande de l'émission, la méthode de L'auto battement modal (self mode beating) a été utilisée. Le spectre du battement est étudié à l'aide d'un analyseur de spectre électrique couplé à un photodétecteur. La largeur de bande de la note de battement à 1490 nm est d'environ 12,5 kHz, 20 dB sous le maximum. En assumant que le spectre présente une distribution lorentzienne, la FWHM du mode de la cavité externe est estimée à 675 Hz. À l'aide de la même mesure, la largeur de bande d'un DFECL de 67 cm de cavité fut estimée à 2 kHz.

Le taux de suppression des modes secondaires (SMSR) a aussi été étudié par battement hétérodyne : en faisant battre le rayonnement de 2 lasers identiques. Les modes secondaires présentaient une atténuation de 15 à 20 dB par rapport à la raie la plus forte. On montre que le SMSR est toujours d'au moins 15 dB et qu'il demeure 5 à 6 modes longitudinaux dans le spectre d'émission du DFECL.

## 5. Accordabilité des DFECLs

Les sources lasers accordables sont d'une grande utilité dans plusieurs domaines tels la spectroscopie, les senseurs, les radars et les communications optiques. Les lasers large bande sont particulièrement utiles pour l'implantation du paradigme DWDM. En ce qui a trait à la génération optique de micro-ondes, des lasers de largeurs d'émission moins importantes font amplement l'affaire.

On contrôle généralement la fréquence d'émission des lasers à cavités externes en ajustant les longueurs de celles-ci ou en ajustant la réponse spectrale de réflectivité du FBG faisant office de miroir. Ceci est effectué en changeant la période de Bragg du réseau réflecteur par étirage mécanique ou par chauffage et dilatation thermique.

L'accordabilité du réseau dynamique présent dans l'EDF s'opère d'une différente manière. Le temps de vie des ions Erbium est relativement long. Cette caractéristique du réseau non linéaire aide à amortir les changements rapides de longueurs d'onde

d'émission en stabilisant celle-ci. Il est nécessaire de varier la fréquence de l'onde stationnaire se propageant le long de L'EDF. Il est aussi possible de modifier la longueur d'onde d'émission en variant le courant traversant la diode laser par l'entremise du facteur de Henry.

Les résultats expérimentaux montre la possibilité d'accorder la longueur d'onde d'émission du DFECL sur  $60\text{ pm}$  en variant le courant de  $160\text{ mA}$  de manière linéaire. La pente de la réponse freq.  $V_s$  courant est de  $50\text{ MHz/mA}$ . Par ailleurs, une variation de la température d'opération de la diode laser a généré la possibilité d'accorder la longueur d'onde sur  $100\text{ pm}$  au taux de  $25\text{ pm/}^\circ\text{C}$  ( $3\text{ GHz/}^\circ\text{C}$ ). L'accordabilité du réseau dynamique induit par le FBG externe n'est pas affectée par la modulation de courant et de température aux bornes de la diode. La puissance d'émission peut donc être ajustée par un ajustement du courant et de la température.

Puisque la génération optique de micro-ondes nécessite des fréquences de modulations de l'ordre de quelques GHz à quelques dizaines de GHz, l'expérience montre que le contrôle direct de la longueur d'onde d'émission d'un DFECL peut constituer une avenue simple et abordable de contrôle de la fréquence d'émission micro-onde. En comparaison, les lasers DFB ont des réponses de  $1\text{ GHz/mA}$  et de  $24\text{ GHz/}^\circ\text{C}$ , ce qui en fait des dispositifs beaucoup trop sensibles pour leur implantation systématique. La faible sensibilité des DFECLs permet donc de diminuer l'importance des boucles de rétroaction électroniques nécessaire à l'opération en fréquence unique et ainsi de simplifier les systèmes.

## 6. DFECL pour les applications ROF

La modulation directe de la largeur de bande des lasers est limitée par la fréquence de relaxation des photons ou la fréquence de la cavité résonante. L'utilisation d'un

absorbant saturable dans la cavité, la largeur de bande de modulation directe d'un DFECL peut être augmentée.

Les expériences de modulation en fréquence unique ont permis de montrer les oscillations de relaxation inhérentes à la technique de modulation près de la fréquence de résonance du système. Au fur et à mesure que la fréquence de modulation est augmentée au-delà de la fréquence de résonance de la cavité, la transmission du DFECL devient périodique. La période de la réponse est exactement égale à la fréquence de résonance de la cavité. On note 25 dB d'isolation entre les pics et les creux de la réponse. Les pics de transmission débutèrent à s'atténuer à partir d'une fréquence de modulation de 2,8 GHz. L'utilisation d'une meilleure interface RF et l'optimisation de la longueur de la cavité pourraient permettre d'augmenter la largeur de bande de modulation.

La stabilisation modale (mode locking) produite par l'utilisation de l'absorbant saturable permet d'augmenter la réponse en transmission d'un DFECL pour des multiples de la fréquence de résonance de la cavité. Pour ces fréquences d'opération, la largeur de bande de modulation est aussi augmentée. Ceci permet de moduler un signal micro-onde de largeur spectrale fine sur chacun des pics de transmission du DFECL et ce, avec une très bonne isolation entre les canaux.

Nous avons modulé le DFECL avec le 22<sup>ième</sup> multiple de la fréquence d'opération de la cavité soit autour de 2,4 GHz. Le rapport signal sur bruit après transmission est d'environ 50 dB. Avec une largeur de bande FM de 10 MHz, la modulation directe du DFECL à 2,4 GHz n'a produit aucune distorsion du spectre. Pour une largeur de bande FM de 20 MHz, les distorsions sont faibles. Ce résultat montre bel et bien l'applicabilité d'une transmission ROF par modulation directe d'un DFECL.

L'OFDM (orthogonal frequency division multiplexing) est une méthode de modulation permettant de transmettre une grande quantité de données sur support d'onde radio. Chaque sous-porteuse est modulée en quadrature d'amplitude (QAM) à un débit de symboles faible. La fréquence QAM est similaire à celle utilisée dans le

paradigme à porteuse unique pour la même gamme de fréquence. L'OFDM est la méthode utilisée pour les systèmes de communications large bande sans fils tel le Wi-Fi (IEEE 802.11 a/g).

Le signal OFDM fut appliqué aux bornes du DFECL par modulation directe selon la norme IEEE 802.11 a/g. Une modulation 64-QAM OFDM avec un taux maximum de 54 Mbits/sec fut implémentée avec une largeur de bande de 20 MHz. Une porteuse RF de 2,4668 GHz fut précisément fixée pour maximiser la transmission. L'intensité RF fut tour à tour variée de 0 dBm à 10 dBm par incrément de 2,5 dBm. Le spectre du signal OFDM reçu présente un rapport signal sur bruit de 35 à 45 dB. Le signal RF de plus haute puissance produisit le meilleur rapport signal sur bruit.

L'EVM (error vector magnitude) est un test diagnostique qui permet de vérifier la qualité d'un lien de transmission OFDM. Cette mesure évalue la valeur RMS de la variation du vecteur d'erreur en fonction du temps lors des transitions de l'horloge (à la fin d'un bloc de symboles). Plus petit est le rapport EVM, meilleure est la transmission du lien. Durant les expériences sur un DFECL, l'EVM a diminué avec une augmentation de la puissance de modulation RF. Cette réponse diffère de celle du laser modulé à l'externe où on a plutôt noté une augmentation de L'EVM avec l'augmentation de la puissance RF. Cette hausse est causée par des distorsions de troisième ordre produite par le modulateur externe.

Les tests de modulation directe confirment donc la possibilité d'utiliser le DFECL pour des transmissions ROF implémentant le paradigme IEEE 802.11 a/g.

## 7. DFECL à fibre totalement dopées

Le réseau dynamique formé dans la fibre dopée d'un DFECL est l'élément principal permettant d'obtenir une raie d'émission stable et très fine. Un réseau dynamique long permet de réduire la largeur de la raie d'émission mais, en contrepartie, plus longue est

la fibre dopée, plus longue est la cavité ce qui réduit l'espace entre les modes et ainsi rend difficile la suppression de modes secondaires.

Une fibre optique standard permet à deux modes de polarisations distinctes et d'indices effectifs légèrement différents de se propager. Cette dispersion modale (PMD) devient un paramètre important à contrôler lorsque la largeur de bande du laser devient très fine. Une fibre PM, à maintien de polarisation peut être utilisée pour réduire l'impact de la PMD.

L'analyse théorique montre que l'introduction de fibre dopée dans la cavité externe peut augmenter le SMSR. La partie de fibre non dopée ne sert alors qu'à contrôler le nombre de modes oscillant. Un nouveau design de DFECL constitué d'un mécanisme de couplage à lentille fibré a été réalisé. Celui-ci consiste en la fusion d'un FBG très près de l'EDF. Le design indique qu'une longueur de 26 cm d'EDF est optimale. Le FBG sélectionné présentait une réflectivité de 9 dB centrée à 1528 nm et de largeur de bande de 0,2 nm.

Le SMSR de ce laser fut mesuré à plus de 50 dB et l'opération monomode a été démontrée. Le SMSR externe de ce laser fut ensuite mesuré par battement hétérodyne. Le SMSR externe est de 45 dB. À l'aide de la même mesure, la largeur de bande d'un DFECL fut estimée à 350Hz.

Le nouveau DFECL possède une cavité constituée de 100% d'EDF. Ceci permet d'obtenir un écart plus important entre les modes de cavité externe. Ceci permet de réduire de manière plus substantielle les modes secondaires et ainsi d'opérer en régime monomode.

## 8. Conclusion

On a réalisé des DFECL à 1490 et 1530 *nm* lors de notre étude. Les caractéristiques de stabilité fréquentielle et de puissance des dispositifs ont été mesurées. Le grand ratio de suppression des modes secondaires, l'accordabilité fréquentielle et la possibilité de modulation directe des DFECLs construits permet d'entrevoir leur utilisation dans les communications ROF en raison de la faible largeur de leur raie d'émission.



## **LIST OF PUBLICATIONS RELATED TO THE THESIS**

### **JOURNAL PAPERS**

R.N. Liu, I.A. Kostko, R. Kashyap, K. Wu, and P. Kiiveri, "Inband-Pumped, Broadband Bleaching of Absorption and Refractive Index Changes in Erbium Doped Fiber", Optics Communications, Vol. 255, pp.65-71, 2005.

R. Liu, I. A. Kostko, K. Wu, and R. Kashyap, " Side mode suppression using a doped fiber in a long external-cavity semiconductor laser operating at 1490 nm", Optics Express Vol.14, No.20, 9042, 2006.

Runnan Liu, Irina A. Kostko, Ke Wu, and Raman Kashyap, "Stable and continuous wavelength tuning of a hybrid semiconductor laser with an erbium-doped fiber external cavity", Optics Letters, Vol. 32, Issue 12, pp. 1635-1637, 2007

## CONFERENCE PAPERS

Runnan Liu, Irina Kostko, Ke Wu, Raman Kashyap, "Tuning characteristics of a long erbium doped fibre external cavity semiconductor laser for radio-over fibre applications", Proc. SPIE Vol. 6343, 63432J, 2006,

Runnan Liu, Irina Kostko, Ke Wu, Raman Kashyap, "Optical generation of microwave signal by doped fiber external cavity semiconductor laser for radio-over-fiber transmission.", Proc. SPIE Vol. 5971, 59711W, 2005,

R. Liu, K. Wu, and R. Kashyap, "Microwave transmission by direct modulating an ultra-long doped fiber external cavity semiconductor laser", ISATED APR2007, May 30th - Jun 2nd, Montreal, 2007

R. Liu, K. Wu, and R. Kashyap, "Direct modulation of an ultra-long doped fiber external cavity semiconductor laser at multiples of the cavity resonant frequency", Proc. SPIE, Vol: 6796, Ottawa, Jun4-6, 2007,

F. Guay, R. Liu, D. Deslandes, R. Kashyap, K. Wu, "Distributed feedback EBS in a coaxial cable by means of periodical mechanical section modification" ANTEM/URSI 2006. pp. 565-8., Montreal, Canada, July 2006.

Runnan Liu, M. E. Mousa Pasandi, Sophie LaRochelle, Jianping Yao, Ke Wu and Raman Kashyap, "OFDM signal transmission by direct modulation of a doped fiber external cavity semiconductor laser", Presentation at OFC 2008, Feb. 24-28, San Diego, USA

Runnan Liu, Howard Rideout, Joe Seregelyi, Ke Wu and Raman Kashyap, "A fully erbium doped fiber long external cavity laser with 45 dB side mode suppression", Photonics North 2008, Montreal, June2-4, 2008

## TABLE OF CONTENTS

ACKNOWLEDGEMENTS .....	v
RÉSUMÉ .....	vii
ABSTRACT .....	x
CONDENSÉ EN FRANÇAIS .....	xiii
LIST OF PUBLICATIONS RELATED TO THE THESIS .....	xxiv
JOURNAL PAPERS .....	xxiv
CONFERENCE PAPERS .....	xxv
TABLE OF CONTENTS .....	xxvi
LIST OF FIGURES .....	xxix
LIST OF ACRONYMS .....	xxxii
Chapter 1 Introduction .....	1
1.1 Motivation .....	1
1.1.1 Optical Microwave Transmission .....	3
1.1.2 Laser Sources .....	7
1.2 Objectives .....	12
1.3 Thesis Outline .....	12
1.4 Original Contributions .....	15
Chapter 2 Laser sources .....	17
2.1 Introduction .....	17
2.2 Semiconductor lasers .....	17
2.2.1 Line-width of semiconductor laser .....	18
2.2.2 Oscillating mode of laser cavity .....	20
2.2.3 Direct modulation of semiconductor laser .....	23
2.3 DFB and DBR lasers .....	24
2.4 External Cavity Laser .....	27
2.5 Fiber Bragg Grating .....	30
2.6 Fiber Grating External Cavity Laser .....	34

2.7 Conclusion.....	37
Chapter 3 The rare earth doped fiber.....	39
3.1 Introduction .....	39
3.2 Erbium Doped Fiber.....	39
3.2.1 Absorption Modification of EDF .....	44
3.2.2 Doped fiber for lasers.....	46
3.3 Self pumped absorption of EDF .....	48
3.3.1 EDF absorption bleaching.....	48
3.3.2 Whole band absorption bleaching of the EDF .....	52
3.4 Doped fiber laser .....	57
3.4.1 Doped Fiber External Cavity Laser (DFECL) .....	58
3.4.2 Spatial Hole Burning.....	59
3.4.3 Dynamic Grating.....	61
3.5 Conclusion.....	65
Chapter 4 Narrow Line-width and Stability of DFECL .....	67
4.1 Introduction .....	67
4.2 Doped Fiber External Cavity Laser.....	68
4.3 Design and Fabrication of New DFECL .....	70
4.4 The stability of DFECL .....	73
4.5 Simulations for DFECL.....	74
4.6 The Line-width Measurement of the DFECL .....	75
4.7 Experiment of line-width measurement with self mode beat note .....	78
4.8 SMSR Measurement by self mode beating .....	80
4.9 SMSR measurement by heterodyne beating.....	84
4.10 Conclusion.....	89
Chapter 5 Tuning Characteristics of The DFECL .....	90
5.1 Introduction .....	90
5.2 Transient Response of DFECL.....	91
5.3 Tuning the DFECL .....	95

5.4 Conclusion .....	99
Chapter 6 DFECL for ROF applications .....	101
6.1 Introduction .....	101
6.2 Resonance enhanced direct modulation .....	102
6.3 Direct Modulation of DFECL .....	104
6.4 Narrow Band Microwave Transmission.....	108
6.5 Transmission from DFECL to an antenna.....	110
6.6 OFDM signal transmission with DFECL .....	112
6.7 Conclusion.....	117
Chapter 7 Fully doped fiber DFECLs.....	119
7.1 Introduction .....	119
7.2 Design of a fully EDF external cavity laser .....	119
7.3 Experiment and results .....	121
7.4 Conclusion.....	126
Chapter 8 Conclusion .....	127
8.1 Thesis overview.....	127
8.2 Direction for future work.....	130
REFERENCES.....	133

## LIST OF FIGURES

Figure 1-1 Schematic diagram of the Radio Over Fiber system.....	1
Figure 2-1 Schematic structure of a Fabry-Perot semiconductor laser.....	18
Figure 2-2 Schematic structure of DFB laser.....	26
Figure 2-3 Schematic structure of DBR laser .....	26
Figure 2-4 Schematic structure of external cavity laser.....	28
Figure 2-5 Schematic of a fiber Bragg grating.....	31
Figure 2-6 Grating reflectivity changed along the fiber.....	32
Figure 2-7 Schematic of fiber grating external cavity laser .....	34
Figure 2-8 Part of light spectrum of a FP semiconductor laser.....	36
Figure 2-9 Light spectrum of the FGECL built with the broad line-width FP laser.....	36
Figure 3-1 Absorption and gain spectra of an EDFA .....	41
Figure 3-2 Schematic illustration of EDF pumping scheme.....	41
Figure 3-3 Doped fiber laser with two FBG .....	46
Figure 3-4 Doped fiber external cavity laser .....	47
Figure 3-5 The doped fiber works as a two level system.....	47
Figure 3-6 The setup for EDF absorption measurement.....	49
Figure 3-7 The net absorption of EDF measurement results .....	51
Figure 3-8 Experiment set up for inband pump absorption measurement.....	53
Figure 3-9 The bleaching spectrum of EDF with pumping at 1532 nm .....	54
Figure 3-10 The bleaching spectrum of EDF with pumping at 1554nm .....	55
Figure 3-11 Schematic of the external cavity semiconductor laser .....	58
Figure 3-12 Schematic Waves in DFECL.....	59
Figure 3-13 The spectra of refractive index change of the EDF at pump wavelengths of 1532 nm and 1554 nm at pump powers of 2.7 dBm and 3.3 dBm, respectively. Dotted line shows spectrum of the refractive index change at -27 dBm pump ..	64
Figure 4-1 Schematic of the external cavity semiconductor laser .....	68

Figure 4-2 Absorption in erbium-doped fiber: (a) absorption at 1490 nm as a function of pump power; (b) bleaching of the whole absorption band when the erbium-doped fiber is pumped at 1490 nm (Pump power decreased by inline attenuation) .....	73
Figure 4-3 Long term stability of the DFECL .....	74
Figure 4-4 Simulated spectrum of DFECL-2: 200mA (solid) and 220 mA (dashed).....	75
Figure 4-5 Setup of line-width measurement by self mode homodyne beating .....	79
Figure 4-6 The beat spectrum of the DFECL-1 (EC 95-cm-long).....	79
Figure 4-7 the mode beat note measurements of an ECL .....	81
Figure 4-8 The mode beat note measurements of a DFECL.....	81
Figure 4-9 The setup for microwave generation by beating two DFECLs .....	85
Figure 4-10 measurements of the heterodyne beat-note of the two DFECLs (BW=13GHz).....	86
Figure 4-11 measurements of the heterodyne beat-note of the two DFECLs (BW=3GHz) .....	86
Figure 4-12 The derived light mode of DFECL from the experiment of DFECL heterodyne beat note .....	87
Figure 4-13 Calculation of the dynamic grating bandwidth divided by the spacing the in DFECL .....	88
Figure 5-1 Setup for output of DFECL measurement.....	93
Figure 5-2 Switch on/off experiment for measuring the dynamic grating setup characteristics.....	94
Figure 5-3 Wavelength stability of DFECL with switch on/off at $I = 120$ m.....	94
Figure 5-4 (a) Wavelength and (b) power tuning by changing the driving current laser diode.....	96
Figure 5-5 The Wavelength tuning by changing the temperature of the laser diode.....	97
Figure 5-6 The wavelength tuning of DFECL as a function of drive current and temperature.....	98
Figure 6-1 Setup for DFECL direct modulation .....	106
Figure 6-2 Transmission response of direct modulation of long DFECL.....	107

Figure 6-3 The setup for microwave transmission by DFECL .....	108
Figure 6-4 The narrow bandwidth signal transmission with a DFECL .....	109
Figure 6-5 The received spectrum from DFECL direct modulation.....	109
Figure 6-6 The transmission of 10 MHz bandwidth FM wave from DFECL direct modulation .....	110
Figure 6-7 The transmission of 20MHz bandwidth FM wave from DFECL direct modulation .....	110
Figure 6-8 Set-up for directly modulating a DFECL with various measuring points...	111
Figure 6-9 Direct Modulation of DFECL with 20MHz bandwidth FM signal at 0 dBm RF carrier, (A): Spectrum of RF source, (B): the spectrum with only antenna transmission, (C): received spectrum at photo-detector after directly modulating the DFECL, and RF amplifier, (D), the spectrum from the photo-detector after directly modulating the DFECL and RF amplifier and antenna transmission. (E), received spectrum photo-detector after directly modulating the DFECL .....	111
Figure 6-10 The setup of OFDM direct modulation .....	113
Figure 6-11 The receive OFDM spectrum from direct modulating a DFECL .....	114
Figure 6-12 The receive EVM from direct modulating a DFECL.....	115
Figure 6-13 The external OFDM modulation setup.....	116
Figure 6-14 EVM measurements for DFECL direct modulation and DFB external modulation .....	116
Figure 7-1 Calculation of the dynamic grating divided by the mode spacing in the DFECL .....	120
Figure 7-2 Schematic structure of fully EDF external cavity laser.....	121
Figure 7-3 Doped fiber lens for the DFECL .....	122
Figure 7-4 Optical spectrum of fully EDF external cavity laser.....	123
Figure 7-5 Self mode beat note of the fully EDF external laser .....	123
Figure 7-6 Spectrum of Beating the DFECL with a single mode tunable laser.....	124
Figure 7-7 The line-width of DFECL measured with self beat note.....	125



## LIST OF ACRONYMS

AlGaAs	Aluminum Gallium Arsenide
AM	amplitude modulation
AR	anti-reflection
ASE	amplified spontaneous emission
BPSK	binary phase shift keying
CW	continuous wave
DBR	distributed Bragg reflector
DF	doped fiber
DFB	distributed feedback laser
DFECL	doped fiber external cavity laser
DWDM	dense wavelength division multiplexing
ECL	external cavity laser
EDF	erbium doped fiber
EDFA	erbium doped fiber amplifier
EDFL	erbium doped fiber laser
ESA	electric spectrum analyzer
EVM	error vector magnitude
FBG	fiber Bragg grating
FGECL	fiber grating external cavity laser
FM	frequency modulation
FP	Fabry-Perot
FSR	free spectral range
FWHM	full-width half-maximum line-width
GaAs	Gallium Arsenide
IMDD	intensity modulation direct detection
IQ	In phase component / quadrature component
LD	laser diode

LiNbO <sub>3</sub>	Lithium Niobate
MMW	millimeter wave
MZI	Mach-Zehnder interferometer
MZM	Mach-Zehnder modulator
OC	optical coupler
OFDM	orthogonal frequency division multiplexing
OIL	optical injection locking
OPLL	optical phase locked loop
OIPLL	optical injection phase locked loop
OSA	optical spectrum analyzer
PD	photodetector/photodiode
QAM	Quadrature amplitude modulation
RIN	relative intensity noise
RMS	root mean square
ROF	radio over fiber
RF	radio frequency
SMF	single mode fiber
SMSR	side mode suppression ratio
UV	ultra violet
VSA	vector spectrum analyzer
VSG	vector signal generator
WDM	wavelength division multiplexing

## CHAPTER 1 INTRODUCTION

### 1.1 Motivation

Radio over fiber (ROF), or microwave photonics, is an optical-microwave hybrid technique [Stephens, Joseph, and Chen 1984; Cooper 1990; Merrett, Cooper, and Symington 1991; Ogawa, Polifko, and Banba 1992]. With the radio over fiber system, the electromagnetic waves can be generated or transmitted over the fiber optic communication system to remote locations.

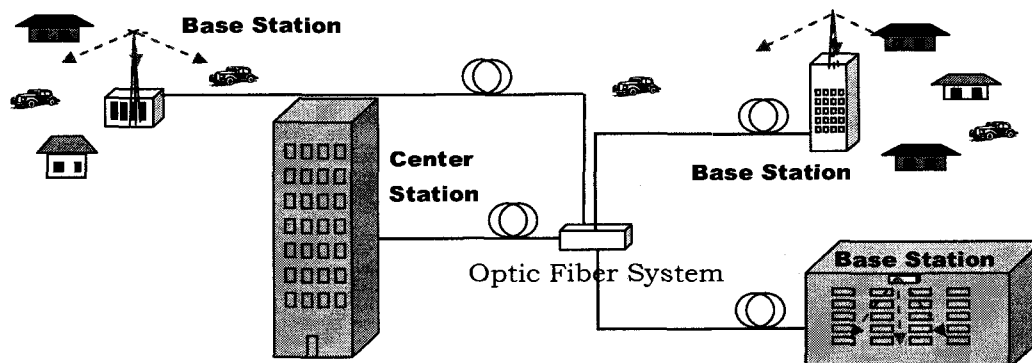


Figure 1-1 Schematic diagram of the Radio Over Fiber system

The radio over fiber system is generally structured with central stations, the fiber optic communication system and the remote base stations (as shown in Figure 1-1). The radio waves modulate the light wave and are transmitted on the fiber optic systems via optical transmitters. In an optical receiver, the radio waves are demodulated from the received light wave. Both the central stations and the base stations may have optical transmitters and optical receivers. In the central stations, as the size and power consumption is not crucial, good performance devices are preferred to transmit high quality signals. Base stations are supposed to be located everywhere in the country. Due to the large number of the base stations, devices for base stations are required with a small size and low cost. As less processing elements are preferred in a base station

between the optical devices and antennas for mobile units, the light transmitted to the base station must be of good quality.

Since the frequency of a light wave is as high as 200 THz, the frequency difference between radio frequency (RF) (10 kHz- 30 GHz) and microwave (300 MHz-300GHz) is a relatively small fraction. As it is often necessary to optically modulate in different frequency regimes, in this thesis, we do not make a distinction between radio frequency wave and microwave transmission.

The major components for the ROF are optical transmitters, transmission media, and receivers. The optical transmitters can be directly modulated laser sources or with external modulators. The electrical signals are uploaded to the transmitted light for optical communication.

For the fiber optic transmission system, the requirements are not much different for the source when comparing ROF communication and digital fiber optic communication. The existing fiber optic system can be used for radio over fiber communications. As the fiber optic transmission has been extensively studied in fiber optic communication system, the studies for the ROF are mainly on the structures: transmitters and receivers. All these work on the basis of opto-electronic conversions for the purposes of low loss, low noise, simple structure, and high efficiency.

The advantages of fiber optic communication are low loss for long distance transmission and broad bandwidth for high capacity transmission [Agrawal, G.P. 2002]. The early optical applications began with free space transmission. With the realization and development of optical fiber, long distance transmission became available with very low loss fiber. Since then, optical communication has been mostly based on the fiber optics. With the optical fiber low cost, the cost of long distance communication system has decreased significantly. The silica optical fiber is the most used transmission media. For this fiber, the optical wavelengths are typical chosen to be 1.3 and 1.55  $\mu\text{m}$ . The 1.55  $\mu\text{m}$  wavelength corresponds to the minimum transmission loss of about 0.2 dB/km.

Optical fiber dispersion is another problem for large bandwidth long distance signal transmission. Dispersion can induce errors in high-bandwidth transmission, even when the received signal intensity is high. Wavelength of 1.3  $\mu\text{m}$  corresponds to the lowest dispersion for silica fiber transmission.

At the receivers, photo detectors play important roles, where the electrical signals are demodulated from the optical carrier. The photoreceivers also affect the system performance with respect to modulation bandwidth, the noise, and linear dynamic range. Whichever transmission media and receivers are used, the signals from the transmitters should be of good quality.

### **1.1.1 Optical Microwave Transmission**

Optical microwave transmission is performed by applying the microwave to either the laser sources or the modulators to modulate the light wave [Seeds 2002]. There are many approaches for signal modulations; such as intensity modulation, frequency modulation and phase modulation, etc. One simple way for optical microwave generation and detection is with intensity modulation direct detection (IMDD) method [Madhumita Bhattacharya, Anuj Kumar Saw, and Taraprasad Chattopadhyay 2003; Sarker, Yoshino, and Majumder 2004]. Other studies to convert frequency or phase modulation to intensity modulation have also been reported [Jun Wang, Fei Zeng, and Jianping Yao 2005]. IMDD provides a simple way to modulate and receive the RF signals.

Essentially, three approaches are mainly used for the transmission of microwave signals over optical fiber links with the optical sources direct modulation, external modulation, and microwave remote optical generation [Seeds 2002]. All of these approaches can be used as intensity modulation.

## **Laser Direct Modulation**

An interesting feature of the semiconductor laser is that it can be modulated directly. Directly modulating a semiconductor laser is a simple and low cost technique to generate microwave signals and transmit them over optical fiber networks. Direct modulation of laser diodes is based on the modulation of the electron flowing through the semiconductor diode to generate a modulated optical signal [Olesen and Jacobsen 1982; Agrawal 1984b; Dods, Ogura, and Watanabe 1993]. Conceptually, any laser can be directly modulated, but it is easiest to modulate a semiconductor laser and the most widely used device for fiber optic communications. By modulating the drive current, a microwave or RF signal can modulate the intensity of the emitted light. The laser light output can be linearly proportional to the drive current over a large current range. Unfortunately, the change in the laser current also changes the optical wavelength [Agrawal 1984b; Agrawal, G.P. and Dutta, N.K. 1993]. This is a wavelength chirping phenomenon and results in frequency modulation superimposed on the wanted intensity modulation. The origin of the chirp relates to the carrier-induced index change accompanying the modulation-induced gain variations. The wavelength chirp leads to a significant dispersion penalty in optical communication systems and is often the limiting factor in their performance. Direct modulation of the semiconductor laser by its drive current can cause amplitude as well as frequency modulation of the laser light [Paoli and Ripper 1970]. Direct modulation usually has low modulation bandwidth. Although cut-off frequencies (or bandwidth) with laser direct modulation can be above 33 GHz [Weisser, Ralston, Eisele, Sah, Hornung, Larkins et al. 1994], commercially available low-cost laser diodes usually have cut-off frequencies of about 10 GHz or below.

The direct modulation performance of a laser largely depends on the fundamental characteristics of a laser diode. The study of direct modulation is important for understanding the limitations of laser sources.

## Modulation with External Modulator

Although RF modulation can be achieved in the easiest way by applying direct modulation to lasers, these are still limited [Cox, Betts, and Johnson 1990]. The first reason is due to the bandwidth limitation of direct modulation, and is normally suitable only for low frequency modulation (usually less than a few GHz). The second reason is the change in the laser current can cause intensity modulation accompanied with the unwanted frequency modulation. The third reason is the gain limitation in direct RF modulation.

These limitations of direct modulation can be solved by using external modulation. In this case, the laser light is simply the CW carrier, and it can be kept constant. The RF or microwave signals are applied to an external modulator, to modulate the light carrier [Simons, R. 1990; Cox, Betts, and Johnson 1990; Sakamoto, Spickermann, and Dagli 1995; Sakamoto, Spickermann, and Dagli 1995; Chen, Fetterman, Chen, Steier, Dalton, Wang et al. 1997; Chen, Fetterman, Chen, Steier, Dalton, Wang et al. 1997; Noguchi, Mitomi, and Miyazawa 1998; Noguchi, Mitomi, and Miyazawa 1998]. The external optical modulation function is usually based on two nonlinear optical effects: electro-optical in conjunction with the principle of interferometric modulation; and electroabsorption modulation, which depends on the change in the absorption of a semiconductor as a function of current. Since the RF link gain for external modulation is related to the electro-optic coefficient, very high electro-optic gain can be obtained.

Furthermore, the noise figure is an important parameter in laser modulation. In the case of direct modulation, the noise figure is influenced by wavelength chirp. As the wavelength in direct modulation is related to the drive current, the modulated drive current can cause wavelength chirp. While in the case of external modulation, it is not necessary to change the drive current of the laser, so there is less noise from the laser source. The light source should be of high quality and its performance not be influenced by modulation. The external modulators are usually designed to have high electro-optic

conversion efficiency; they have high modulation gain for the RF signal, although they may also induce some frequency chirp depending on the bias point [Guohua Qi, Jianping Yao, Seregelyi, Paquet, Belisle, Xiupu Zhang et al. 2006; Jun Wang and Jianping Yao 2006; Sisto, LaRochelle, and Rusch 2006].

The drawback of external modulation is the output optical power since the external modulator is usually designed with optical waveguide, there is a power limitation due to the onset of optical damage, and may generally be limited to  $<100\text{mW}$ . Further, optical coupling to and from the modulator has additional insertion loss. For long distance or high power transmission, an extra optical amplifier is sometimes needed. The external modulation scheme is more complex in structure and has a higher cost than the direct modulation scheme.

The performance of transmission with external modulation largely depends on the characteristics of the external modulator. As, this project is the study of new laser sources for ROF applications, the details of external modulation are not discussed in this thesis.

## **Microwave optical generation**

Heterodyning two semiconductor lasers to generate a beat signal is a well investigated topic [Goldberg, Taylor, Weller, and Bloom 1983; Wake, Lima, and Davies 1995; Johansson and Seeds 2001]. It is particularly advantageous in fiber-radio applications, because it can reduce hardware complexity of the base station and overcome limitations in transmission imposed by fiber chromatic dispersion.

Optical microwave (or millimeter wave) generation is based on the principle of remote heterodyning. Two or more optical signals are simultaneously transmitted and are mixed at the receiver. This mixing gives a heterodyned optical signal realized by the nonlinear response of the photodetector (as it is a square-law detector) itself, or be



detected separately and down-converted in an electrical RF mixer. One or more of the heterodyning microwaves cross-products can be generated in this way.

The generated microwave frequency is given by the wavelength difference of two lasers, and there is no frequency limitation for the generated microwave (millimeter wave), as it can be up to THz, limited by the detection scheme. Thus, an external modulator is not necessary for optical microwave generation. The performance of laser sources for optical microwave generation is critical. A high power, low noise, and stable laser are preferred. As the generated microwave is transmitted with the light carrier, the transmitted power can be high, and a few or no optical repeaters may be needed in the optical transmission system. The receivers can also be simply a photodetector to generate at the beat frequency.

A free-running semiconductor laser typically has the line-width of around 50 MHz. Its wavelength is strongly temperature and current dependent, typically 10 GHz/°K and 1 GHz/mA, respectively. Most laser diode controllers have a control resolution of 0.1 °C and 0.1 mA. Thus, the laser normally has a ~100 MHz frequency fluctuation. Special control techniques are required to obtain a spectrally pure microwave heterodyned signal for ROF applications. This can be achieved with either special laser sources with ultra-stable wavelength and narrow spectral line-width, or with lasers and optical feedback [Goldberg, Yurek, Taylor, and Weller 1985; O'Reilly, Lane, Heidemann, and Hofstetter 1992; Ramos and Seeds 1992].

The laser source is the major component for all of these transmission techniques. A stable laser source with low noise, narrow line-width would benefit these approaches for optical microwave transmission in radio over fiber application.

### **1.1.2 Laser Sources**

Laser sources provide the optical carrier for signals transmission. The performance of the sources largely affects the performance of the communication system. From the

point view of the RF optical link, the features that are considered here are: RF gain, frequency response, noise figure, and dynamic range [Cox, Betts, and Johnson 1990; Roussell, Helkey, Betts, and Cox 1997]. The RF gain is the function of RF signal transmission gain of the optic-electric link system. The frequency response is the frequency transfer function of the optic-electric system. The noise figure expresses the noise generated in the system. The intensity modulation (IM) free dynamic range is a parameter where multiple RF frequencies are simultaneously present. IM-free dynamic range is defined as the maximum difference between the noise floor and the fundamental output which produces distortion terms of equal amplitude to the noise floor. As the parameters are decided by both the laser source and photodetector, they can be used for laser characterization if the photodetector is fixed for comparison.

From the optical regime, the consideration of choosing lasers for RF optical communication is dependent on the power, laser's stability, and the light spectrum line-width, modulation bandwidth, linearity and cost. The power stability influences intensity noise. The wavelength stability is related to frequency noise. The spectral line-width is due to phase noise, and the modulation bandwidth is limited by the laser's frequency response.

Lasers began by the development of ruby MASER (Microwave Amplification by Stimulated Emission of Radiation) [Maiman 1960], and after that, was realized as solid state and the gas lasers [Javan, Bennett, and Herriott 1961]. The development of semiconductor lasers was a major development for optical communication [Hayashi, Panish, Foy, and Sumski 1970]. Semiconductor lasers are compact, are monolithically manufactured, have a high power conversion efficiency, and available for communication wavelengths.

The semiconductor laser is available for direct modulation at microwave frequencies via the injected current. Compared to other types of lasers, a semiconductor laser offers

two distinct advantages; which is its compact size and the possibility of direct modulation through the variation in applied current.

The optical loss and dispersion [Agrawal, G.P. 2002] are two main features for fiber optic transmission and are functions of the wavelength for typical single mode silica fiber. According to the optic fiber transmission characteristics, 1.3 micron and 1.5 micron are two best wavelength windows for the fiber optic communication with low loss or low dispersion. The choice of the operating wavelength is therefore dependent on the proposed transmission loss and dispersion characteristics of the system. At the wavelength of 1.5 microns, standard silica optical fiber has the lowest transmission loss. At this wavelength, light can be transmitted over 100 km at moderate bit rates (such as 20 Gb/s), without amplification. At a high bit rate, the repeater spacing is limited not necessarily by the fiber loss but rather by the extent of fiber dispersion. To solve the problem, one solution is to use the zero dispersion wavelength at 1.3 micron, where its transmission loss is relative high.

The development of erbium doped fiber amplifier (EDFA) has benefited fiber optic communications greatly because it simplifies multi-channel amplification and is directly compatible with optical fibres. The EDFA has become one of the most used devices for long distance fiber-optic communication. Since 1.5 micron window is the best wavelength region for erbium doped fiber amplifier, most long distance fiber-optic communications are in this band. Therefore, at this wavelength, in order to decrease the fiber dispersion, a narrow line-width laser source is really a good choice for long distance fiber optic communication. Dispersion shifted fibre reduces dispersion in this window, but has a lower threshold for nonlinear effects. The solution for this wavelength is to use narrow line-width lasers, which reduce the effect of dispersion.

The line-width of the laser is broadened due to phase noise. Line-width reduction has been studied, which can help lower chirp for optical communication [Henry 1982; Henry 1986; Olsson, Henry, Kazarinov, Lee, and Johnson 1987]. Although gas lasers

provide very good performance in stability and narrow line-width, the large size, low direct modulation bandwidth and size limit their application [Wyatt, Smith, and Cameron 1982].

Compact semiconductor lasers have been developed successfully for optical communication, but the line-width and its stability are not always as desired. A normal Fabry-Perot (FP) semiconductor laser has a very broad line-width ( $\sim$  nm). With integrated distributed feedback, a free running Distributed Feedback (DFB) laser has a line-width of  $\sim 10$  MHz ( $\sim 0.01$  pm). An external cavity is used to enhance the performance by narrowing the line-width, and the peak power of a semiconductor laser is also increased [Statz, Tang, and Lavine 1964; Hayashi, Panish, and Foy 1969; Fleming and Mooradian 1981; Kazarinov, Henry, and Logan 1982; Agrawal 1984a; Vahala, Paslaski, and Yariv 1985; Henry and Kazarinov 1986; Kazarinov and Henry 1987; Olsson, Henry, Kazarinov, Lee, and Johnson 1987; Yariv, A. 1991; Timofeev, Simin, Shatalov, Gurevich, Bayvel, Wyatt et al. 2000b]. External cavity semiconductor lasers can have line-width as low as  $\sim 50$  kHz. External cavity semiconductor laser has been demonstrated to have narrow line-width and are highly stable for optical communications [Campbell, Armitage, Sherlock, Williams, Payne, Robertson et al. 1996; Timofeev, Bayvel, Midwinter, Wyatt, Kashyap, and Robertson 1997; Timofeev, Bayvel, Wyatt, Kashyap, Lealman, and Maxwell 1998; Timofeev, Kostko, Bayvel, Berger, Wyatt, Kashyap et al. 1999].

A doped fiber external cavity semiconductor laser (DFECL) is developed from the fiber grating external cavity laser, and has many of the advantages of the external cavity laser [Loh, Laming, Zervas, Farries, and Koren 1995b; Timofeev and Kashyap 2003]. The simplicity of the DFECL makes fabrication easy and inexpensive, as it can be simply assembled with readily available components. The DFECL has the characteristics of high power, stable wavelength, and a narrow spectral line-width. This laser is a potential source for radio over fiber applications.

External optical feedback is a technique used to narrow the line-width and stabilize the wavelength in CW lasers. Optical injection locking (OIL) is one approach of optical feedback locking to decrease the lasers phase noise and synchronize the lasers for beating [Wyatt, Hodgkinson, and Smith 1983; Moses, Turner, and Tang 1976; Spano, Piazzolla, and Tamburrini 1985; Lidoyne, Gallion, Chabran, and Debarge 1990; Hui, D'Ottavi, Mecozzi, and Spano 1991; Bouyer, Gustavson, Haritos, and Kasevich 1996; Laperle, Svilans, Poirier, and Tetu 1999]. Injection locking of two semiconductor slave lasers to different frequency modulation sidebands of a semiconductor master laser, which is modulated with a microwave source has been reported in the literature [Spano, Piazzolla, and Tamburrini 1985; Godard, Pauliat, Roosen, and Ducloux 2004]. Therefore, slave lasers are correlated in their phase noise. The main practical limitation for optical injection locking is that the locking range is usually small (typically a few hundred megahertz), so that the temperature of the slave lasers must be controlled with milli-Kelvin precision, or lasers must be monolithically integrated to achieve thermal tracking [Chen, Fetterman, Chen, Steier, Dalton, Wang et al. 1997]. An alternative technique for correlating the phase noise of the heterodyne sources is to use an optical phase-lock loop (OPLL) [Enloe and Rodda 1965; Steele 1983; Grant, Michie, and Fletcher 1987; Ramos and Seeds 1990; Kazovsky and Jensen 1990; Ramos and Seeds 1992; Johansson and Seeds 2001; Biswas and Bhattacharya 2001]. The outputs from the two sources are coupled to a photodetector, producing a signal at the difference frequency between the wavelengths of the sources. This signal is compared with a microwave reference frequency in a mixer, and after appropriate filtering the output phase error signal is used to tune the slave laser. Therefore, the frequency difference exactly equals the reference. This has been demonstrated for narrow-line-width gas lasers [Enloe and Rodda 1965]. For practical realization of OPLLs, the loop delay should be small enough to ensure that phase fluctuations of the optical sources are accurately cancelled. With the optical feedback locking, the source line-width can even narrow further, to as narrow as 10 MHz, with the phase noise better than -100 dBc/Hz at the offset of 10 kHz [Lidoyne, Gallion, Chabran, and Debarge 1990]. A line-width of

10 Hz has also reported in [Goldberg, Yurek, Taylor, and Weller 1985]. Furthermore, combined with the OIL and OPLL, optical injection phase lock loop has reported to have a wide lock range without loop delay limitation [Bordonalli, Walton, and Seeds 1996; Bordonalli, Walton, and Seeds 1999], but is rather complicated.

## **1.2 Objectives**

The objective of this thesis is to investigate a new laser source for the purpose of radio over fiber applications. This laser should have attractive characteristics, such as narrow line-width, stable wavelength, suitable modulation bandwidth and simple structure.

The DFECL is shown to have a very narrow line-width and is stable in its free running state. It may have many advantages for radio over fiber applications. Although the DFECL was originally reported several years ago, the mechanism of how the doped fiber performs in the external cavity had not been clearly reported before this study was undertaken.

This thesis study includes:

Study of the doped fiber characteristics for DFECL

Study of the line-width of the DFECL

Study of the stability of the DFECL

Study of the tunability of the DFECL

Study of the modulation performance of the DFECL

## **1.3 Thesis Outline**

This thesis is organized in chapters as follows:

In chapter 2, lasers for radio over fiber applications are reviewed. The radio over fiber application is the study of hybrid microwave and photonics. The transmitter is one of the key parts of the radio over fiber system. The light carrier provided by optical sources can affect the performance of the whole system. Stable and narrow line-width lasers are the ideal source for radio over fiber application. As the simplest semiconductor laser for ROF applications, the FP lasers are first introduced. Improvements from the FP laser, are DFB and DBR lasers which demonstrate better performance. Composed with FP lasers, a simple external cavity laser structure shows further improvement in performance. With fiber Bragg gratings, all fiber fiber lasers can be made with very low cost and high performance. This is shown to be the basis for building new and better laser sources. Finally, we show how the DFECL differs from these lasers.

In chapter 3, the study of the doped fiber is presented. Rare earth doped fiber is an important optical component for fiber optic communications. The early studies of doped fiber are mainly focused on the characteristics for optical fiber amplifiers and lasers. Besides being used as an optical fiber amplifier and fiber lasers, the doped fiber can also be used in laser in an external cavity. The mechanism of doped fiber used in external cavity lasers was not clearly understood before this study; and assumptions needed to be verified. In this chapter, the characteristics of the doped fiber for the purpose of making ultra narrow line-width stable external cavity laser are presented. The experimental results show that a high power narrow line-width pump leads to absorption bleaching of the entire absorption band in the doped fiber.

In chapter 4, the detailed fabrication of new DFECLs is presented. The structure of doped fiber external cavity laser is theoretically analyzed. The analysis presented shows that the absorption bleaching of the doped fiber leads to spatial absorption modulation, forming a dynamic grating in the external cavity. The dynamic grating strengthens the reflection of the oscillating waves in the cavity, leading to narrowing of the line-width and stabilization of the wavelength. The new DFECLs demonstrated in this work

operate at 1490 nm wavelength, the edge of the absorption range of the erbium doped fiber. Building a DFECL at this wavelength verifies that the DFECL can be built in the whole absorption bandwidth of erbium doped fiber. A new fully doped fiber external cavity laser at  $\sim 1530$  nm will be presented in chapter 7.

Studies on the fundamental performance of these new DFECLs are also presented. The experimental results demonstrate that the new lasers are very stable in wavelength. The line-width of the new lasers is in the order of kHz, measured by self mode beating. The side-mode suppression ratio of the laser was also measured. With the theoretical analysis, as well as the derivation from experimental measurements, it is found that the new laser side-mode suppression can be  $\sim 20$  dB. An optical microwave generation experiment is demonstrated with the new DFECL using heterodyne beating. With the simulation and experimental results, an optimized design is also suggested.

Tunable lasers are extremely attractive for radio over fiber communication and optical communications. In chapter 5, the study of tunability of the DFECL is investigated. The analysis shows that the external cavity modes are very close together, and the dynamic grating allows the stable wavelength from the DFECL to be slowly tuned. The doped fiber external cavity laser can be either tuned over a wide range by the external fiber Bragg grating, or fine tuned with the dynamic grating in the doped fiber. It is found that the fine tuning with the dynamic grating has a tuning rate as low as 50 MHz /mA, compared to  $\sim 1$  GHz/mA for a DFB laser. The optical tuning resolution can be as low as 5 MHz with the current control resolution of 0.1 mA. The DFECL wavelength tuning may also be realized with temperature. The fine tuning characteristic is extremely useful for radio over fiber applications.

In chapter 6, the modulation performance of DFECL is presented. Due to the ultra long external cavity, the DFECL has very narrow mode spacing. Therefore, the low cavity resonance limits the direct modulation bandwidth of DFECL. However, it is shown that with the saturable absorber inside the external cavity, the long cavity DFECL



can be directly modulated at its resonant frequency. Narrow bandwidth microwave can be generated and transmitted at multiples of the resonant frequency. Experiments show that the DFECL can be directly modulated at the 22<sup>nd</sup> multiples of its cavity resonant frequency. For the DFECL under test, the transmission bandwidth can be as broad as 20 MHz. 64-QAM OFDM modulation signal has been transmitted by directly modulating the long DFECL at 2.5 GHz, with the data satisfying the IEEE802.11a/g standard.

In chapter 7, a latest DFECL with a fully doped fiber in its external cavity is presented, also operating in the 1530nm window. To verify the theoretical analysis in the previous chapters, this fully EDF external cavity laser was built with a tapered lens directly on the EDF, and the EDF spliced very close to the FBG. By directly coupling to the laser diode, this laser presents a side mode suppression ratio better than 45 dB, with a mode spacing of about 400 MHz.

In chapter 8, the conclusions of the studies are presented and discussed. In this thesis, the doped fiber external cavity laser, the fabrication of new lasers and their many characteristics have been studied. Experiments are also reported with these lasers for the first time. As the DFECLs can be developed further, in this chapter, future research is suggested for building better DFECL for radio over fiber. Some of this research is currently being undertaken in our lab and new applications are being investigated.

## **1.4 Original Contributions**

The original contributions of this thesis have stemmed from the analysis, design, fabrication and measurement of novel DFECL for radio over fiber applications. Publications arising from this work have been already listed. The contributions are listed as follows.

First experimental report of whole-band absorption bleaching of the doped fiber when pumping with an in-band narrow line-width pump laser.

Detailed experimental and theoretical study the dynamic grating phenomenon in the doped fiber inside the external laser cavity.

Built the first DFECL at a wavelength of 1490 nm, which is at the edge of absorption band of an erbium doped fiber.

Demonstration of a novel simple approach for ultra narrow line-width laser measurement.

Demonstration of optical microwave generation with two independent narrow line-width DFECLs.

Experimental demonstration of the DFECL's long term stability.

Experimental demonstration of the DFECL transient response. The result indicates that the dynamic grating has a slow response.

First demonstration of the fine tuning of the DFECL by control of the current and temperature of the semiconductor laser chip. The slow and small wavelength tuning range of the laser is attractive for microwave photonics generation.

First demonstration of the direct modulation of the DFECL at the 22nd multiples of cavity resonance frequency. The data bandwidth was 20 MHz.

Demonstration of the microwave signals transmission using an antenna system by directly modulating a DFECL at 2.4 GHz.

First demonstration of the 64-QAM OFDM signal transmission by direct modulating the long DFECL at 2.5 GHz frequency at 1490 nm.

Built the first fully erbium doped fiber external cavity laser operating at 1530 nm.

## CHAPTER 2      LASER SOURCES

### 2.1 Introduction

The major researches in radio over fiber application are in microwave generation and transmission with fiber optics. Optical microwave generation and transmission is done by applying the microwave signal to a laser source or modulator to modulate the light wave. Essentially, from the viewpoint of the optical transmission, three approaches are generally used for the transmission of microwave signals over optical fiber links with the optical sources: direct modulation, external modulation, and RF remote optical generation [Seeds 2002].

Laser sources provide the optical carrier for transmission signals. The performance of a source has a profound effect on the performance of the communication system.

In this chapter, several related laser sources and techniques are reviewed, especially the external cavity laser and its relationship to our new laser with the doped fiber external cavity.

### 2.2 Semiconductor lasers

Semiconductor lasers operate at wavelengths for fiber-optic communications, spanning several bands (1.3 microns, S, C and L-bands) with different gain materials. The two popular materials systems are the GaAs/Al<sub>x</sub>Ga<sub>1-x</sub>As and In<sub>1-x</sub>Ga<sub>x</sub>As<sub>y</sub>P<sub>1-y</sub>/InP. GaAs lasers operate in the wavelength range of 0.75-0.9  $\mu\text{m}$ , whilst InGaAsP lasers operate in the range of 1.1-1.6  $\mu\text{m}$ .

For a laser to operate, a gain media for amplification is required, as well as a cavity for oscillation [Statz, Tang, and Lavine 1964; Hayashi, Panish, and Foy 1969; Yamada and Suematsu 1979; Kazarinov, Henry, and Logan 1982; Agrawal 1987; Yariv, A. 1991; Agrawal, G.P. and Dutta, N.K. 1993]. The gain medium is used to amplify the

electromagnetic field propagating inside a cavity formed with two mirrors. In the semiconductor laser, the oscillating light is wave-guided [Agrawal, G.P. and Dutta, N.K. 1993]. The optical mode is confined in the lateral direction. The semiconductor material is electrically pumped using a forward biased p-n diode structure. The charge carriers injected into a thin active layer stimulate recombination, and through feedback light waves passing through this region are then amplified by stimulated emission. The feedback mechanism is in the form of mirrors at the facets of the laser. As the refractive index difference between the semiconductor material and free space is large ( $\sim 3.4$ ), the cleaved ends of lasers act as mirrors and provide the sufficient optical feedback with a reflectivity of 0.3 each for overcoming the internal losses and to achieve lasing at the appropriate current bias, a schematic of the laser is shown in figure 2-1.

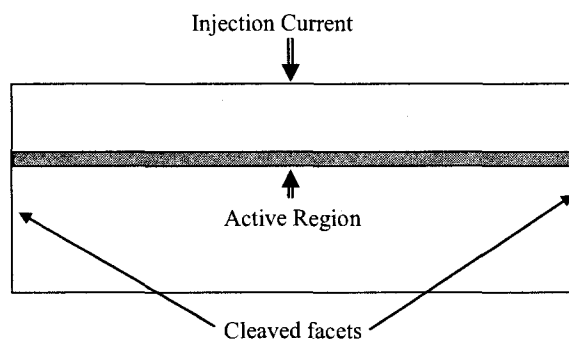


Figure 2-1 Schematic structure of a Fabry-Perot semiconductor laser

### 2.2.1 Line-width of semiconductor laser

In general, the line-width of the laser source can be thought of as the fluctuations in the phase of the optical field [Lax and Louisell 1967]. These fluctuations arise from spontaneous emission events, which discontinuously alter the phase and intensity of the lasing field. Besides the instantaneous phase change caused by spontaneous emission, there is a delayed phase change resulting from the instantaneous change in field intensity.

Narrow line-width and highly stable lasers are critically important in fields as diverse as optical communications, laser cooling and atomic frequency standards. When designing a laser system, the identification and removal of frequency noise sources are crucial for narrow line-width operation.

In a semiconductor laser, spontaneous emissions generate photons of random phase and direction. These discontinuously alter the phase and intensity of the lasing field [Fleming and Mooradian 1981; Henry 1982; Henry 1986].

The spectral line-width of semiconductor laser diodes is given by [Henry 1982]:

$$\Delta f = \frac{R}{4\pi N} (1 + \alpha^2) \quad (2-1)$$

Where  $N$  is the average photon number in the cavity, and  $\alpha$  is the line-width enhancement factor.  $R$  is the spontaneous emission rate coupled to the lasing mode and is equal to the stimulated emission rate of one laser photon.  $R$  is obtained from the Einstein relation as:

$$R = v_g g n_{sp} \quad (2-2)$$

Where,  $v_g$  is the group velocity of light, and  $g$  the threshold gain.  $n_{sp}$  is called the spontaneous emission factor, which is given by

$$n_{sp} = \frac{1}{1 - \exp[-(eV - h\nu)/kT]} \quad (2-3)$$

Where,  $h\nu$  is the photon energy, and  $eV$  the quasi-Fermi level separation and  $kT$  is the thermal energy.

Therefore, the line-width of a semiconductor is energy, wavelength and temperature related.

In reality, due to the quantum fluctuation, the laser output exhibits intensity as well as phase fluctuations. The maximum intensity noise is in the vicinity of the laser threshold and then decreases rapidly with an increase in the drive current. The intensity noise shows a peak near the relaxation oscillation frequency as a consequence of the laser's intrinsic resonance. Phase fluctuations produce spectral broadening of each longitudinal mode and are responsible for the observed linewidth.

### 2.2.2 Oscillating mode of laser cavity

Most communication semiconductor lasers operate in the fundamental spatial mode in the transverse direction. Due to the waveguide in the semiconductor gain media, the longitudinal modes then determine the oscillating waves in the laser cavity.

As mentioned earlier, in a simple semiconductor laser constructed with cleaved facets, the refractive index difference of the media and air makes the facets perform as mirrors. Part of the light reflects back into the cavity. This forms a Fabry-Perot (FP) cavity. Both the internal loss and mirror loss can be regarded the same for all the FP cavity modes. All the lasing modes form the lasing gain spectrum. By increasing the current, the gain in a semiconductor laser increases. When the gain peak is equal to the loss, the mode at this wavelength starts to lase. The mode which has the largest gain becomes the dominant mode.

Considering the longitudinal modes, for a semiconductor laser of length  $L$ , the short central region provides the optical gain and the cleaved facets forms a FP cavity. The feedback of the cavity reflection provides the laser oscillation.

The lasing modes should satisfy the phase condition of the cavity oscillation [Agrawal, G.P. and Dutta, N.K. 1993].

$$2n_0k_0L = 2m\pi \quad (2-4)$$

Where  $k_0 = 2\pi f / c$  is the wave number,  $n_0$  is the refractive index of the media.

The lasing frequency  $f$  is given by:

$$f_m = \frac{mc}{2n_0L} \quad (2-5)$$

Where  $f_m$  often referred to as the cavity resonance frequency, is the frequency of the  $m_{th}$  longitudinal mode of a FP cavity with an optical length,  $n_0L$ .  $n_0$  is frequency dependent, with the relation,

$$\Delta(n_0f) = n_0(\Delta f) + f(\Delta n_0) \quad (2-6)$$

The gain spectrum of semiconductor laser is usually very broad (~10 THz), so that many longitudinal modes of the FP cavity experience gain simultaneously.

The mode spacing is thus given by

$$\Delta f = \frac{c}{2n_gL} \quad (2-7)$$

Where,  $n_g = n_0 + f(\partial n_0 / \partial f)$  is the group index of the dispersive semiconductor material.

The linewidth of a mode broadened by spontaneous emission plays an important role for the spectral characteristics of a semiconductor laser. A simple approximation is that the gain decreases quadratically from its peak [Agrawal, G.P. and Dutta, N.K. 1993]

$$G(\omega) = G_0 \left[ 1 - \left( \frac{f - f_0}{\Delta f_g} \right)^2 \right] \quad (2-8)$$

Where  $f_0$  is the frequency at the peak with maximum value of gain,  $G_0$ ,  $\Delta f_g$  is the frequency spread over which the gain is nonzero on either side of the gain peak, and  $f$  is only in the region where  $G(f) \geq 0$ .

Under ideal conditions, one main mode reaches the threshold and starts lasing. The other modes do not reach the threshold; their gain remaining less than that of the main mode, as the gain is depleted by the lasing mode. In this condition the laser remains in a single longitudinal mode. Practically, the mode spacing of a normal semiconductor laser is very small, it is difficult to suppress the side modes and achieve single mode operation at a current above this condition. The neighbouring modes on each side of the main mode carry a significant proportion of the laser power together with the main mode.

Multimode behaviour in FP semiconductor lasers has been explained with several mechanisms. Spatial hole-burning is a result of the standing wave nature of the optical mode and is known [Statz, Tang, and Lavine 1964] to lead multimode oscillation.

The number of modes can be calculated from the ratio of gain frequency region and the mode spacing, as:

$$M = 2m + 1 \cong \frac{\Delta f_g}{\Delta f} \quad (2-9)$$

The side mode suppression ratio (SMSR) is the amplitude ratio of the maximum mode to the first side mode. Including the effects of spontaneous-emission and the photon-lifetime, the side mode suppression can be represented as:

$$SMSR = 1 + \frac{P_0}{\tau_p R_{sp}} \left( \frac{\Delta f}{\Delta f_g} \right) \quad (2-10)$$

Where  $\tau_p$  is the photon lifetime,  $R_{sp}$  is the spontaneous emission spectrum;  $P_0$  is the main mode power. The SMSR increases with increasing lasing power.



For optical fiber communication systems, the longitudinal side-modes are undesirable, because they cause pulse spreading in the presence of fiber dispersion, thereby degrading system performance. One approach to achieve single mode lasing is to narrow the gain region for a large mode spacing.

The mechanism of spatial hole burning destabilizes the main mode. Such a nonlinear process tends to beat the lasing and the non-lasing modes. The beat frequency modulates the carrier population. The carrier population changes the mode gain and refractive index. Both are at the beat frequency, and these then lead to dynamic gain and index gratings. According to Bragg diffraction, these gratings couple the longitudinal modes. In this state, the power distribution is caused by the so called four-wave mixing process [Kazarinov, Henry, and Logan 1982; Agrawal 1987]. This mechanism has been used to explain large SMSR values of index guided AlGaAs lasers [Kazarinov, Henry, and Logan 1982].

### **2.2.3 Direct modulation of semiconductor laser**

Transient or dynamic response of a semiconductor laser is essential for digital optical fiber communications. In the case of direct modulation, the drive current is modulated by the high frequency signals.

A normal semiconductor laser may have a switch-on transient time of less than 1 ns. Within the time regime of the modulating pulse, the power distribution among various longitudinal modes varies periodically as the laser goes through relaxation oscillations [Paoli and Ripper 1970]. The semiconductor laser exhibits poor side mode suppression under dynamic conditions, especially close to threshold. If it is modulated with high frequency for optical communication, it may be difficult to reach a steady state.

These oscillations, referred to as relaxation oscillations, are a manifestation of an intrinsic energy resonance, in which system energy oscillates between the electron and photon populations. The electron and photon populations oscillate in the dynamic state.

This relaxation oscillation is due to the intrinsic resonance in the nonlinear laser system. The natural frequency of relaxation oscillations is in the gigahertz range and plays an important role in determining device response. Relaxation oscillations take several nanoseconds to become sufficiently damped for mode intensities to reach their steady state values.

When a semiconductor laser is directly modulated, quantum fluctuations in any laser introduce both intensity and phase noise. This is because the drive current modulation of semiconductor lasers results in an amplitude modulation, due to a change in the laser's operating point; meanwhile, it also results a frequency shift of the emission, due to the alteration of the optical path-length of the laser cavity [Dandridge and Goldberg 1982]. This frequency chirping phenomenon is often a limiting factor in the performance of directly modulated communication systems.

Because of an intrinsic resonance of the device it was found that the response peaks at the relaxation-oscillation frequency, and the modulation efficiency drops sharply for modulation frequency greater than the relaxation oscillation frequency. Although theoretically the direct modulation 3dB bandwidth can reach the relaxation oscillation frequency, practically, due to the electrical parasitics and the response no longer being linear with frequency, the useful bandwidth is much lower than the relaxation oscillation frequency.

Normally, conventional FP semiconductor lasers have relatively broad line-widths. Also, the stability and modulation bandwidth are also not satisfactory for high speed optical communication, although it is very attractive because of its low cost and simple structure. Other approaches are needed to help the laser diode to narrow the line-width.

## **2.3 DFB and DBR lasers**

A normal FP semiconductor laser has the drawbacks of low side-mode suppression, broad line-width, and unstable intensity. This makes conventional semiconductor lasers

unacceptable for some optical communication applications, such as DWDM, and optical microwave generation of ROF.

Most FP semiconductor lasers emit multi longitudinal mode light, as the media has broad bandwidth gain, and the facet reflectivity is also broadband. The gain spectrum is usually much wider than the longitudinal mode spacing. One way to improve the mode selectivity is to make the feedback wavelength selective, so that the cavity reflective losses are different for longitudinal modes. In other words, the feedback selection can help to select the main longitudinal mode. In this way, the selected wave gets higher reflection than the other waves and reaches the lasing threshold first.

Distributed feedback (DFB) and distributed Bragg reflector (DBR) semiconductor lasers are two important types of monolithic single mode semiconductor lasers [Agrawal, G.P. and Dutta, N.K. 1993], as shown in figure 2-2 and figure 2-3. The DFB and DBR lasers were developed in parallel in the 1980s. They both have similar light emission characteristics. In these lasers, a holographic method or an e-beam lithographic technique together with chemical etching technique are used to form a grating with sub-micrometer periodicity during the fabrication. After these gratings are formed, multiple epitaxial layers are re-grown to form the complete epitaxial structure. The periodic perturbation of refractive index provided by these gratings couples the waves propagating in the forward and backward directions. Due to the technological complexity in the fabrication process, these lasers are more expensive than FP lasers, since the grating parameters are strongly dependent on the material and structural parameters.

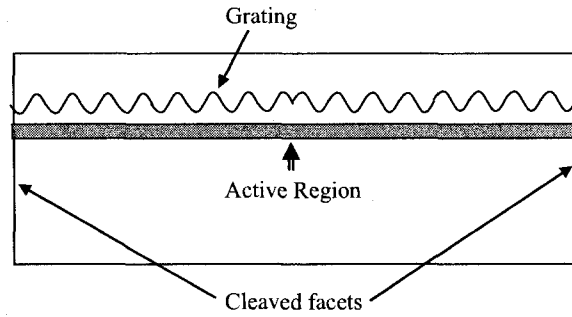


Figure 2-2, Schematic structure of DFB laser

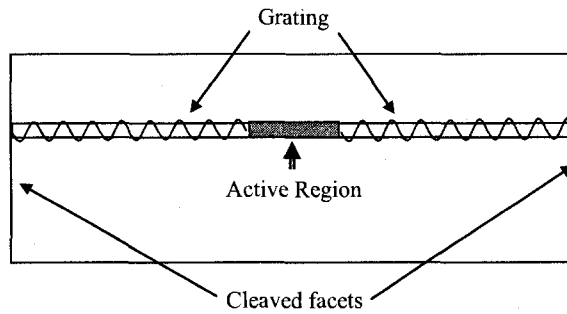


Figure 2-3, Schematic structure of DBR laser

In a DBR laser, the feedback and wavelength selection regions exist only at the ends of the diodes. These feedback regions act as wavelength selective mirrors. In a DFB laser, the grating is distributed throughout the cavity. Usually the grating is shifted by a quarter-wave in the middle to provide large side mode discrimination. Mode selectivity of the DFB or DBR results from the Bragg condition. The Bragg diffraction process assures the laser lases only at the wavelength,  $\lambda_{Br}$  satisfying the Bragg condition [Agrawal, G.P. and Dutta, N.K. 1993]:

$$m\lambda_{Br} = 2n\Lambda \quad (2-11)$$

Where  $\Lambda$  is the grating period,  $n$  is the mode index, and  $m$  is an integer that designates the order of the Bragg diffraction; normally,  $m = 1$ . The mode with the greatest reflective achieves the most gain in the laser media. The side modes get less gain and are suppressed. SMSR values of  $\sim 1000$  (30 dB) are readily obtained at power levels of a

few milliwatts. As a comparison, for the FP laser, a typical SMSR value falls in the 10-20 range, and greater than 50 is difficult to achieve.

Similar to an FP laser, the light-current (L-I) characteristics of a DFB laser is temperature dependent. The DFB lasers outperform conventional FP lasers, and can possibly work in the temperature range of 20-108°C with fewer mode hops. There is a wavelength shift as a function of temperature at a rate about 0.09 nm/°C. This happens because the refractive index varies with temperature, which causes the etched Bragg grating wavelength to change. The rate of change of wavelength as a function of temperature is much higher for FP lasers, which is ~0.5 nm/°C. However, the line-width of a DFB laser can be <200 kHz.

The side modes can affect the modulation when the frequency is greater than half of the mode spacing. Conventional FP lasers suffer from a limitation in the modulation bandwidth, because they are multimode. DFB or DBR laser can therefore have a much improved direct modulation bandwidth. Over 40 GHz modulation bandwidth can be realized [Knodl, Hanke, Saravanan, Peschke, Macaluso, and Stegmuller 2004; Yi Luo, Bing Xiong, Jian Wang, Pengfei Cai, and Changzheng Sun 2006].

## 2.4 External Cavity Laser

One alternative to the monolithic DFB and DBR lasers is an external cavity semiconductor laser (ECL) by using external wavelength selective optical elements. This ECL laser can be structured with an extra cavity outside the FP semiconductor laser diode. The simplest case is to use an external mirror as the feedback element [Agrawal, G.P. and Dutta, N.K. 1993].

One successful technique is to add a passive section into the laser cavity by antireflection (AR) coating the laser facet and adding an external reflector several tens of centimetres away from the facet [Fleming and Mooradian 1981; Agrawal 1984a; Henry 1986; Kazarinov and Henry 1987; Olsson, Henry, Kazarinov, Lee, and Johnson

1987], as shown in figure 2-4. The external cavity is formed between the reflectors from one laser facet to the other mirror. As the cavity length is increased, the new oscillating profile changes the original FP modes to the new cavity modes. At the same time, the mode spacing becomes smaller and SMSR also decreases.

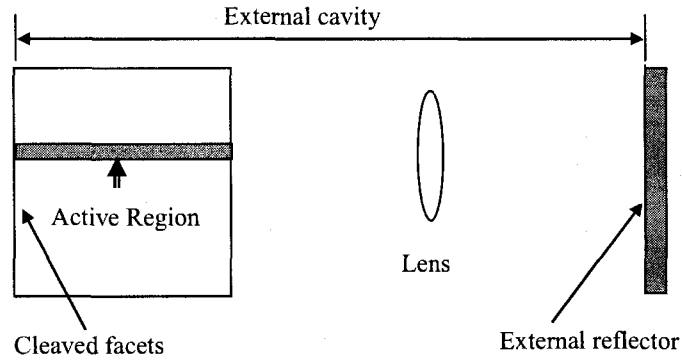


Figure 2-4, Schematic structure of external cavity laser

An improvement to this technique is to use wavelength selective reflector, e.g. Bragg grating is most commonly used for an external reflector. The distributed feedback can also be used to provide a Bragg grating that can be placed at the end of the external cavity [Henry and Kazarinov 1986; Agrawal and Henry 1988]. In these external cavity schemes, mode selectivity arises from interference between the waves propagating in the two directions. Since the reflectivity of the external mirror is wavelength dependent, an additional mode selective mechanism can be introduced, if the feedback from the far end of the external cavity is dispersive.

The external cavity provides another Fabry-Perot cavity, and compounded with the semiconductor laser cavity, forms a new loss profile, as the oscillating mode spacing is related to the cavity lengths.

The longitudinal mode spacing of a laser can be defined as:

$$\Delta\lambda_{MS} = \frac{\lambda^2}{2nL} \quad (2-12)$$

Where  $\lambda$  is the wavelength,  $n$  is the refractive index,  $L$  is the length of oscillating cavity. As an example, with a cavity length less than 1 cm, at a wavelength of 1500 nm, the mode spacing is greater than 0.75 nm; therefore it is possible to select one longitudinal mode with a narrow bandwidth Bragg grating.

As stated before, the laser line-width narrows approximately as the square of the external reflector separation [Fleming and Mooradian 1981]. In the case of the external cavity semiconductor laser, the line-width can be further reduced by increasing the length of the external cavity [Kazarinov and Henry 1987].

$$\Delta\lambda \sim \frac{1}{(1 + U_1 L_1 / U_0 L_0)^2} \quad (2-13)$$

Where,  $U_1$  and  $L_1$  are the optical energy density and length of the passive part,  $U_0$  and  $L_0$  are those of the semiconductor part of cavity, respectively.

Wyatt and Devlin have reported stable single-mode operation with a line-width of only 10 kHz with an external cavity [Wyatt and Devlin 1983]. At the same time, the increase in the total cavity length has the effect of increasing the photon lifetime. This results a larger number of intra-cavity photons at a given output power, and thus the line-width of the single longitudinal mode decreases [Ikegami and Suematsu 1968].

$$\tau_{ph} = \left\{ c \left( \frac{\ln(1/R)}{L} + \alpha \right) \right\}^{-1} \quad (2-14)$$

Where  $\alpha$  is the loss per unit length,  $R$  is reflectivity at the cleaved sides,  $L$  is the cavity length and  $c$  is the velocity of light in the junction.

The frequency chirp and line-width are also reduced by coupling the semiconductor laser to the resonator. The physical mechanism is the frequency dependent optical feedback into the laser cavity from the high-Q resonator, by the external passive resonator. The analysis of this laser shows that under CW or low-frequency operation

the reductions in the adiabatic chirp and the line-width are simply related [Kazarinov and Henry 1987]. The enhancement of the relaxation-oscillation frequency and the reduction of the line-width have been observed for an external reflector [Vahala, Paslaski, and Yariv 1985]. The relation between chirp and line-width reductions was verified [Olsson, Henry, Kazarinov, Lee, and Johnson 1987] using an external Bragg reflector. Under the same operating conditions the line-width is reduced by the square of the chirp reduction factor [Henry and Kazarinov 1986]. The dynamic performance of such an external cavity semiconductor laser is improved considerably [Agrawal and Henry 1988].

The single longitudinal mode is selected by the coupled device close to the gain peak with the lowest cavity loss. This provides an approach for wavelength tuning. Wavelength tuning can be achieved by changing the external cavity length, which can be controlled either thermally or electronically [Coquin and Cheung 1988; Sorin and Newton 1988]. The mechanically ruled grating is the simplest scheme for external cavity laser tuneable mirror. The additional advantage here is that the laser wavelength can be tuned over a considerable range by rotating the grating. Using a bulk diffraction grating as the external cavity frequency selective mirror, a 10 kHz line narrowed 1.5 $\mu$ m laser was demonstrated with a 55 nm tuning range [Wyatt and Devlin 1983]. Temperature tuning alters the refractive index, which results in a change in the optical length, this in turn shift the laser cavity modes [Chiba, Fujiwara, Hotta, Takeuchi, and Sasaki 2003; Fletcher and Close 2004]. Electronic tuning was performed by using a piezoelectric transducer, so as to change the length of the cavity [Schremer and Tang 1990; Wei-Chuan Shih, Chee Wei Wong, Yong Bae Jeon, Sang-Gook Kim, and Barbastathis 2002].

## 2.5 Fiber Bragg Grating

An ECL usually has the issue of light alignment and coupling between the optical components. All fiber ECL does not have such problem, as the fiber components can be



spliced with very good optical coupling efficiency. To realize this all fiber ECL, a fiber Bragg Grating (FBG) is needed as the external reflector.

A FBG is an optical fiber device with a periodic or aperiodic perturbation of the effective absorption coefficient or the effective refractive index as a function of length [Kashyap, R. 1999]. An FBG can be roughly classified into two types. Grating that couple modes traveling in the same directions are known as transmission or long period gratings and have periodicities, in the hundreds of microns [Vengsarkar 1997]. Another type of grating is short period grating. Short period or reflection Bragg gratings couple modes traveling in opposite directions and have periodicities less than a micron at 1550nm. The short period grating can be made to have very narrow reflective bandwidth, which is interesting for fiber grating ECLs.

A Bragg Grating can reflect a predetermined narrow or broad range of wavelengths of light incident on the grating, while passing all other wavelengths of the light. A typical FBG usually has low insertion losses, and it is compatible with existing optical fibers used in telecommunication networks. It is a low-cost optical device for very high quality wavelength-selection. FBGs have proven to be attractive in a wide variety of optical fiber applications, especially as narrowband, broadband wavelength selective filters, and tuneable filters.

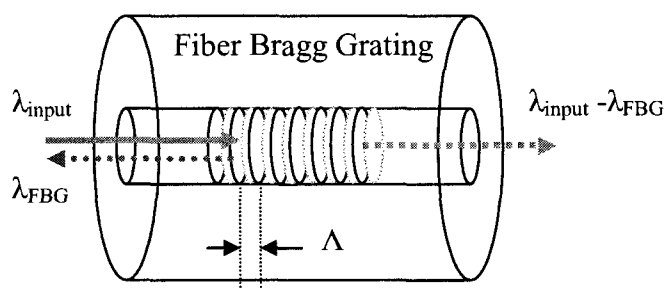


Figure 2-5, Schematic of a fiber Bragg grating

Narrow bandwidth FBG is usually made with uniform period, as shown in figure 2-5, where the mode coupling defines the type of grating. Chirped period FBG can have very

broad bandwidth. Moreover, FBGs can be made complex to meet more complex optical applications.

For a uniform FBG, the refractive index of the fiber is changed with periodic perturbation. [Kashyap, R. 1999]

$$\delta n(z) = \overline{\Delta n} \left\{ 1 + \frac{v}{2} \left( e^{i \left( \frac{2\pi N}{\Lambda} z + \phi(z) \right)} + cc \right) \right\} \quad (2-15)$$

Where  $z$  is along the direction of the fiber axis,  $\overline{\Delta n}$  is the average index change over a grating period,  $v$  is the fringe visibility,  $\Lambda$  is the nominal period or grating pitch, and  $\phi(z)$  is the cumulative phase of the periodic index modulation. A FBG's optical properties can be determined by the variation of the refractive index modulation along the fiber axis  $z$ , incorporation of phase changes in the structure and chirp of the grating.

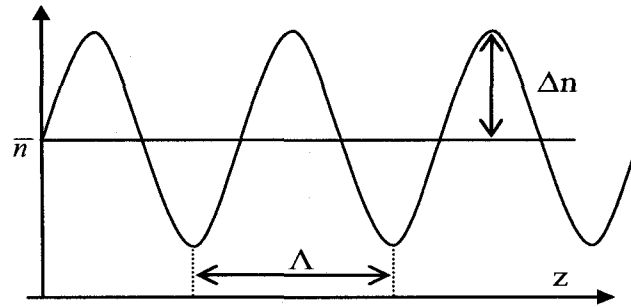


Figure 2-6 Grating reflectivity changed along the fiber

The narrow bandwidth grating at 1500 nm was designed for optical communication [Kashyap, Armitage, Wyatt, Davey, and Williams 1990]. For a uniform FBG, the bandwidth and the peak reflectivity occurs at a wavelength of best phase matching. At the phase matching wavelength, the reflectivity peak [Kashyap, R. 1999] is:

$$|\rho|^2 = \tanh^2(\kappa_{ac} L) \quad (2-16)$$

$\kappa_{ac}$  is the ac coupling coefficient of the FBG. Since

$$\kappa_{dc} \approx \frac{4\pi\eta\overline{\Delta n}}{\lambda} \quad (2-17)$$

For a visibility of unity, the coupling coefficient has a relation of  $\kappa_{ac} = \kappa_{dc}/2$ .

Where,  $\eta \cong 1$  is the overlap integral for identical well-confined modes, and the peak of the Bragg reflection is at

$$\lambda_{\max} = \lambda_B \left( 1 + \frac{\eta\overline{\Delta n}}{n} \right) \quad (2-18)$$

The Bragg wavelength  $\lambda_B$  is defined at the phase matching point for the general case of similar modes.

The Bragg grating period can be presented as

$$\Lambda = \frac{\lambda_B}{2n_{\text{eff}}} \quad (2-19)$$

Where,  $n_{\text{eff}}$  is the effective index of the forward and backward modes of the fiber. The short period grating couples two counter propagating modes at the Bragg wavelength.

The full bandwidth of the FBG, which is defined as twice the bandwidth between the reflection peak and the first zero, is:

$$2\Delta\lambda = \frac{\lambda^2}{\pi n_{\text{eff}} L} \sqrt{(\kappa_{ac} L)^2 + \pi^2} \quad (2-20)$$

Where,  $n_{\text{eff}}$  is the effective refractive index of the FBG,  $L$  is the length of the FBG,  $\lambda$  is the peak reflection wavelength. The FBG reflection spectrum is related to the refractive index modulation and the length of FBG. Because the average refractive index increases continuously with a positive refractive index modulation, the reflection peak

wavelength is longer than the initial Bragg wavelength on commencement of the writing process.

The wavelength of FBG can be tuned via stretching or changing the temperature. The effective index of a propagating mode in the fiber is both temperature and strain sensitive.

$$\Delta n_{eff} = \frac{dn}{dT} \Delta T + \frac{dn}{d\sigma} \Delta \sigma \quad (2-21)$$

Where,  $dn/dT$  is the temperature coefficient of the mode index,  $\Delta T$  is the change in temperature;  $dn/d\sigma$  is the longitudinal stress optical coefficient and  $\Delta \sigma$  is the applied longitudinal stress. The period of the FBG is thus changed by the application of heat or strain. This wavelength tuning is mostly used for tunable filters and tunable lasers.

## 2.6 Fiber Grating External Cavity Laser

A Fiber grating external cavity laser (FGECL) is composed of a semiconductor laser, a piece of a single-mode fiber (SMF), and a narrow-bandwidth FBG. The FGECL has been successfully applied to different applications [Kashyap, R. 1999]. The semiconductor laser diode in FGECL has an anti-reflection-coated output facet. Therefore, the FGECL works as a long external-cavity laser. Due to the fiber waveguide FBG, the FGECL does not have any problem of alignment of external mirrors, and is simple to fabricate.

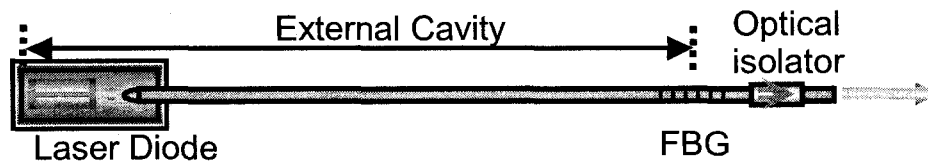


Figure 2-7 Schematic of fiber grating external cavity laser

Since the FBG has a wavelength selective function, the wavelength of the FGECL mode is determined by the diode and fiber refractive indices, as well as by the FBG reflection phase. In general, the current induced variations of these parameters may directly determine the frequency shift. Below the threshold the frequency shift of both the external cavity and FP modes is relatively high due to the unsaturated carrier density. Above the threshold, the frequency shift of FGECL is much less than that of FP lasers [Hansmann, Walter, Hillmer, and Burkhard 1994; Timofeev, Simin, Shatalov, Gurevich, Bayvel, Wyatt et al. 2000a]. It is to be noted that the value of FGECL frequency shift is much lower than that reported for conventional DFB lasers [Hansmann, Walter, Hillmer, and Burkhard 1994]. An ECL with a correct design of an FBG and a high coupling efficiency can have a pure single-mode output spectrum with relatively narrow line-width ( $\sim 50$  kHz) [Timofeev, Simin, Shatalov, Gurevich, Bayvel, Wyatt et al. 2000a].

The mechanism of FGECL is demonstrated by the following experiment. As shown in figure 2-7, the semiconductor laser used was a Fitel 1402 high power FP laser. The lasing light was multi-mode with a very broad gain bandwidth of  $\sim 50$  nm (1450 -1500 nm). The mode spacing was about 0.3 nm, as shown in figure 2-8. The peak wavelength shift with the drive current was in the range of 1480-1490 nm. The peak power was about -8 dBm at a drive current of 145mA. Figure 2-9 gives the output spectrum of the FGECL. The FBG was made with bandwidth of 0.2 nm, at the peak reflective wavelength of 1489 nm. The peak reflectivity of the FBG was  $\sim 6.5$  dB, which is equal to  $\sim 75\%$  reflectivity. The light spectrum of FGECL after the FBG was spliced to the fibre was single mode. The peak wavelength shifted to that of the FBG reflection. The peak power increased to more than 5 dBm at drive current of 160 mA. The peak wavelength shift was only within the range of external cavity FBG bandwidth.

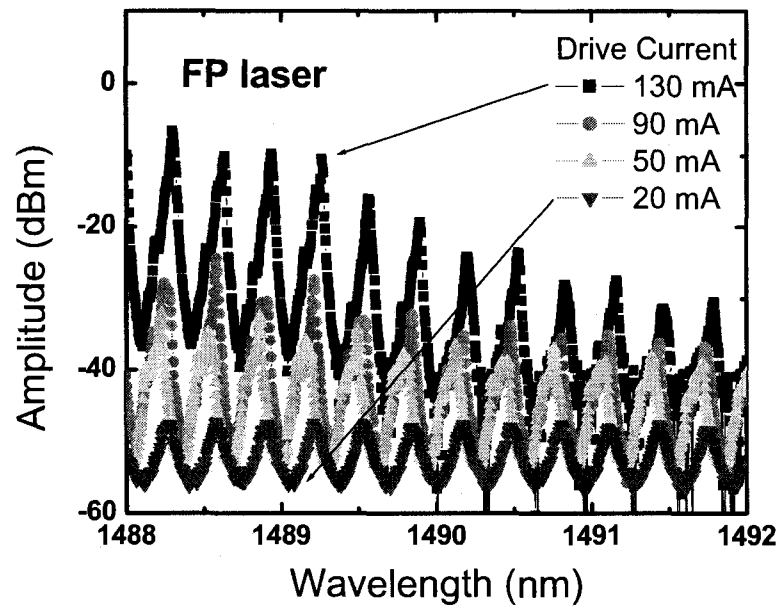


Figure 2-8 Part of light spectrum of a FP semiconductor laser

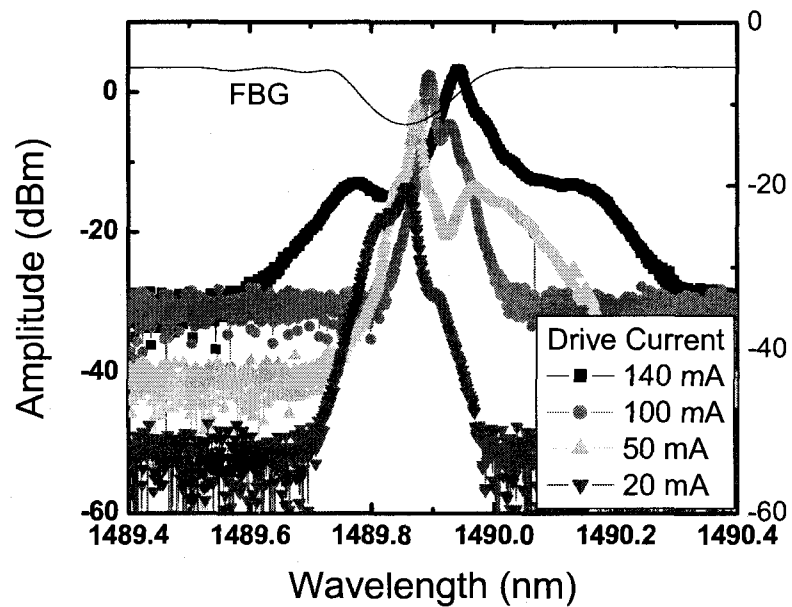


Figure 2-9 Light spectrum of the FGECL built with the broad line-width FP laser.

An advantage of the FGECL is that the temperature sensitivity of a FBG is much lower than that of the semiconductor. Relative to the DFB laser, the FBG reflection

wavelength is a weak function of the ambient temperature, and, hence, there is a weak dependence of the laser operating wavelength [Campbell, Armitage, Sherlock, Williams, Payne, Robertson et al. 1996]. The FBG has a temperature coefficient of wavelength change 6-8 times lower than that of a semiconductor laser [Mantz 1995]. The longer laser formed by the incorporation of the external cavity reduces the line-width in direct relation to  $(1/\text{length})^2$  [Adams, Steventon, Devlin, and Henning 1987].

Another advantage, originating from the presence of a dispersive external cavity [Kazarinov and Henry 1987] is reduced wavelength chirp of the FGECL [Bird, Armitage, Kashyap, Fatah, and Cameron 1991]. As already clear, the lasing wavelength of the FGECL is defined by the FBG [Brinkmeyer, Brennecke, Zuern, and Ulrich 1986; Kashyap, Payne, Whitley, and Sherlock 1994].

A single-frequency FGECL [Park, Rowe, Buus, Reid, Carter, and Bennion 1986; Bird, Armitage, Kashyap, Fatah, and Cameron 1991] was demonstrated as a good source for dense wavelength division multiplexed (DWDM) optical networks. Single channel [Timofeev, Bayvel, Mikhailov, Lavrova, Wyatt, Kashyap et al. 1997] and WDM experiments [Timofeev, Bayvel, Midwinter, Wyatt, Kashyap, and Robertson 1997; Timofeev, Bayvel, Wyatt, Kashyap, Lealman, and Maxwell 1998] performed with FGECL directly modulated with 2.5 GB/s and 10 GB/s signals have confirmed that these lasers are suitable for low penalty transmission over standard single-mode fiber.

After all, FGECL is made with low cost FP laser, and in very simple structure. It has competitive performance in wavelength chirp, narrow line-width. The attractive is that the performance can be further improved with doped fiber inside its external cavity [Loh, Laming, Zervas, Farries, and Koren 1995b; Timofeev and Kashyap 2003].

## 2.7 Conclusion

Radio over fiber is the technique of microwave optical fiber communications. It combines the advantages of the mobility of radio communications and the low loss long

distance communication of fiber optic communications. For microwave photonics applications, the laser sources play a major role as transmitters. Single mode narrow line-width, stable lasers with high modulation bandwidth are desired.

Compact size FP semiconductor lasers with low cost and suitable operating wavelength are needed for radio over fiber communications. As already discussed, FP laser do not possess good stability and narrow line-width. They usually operate multimode, which is not suitable for direct modulation. Many technologies have been used to improve the performance of semiconductor lasers. With an external cavity, FP laser can be built as all fiber FGECL lasers. The FGECL has been shown to have a simple structure and demonstrates competitive performance. Its performance can be improved even further with a doped fiber. The next chapters will now discuss the development of new lasers for this application.



## **CHAPTER 3     THE RARE EARTH DOPED FIBER**

### **3.1 Introduction**

Doped with rare earth materials, normal silica fibers show characteristics of strong optical absorption and stimulated emission in different wavelength regions. Rare-earth doped fiber has been studied for fiber optic communications for more than 20 years. The most interesting applications of rare earth doped fiber was for fiber amplifiers [Digonnet and Gaeta 1985; Desurvire, Simpson, and Becker 1987; Laming, Poole, and Tarbox 1988; Morkel and Laming 1989; Shimizu, Yamada, Horiguchi, Takeshita, and Okayasu 1990; Desurvire, Zyskind, and Simpson 1990; Miniscalco 1991; Giles and Desurvire 1991; Desurvire 1991; Desurvire, E. 2002] and lasers [Shimizu, Yamada, Horiguchi, Takeshita, and Okayasu 1990; Ball and Glenn 1992; Mizrahi, DiGiovanni, Atkins, Grubb, Yong-Kwan Park, and Delavaux 1993; Guy, Taylor, and Kashyap 1995; Pan and Yuan Shi 1995; Loh, Laming, Zervas, Farries, and Koren 1995a; Loh, Laming, Zervas, Farries, and Koren 1995b]. Erbium doped and Ytterbium doped fibers are the media mostly applied for optical fiber amplifiers and fiber lasers. Ytterbium doped fiber has a peak absorption at a wavelength of  $\sim 800$  nm. The absorption peaks in Erbium doped fiber are at 980 nm, and 1480 nm wavelength. The most important characteristic of erbium doped fiber is that its emission-band is in the 1.5 micron wavelength range, which is required for optical fiber communication.

### **3.2 Erbium Doped Fiber**

The characteristics of erbium doped fiber (EDF) can be illustrated with an energy level diagram [Desurvire 1991 Desurvire, E. 2002]. The energy is transformed when the ions change between the levels. When the ions absorb photons, they are excited from lower energy levels to upper energy levels. The ions in upper energy levels return to the bottom of the upper band by phonon relaxation and to the ground state to emit or are

stimulated to emit photons. The stimulated emission wavelength is related to the change in energy between the excited and ground state levels. The most useful emission wavelength of EDF is in the 1.5  $\mu\text{m}$  band and the bandwidth of this emission is about 90 nm wide (1480-1570 nm). The band is in the lowest transmission loss window, and it is the reason why EDF is mostly used for fiber optic communications. The EDF has several useful absorption bands at 800, 980, 1480 nm wavelength, where the emission is relatively weaker, and so these bands are good for EDF pumping. The pump wavelengths used in practical systems are 980 nm by strained-layer quantum well lasers based on GaAs and around 1480 nm by laser diodes based on InGaAsP.

In the 1.5  $\mu\text{m}$  wavelength band, both photon absorption and stimulated emission occur; their relative strengths are almost of the same order of magnitude. Therefore, a photon in this wavelength region can be either absorbed or stimulated and emitted by the EDF. The absorption of the EDF depends on the power and wavelength of pump light. The stimulated emission is also related to the signal light power and wavelength. The gain of erbium doped fiber amplifier (EDFA) can be defined as the ratio of the power of the output signal and input signal. The gain of an EDFA is related to the pump power, pump mode, pump wavelength, fiber length, signal power, and signal wavelength [Digonnet and Gaeta 1985; Desurvire, Simpson, and Becker 1987; Laming, Poole, and Tarbox 1988; Morkel and Laming 1989; Shimizu, Yamada, Horiguchi, Takeshita, and Okayasu 1990]. Corresponding to the absorption and emission spectra of the EDF [Miniscalco 1991; Giles and Desurvire 1991; Desurvire 1991], there is an absorption peak at 1530 nm within the lasing region.

As shown in figure 3-1, the absorption and gain cross-sections have almost the same magnitude. The gain is relatively strong when the wavelength is around 1.54  $\mu\text{m}$ .

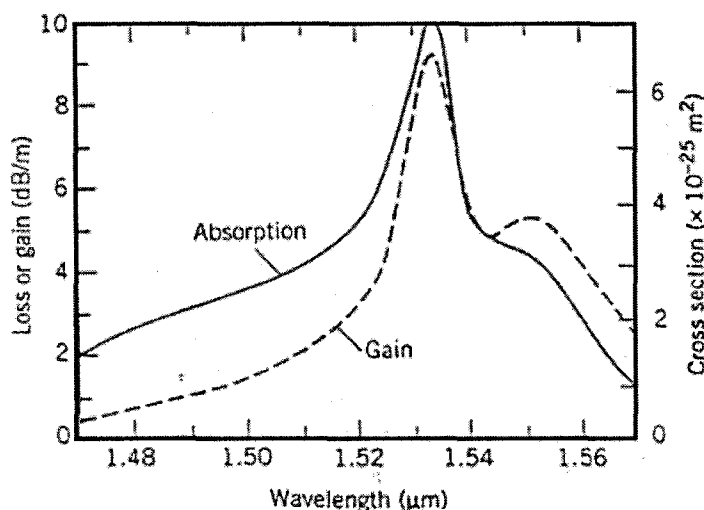


Figure 3-1 Absorption and gain spectra of an EDFA [Giles and Desurvire 1991]

The way to amplify the light is by using additional pump light at the shorter wavelength. In order to have maximum gain, the doped fiber should be saturated by the pump power, so that there is equilibrium between the steady state absorption and emission of photons. The signal light stimulates upper level ions to emit photons which are then amplified. If the pump power is not strong enough to saturate the absorption in the entire length of the doped fiber, the signal power is re-absorbed by the fiber at the far end and the signal amplification gain coefficient is decreased.

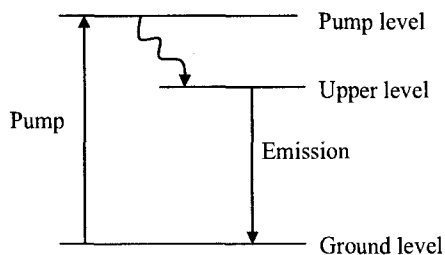


Figure 3-2 Schematic illustration of EDF pumping scheme.

The EDF can be described as a three-level system, as illustrated in figure 3-2 [Desurvire, Zyskind, and Simpson 1990; Desurvire, E. 2002]. With the pump light at 980 nm, erbium ions in doped fiber absorb photons and population inverts from ground

level  ${}^4I_{15/2}$  to the pump level  ${}^2I_{11/2}$ . The life-time of ions in pump level is relatively short being in the order of 1  $\mu$ s; the ions will quickly relax and decay to the upper level  ${}^4I_{13/2}$ . The relaxation process between the pump level  ${}^2I_{11/2}$  and upper level  ${}^4I_{13/2}$  is strongly dominated by fast non-radiative decay. At the upper level  ${}^4I_{13/2}$ , a characteristic fluorescence lifetime of the EDF is about 10 ms [Mita, Yoshida, Yagami, and Shionoya 1992]. Therefore, the erbium ions stay in the upper level  ${}^4I_{13/2}$  with very low relaxation emission, and are ready for stimulated emission. The transition from the upper level  ${}^4I_{13/2}$  to ground level  ${}^4I_{15/2}$  is almost 100% radiative at  $\sim 1.5$   $\mu$ m wavelength. The ions in the upper level  ${}^4I_{13/2}$  then return to the ground state with the emission of photons.

The EDF can also be pumped with light at a wavelength of 1490 nm. A quasi-two-level model is considered for analyzing this case. The optical pump does not pump the erbium ions to the pump energy level  ${}^4I_{11/2}$ , but only to the upper level  ${}^4I_{13/2}$ . The population inversion is between levels of the  ${}^4I_{13/2}$  and the  ${}^4I_{15/2}$ . As the population inversion caused by signals is also within the  ${}^4I_{13/2} - {}^4I_{15/2}$  band, it causes signal line-width broadening and saturation of the transition.

From studies it has been found that all the energy levels can be described by splitting the energy levels into the manifolds of sublevels with the Stark effect [Desurvire 1991]. The Stark splitting of the ground and upper excited states is about 250  $\text{cm}^{-1}$ , which is about 60 nm in wavelength. One general result is that site-to-site variation in the position of the energy levels is of the same order as the Stark splitting between adjacent levels, about 20  $\text{cm}^{-1}$  to 60  $\text{cm}^{-1}$ , (which is about 4 to 12 nm in wavelength), and it is temperature related. The total Stark width of  ${}^4I_{13/2}$  and  ${}^4I_{15/2}$  multiplets has been extrapolated to be in the order of 400  $\text{cm}^{-1}$  to 500  $\text{cm}^{-1}$  [Desurvire and Simpson 1990].

The energy levels are also approximately determined through an analysis of temperature dependence of absorption and emission spectra [Siegman, A.E. 1986]. At room temperature the spectra were found to be representative of a mostly homogeneously broadened line. At thermal equilibrium, the ratio between two adjacent sublevels populations is given by Boltzmann's law, i.e.  $\exp(\Delta E/kT) = 0.78$ , which indicates that a large thermal population exists within each manifold. As the non-radiative decay rate between adjacent energy levels decreases exponentially with the energy gap, intra-manifold relaxation is much smaller between sublevels than it is between main levels. For an EDFA, upper level ions are mostly from pump level instead of the diffusion from adjacent sublevels.

The studies on EDFA have been for high flat gain with low channel cross-talk. Spectral hole burning has an impact in WDM experiments as the strength of a given signal channel will impact the gain spectrum in nearby adjoining channels, in close enough channels, but not channels far removed in wavelength.

The EDF presents homogeneous and inhomogeneous saturation characteristics, determined by the material for fiber [Laming, Reekie, Morkel, and Payne 1989; Desurvire, Giles, and Simpson 1989; Richards, Jackel, and Ali 1998]. The appearance of homogeneous and inhomogeneous spectral hole burning effects at room temperature has been observed with high precision gain measurement [Desurvire, Zyskind, and Simpson 1990; Srivastava, Zyskind, Sulhoff, Evankow, and Mills 1996]. Note that the homogeneous hole line-width is observed to vary with wavelength. This can arise from the difference in non-radiative lifetimes among different Stark sublevels of a multiplet. This spectral hole burning is believed to be through saturation hole burning, which is caused by the change in the absorption in the doped fiber.

In an amplifier pumped at 980 or 1480 nm wavelength, spectral hole burning observed at 1550 nm depends on the host material [Joindot 1992; Sulhoff, Srivastava, Wolf, Sun, and Zyskind 1997; Desurvire, E. 2002], pump wavelength [Yadlowsky

1999], saturated signal wavelength [Rudkevich, Baney, Stimple, Derickson, and Wang 1999], and pump power [Bolshtyansky 2003]. The spectral holes in the 1530–1550 nm band have been reported to be about 1–2 dB in power and have a bandwidth of 3–10 nm. Spectral hole-burning has strong effect on main energy levels relaxation process, but not in the sublevels.

The mechanism of the EDFA is the energy transmission from the pump light to the signal light, due to the absorption and emission. As the lifetime of erbium ions in this upper level is long, the energy can be stored. The absorption of light is wavelength dependent, and the absorption is limited due to the finite number of rare earth ions in the fiber media; however, the rare earth ion number depends on the doping concentration and the fiber length and these can be chosen to suit a particular purpose.

### **3.2.1 Absorption Modification of EDF**

Pump light or signal light can cause the population of the ions to change their distribution. As the absorption changes, through the distribution of ions, the refractive index of the doped fiber is modified. It has been found that both the pump light [Betts, Tjugiarto, Xue, and Chu 1991; Fleming and Whitley 1996] and the signal wavelengths [Friskén 1992; Fischer, Zyskind, Sulhoff, and DiGiovanni 1993; Janos and Guy 1998] in the doped fiber can change the refractive index of the doped fiber. This is due to the large change in the upper-state population which can be achieved with moderate pump powers of a few milliwatts [Thirstrup, Shi, and Palsdottir 1996; Janos and Minasian 1997]. Experimental investigations have examined both pump-induced [Fleming and Whitley 1996] and signal induced [Janos and Guy 1998] refractive index changes. However, relatively small changes in refractive index are observed with similar changes in signal power due to the presence of both absorption and emission cross sections at the signal wavelength [Fleming and Whitley 1996; Janos and Guy 1998].

The analysis of the erbium doped glass system is based on an extension of the model studied deeply for EDFA [Desurvire 1990]. The Kramers–Krönig transform is known to accurately predict pump-induced changes in refractive index in erbium doped fiber amplifiers (EDFA) [Janos and Minasian 1997; Janos and Guy 1998]. Generally, the Kramers–Krönig relationship governs the induced changes in the refractive index and may be expressed as follows [Yariv, A. 1991]:

$$\chi'(\omega) = \frac{1}{\pi} P.V. \int_{-\infty}^{\infty} \frac{\chi''(\omega')}{\omega' - \omega} d\omega' \approx \frac{2}{\pi} P.V. \int_{\omega_1}^{\omega_2} \frac{\omega' \chi''(\omega')}{(\omega')^2 - \omega^2} d\omega' \quad (3-1)$$

where P.V. denotes the Cauchy principle value of the integral and  $\omega$  the angular frequency.  $\omega_1$  and  $\omega_2$  are defined as the frequency range in which the absorption changes are significant.

With the susceptibility  $|\chi(\omega)| \ll 1$ , the refractive index  $n(\omega)$  and absorption coefficient  $\alpha(\omega)$  are given by [Saleh, B.E.A. and Teich, M.C. 1991].

$$n(\omega) \approx n_0 + \frac{\chi'(\omega)}{2n_0} \quad (3-2)$$

$$\alpha(\omega) \approx -\frac{\omega}{n_0 c} \chi''(\omega) \quad (3-3)$$

where  $c$  is the speed of light in a vacuum. By substituting the derivatives of these equations (3-2),(3-3), changes in the absorption coefficient  $\Delta\alpha(\omega)$  may be related directly to changes in refractive index  $\Delta n(\omega)$  using [Yariv, A. 1991; Fleming and Whitley 1996]

$$\Delta n(\omega) \approx -\frac{c}{\pi} P.V. \int_{\omega_1}^{\omega_2} \frac{\Delta\alpha(\omega')}{(\omega')^2 - \omega^2} d\omega' \quad (3-4)$$

Consequently, the changes in the absorption  $\Delta\alpha(\omega)$  affect the refractive index  $\Delta n(\omega)$ .

This refractive index change depends on the absorption change within the absorption band. Therefore, it is wavelength dependent and also power related.

### 3.2.2 Doped fiber for lasers

There are two ways of building a doped fibre laser. One way is to build the laser with a normal laser followed by a doped fiber amplifier, as shown in figure 3.3[Ball and Glenn 1992; Knodl, Hanke, Saravanan, Peschke, Macaluso, and Stegmuller 2004; Yi Luo, Bing Xiong, Jian Wang, Pengfei Cai, and Changzheng Sun 2006]. In this case, short wavelength light is used to pump the ions to the levels higher than the upper emission level. A wave is selected to oscillate within the cavity by FBGs. The oscillating wavelength is in the emission region of the doped fiber. Thus, the doped fiber works exactly with the same principle as a gain media in a semiconductor laser.

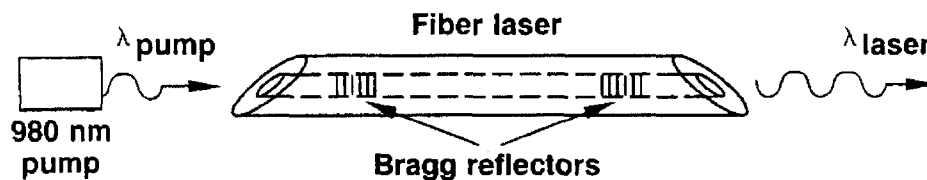


Figure 3-3, Doped fiber laser with two FBG

In a second scheme, shown in Figure 3-4, a doped fiber is placed with the laser diode in the same cavity, which is like the FGECL, but without an additional pump light or the grating. In this instance, the doped fiber acts as an absorber for the light emitted by the semiconductor. Only the oscillating wavelengths from the laser diode go through the doped fiber, composed of the main mode and side modes which are very close to the dominant lasing wavelength in the long cavity. In this case, the doped fiber simply works as an absorbing and bleachable medium.



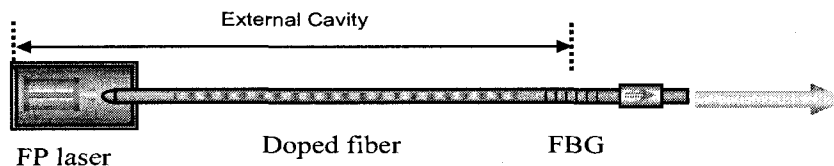


Figure 3-4, Doped fiber external cavity laser

Considering the energy level, as in figure 3-5, there is no normal pump light. The ions cannot be pumped to the pump level. Instead, they are pumped to the upper level by the light oscillating in the cavity is a two-level configuration. With the Fabry-Perot effect, the spectrum of the oscillating light is in a narrow wavelength region. The pumped ions are only distributed within a sublevel of the upper and the ground levels. Light emission is also stimulated by the intra-cavity flux. As the decay rate between adjacent energy levels decreases exponentially with the energy gap [Desurvire and Simpson 1990], the ion diffusion between the adjacent sublevels is very small, and they can be assumed as stay where they were pumped. Therefore, there is very small possibility for non-radiative decay of ions. The absorption feature of doped fiber without a short wavelength pump is different from the case of the EDFA.

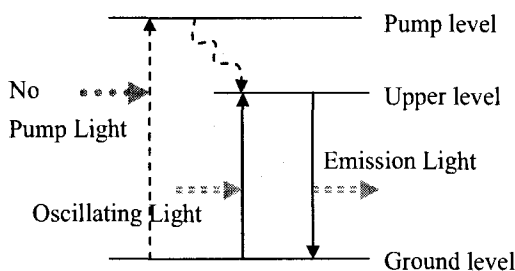


Figure 3-5 The doped fiber works as a two level system

As there is no pump light for the doped fiber external cavity laser, it is self pumped by the oscillating wave. This is a special situation of the doped fiber in laser applications. In the following sections, the performance of EDF in these circumstances is studied in detail.

### 3.3 Self pumped absorption of EDF

Without an extra pump the EDF absorbs the photons and attenuates the light. In the case of a laser composed of the semiconductor, the doped fiber and a FBG, the oscillating wave in the cavity may have a very narrow line-width. For doped fiber lasers without the extra pump, the light oscillating in the cavity lies within a narrow wavelength range due to the FBG's bandwidth.

As the oscillating waves might be at any wavelength within the absorption band, the bleaching of EDF absorption caused by one narrow line-width pump light is truly important for doped fiber study in external cavities.

According to the absorption and emission characteristics, illustrated by the energy level diagram, erbium doped fibre amplifier mostly works while pumping at shorter wavelength and the longer wavelength signal is amplified. Since for the doped fiber laser application, the light wave through the doped fiber is only at a single wavelength or just in a narrow spectral range, the different absorption performance of EDF should be studied for the case of inband pumping. The wavelength of the self-pumping light is in the absorption band of the EDF, from the edge to the middle of the band.

#### 3.3.1 EDF absorption bleaching

The first assumption for study is that only one wavelength is allowed to propagate through the EDF. In the 1.5  $\mu\text{m}$  (1480 nm – 1570 nm) wavelength region, the unsaturated EDF can both absorb photons and emit photons by stimulated emission. Since the absorption and stimulated emission cross-sections are in the same order of magnitude, it is not possible to distinguish between them. In this self pumped case, because the absorption and emission exist simultaneous, the EDF simply behaves as a net absorber, which is the difference between the absorption and the emission. The net

absorption can be experimentally measured by the power loss of the doped fiber with only one narrow line-width source light.

Figure 3-6 is the experimental setup for the self-pumped saturable absorption measurement. Since the absorption at  $1.5\ \mu\text{m}$  is strong, and narrow line-width laser at this wavelength was not very powerful, only a very short piece of EDF can be used, so that the highly doped fiber can be working in the unsaturated and saturated modes with the normal laser source. As both absorption and stimulated emission are wavelength dependent, this net absorption should be considered as wavelength dependent. A JDS SWS-15101 tuneable laser source was used for this self pumped absorption experiment. This source is a stable external cavity laser with a narrow line-width. The laser's full-width at half-maximum (FWHM) line-width was less than  $10\text{pm}$ . The tuneable wavelength was in the range of  $1480\text{nm} - 1540\text{nm}$ . The maximum output power of this JDS laser was less than  $10\ \text{dBm}$ . The output power was measured by an Anritsu ML-901 power meter. In order to have very low insertion loss and accurate reference data, the EDF was spliced to a single mode fiber (SMF). The splicing losses for the whole experiment were measured to be less than  $0.02\ \text{dB}$ . Besides fiber splicing, no reconnection was made during the experiment. As the wavelength change of any laser would cause an intensity change, causing a change in the spectral loss curve, an inline optical attenuator was applied in order to vary the optical power. This measurement was to examine the transmitted loss as a function of the output power in comparison with a doped fiber.

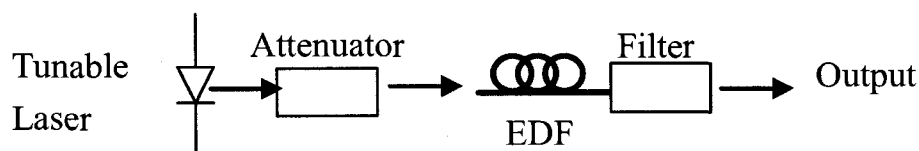


Figure 3-6 The setup for EDF absorption measurement

Theoretical and experimental studies have shown that the absorption of the EDF is proportional to the EDF length. In order to make sure that the absorption of the EDF can be saturated by the input light, only a short piece, 9.5cm long piece of the EDF was used (Liekki Er40-4/125 EDF was chosen for the experiment). This EDF is highly doped with erbium ions with the peak absorption of about 40 dB/m at ~1530nm wavelength, and is suitable for both 980 nm and 1480 nm wavelength pumping.

The results of these measurements are shown in Figure 3-7. The measured output is the net absorption. The input power was measured from the reference light power without the doped fiber inline. The absorption is therefore the power difference between the output power from doped fiber and reference fiber. Our experiments show that the unit length absorption for this fiber is independent of the section length of the fiber measured, which indicates a high degree of homogeneity of the doped fiber. The resulting absorption is in units of absorption. The peak unsaturated absorption is at around 1530nm wavelength, with an absorption of 42.5 dB/m. The EDF unsaturated absorption decreases when the input wavelength is away from the peak wavelength. At 1490 nm, the unsaturated net absorption is ~22.5 dB/m. For the whole wavelength range, the net absorption is positive, which means that without pump light, the doped fiber should first absorb photons, and then emit photons by stimulated emission.

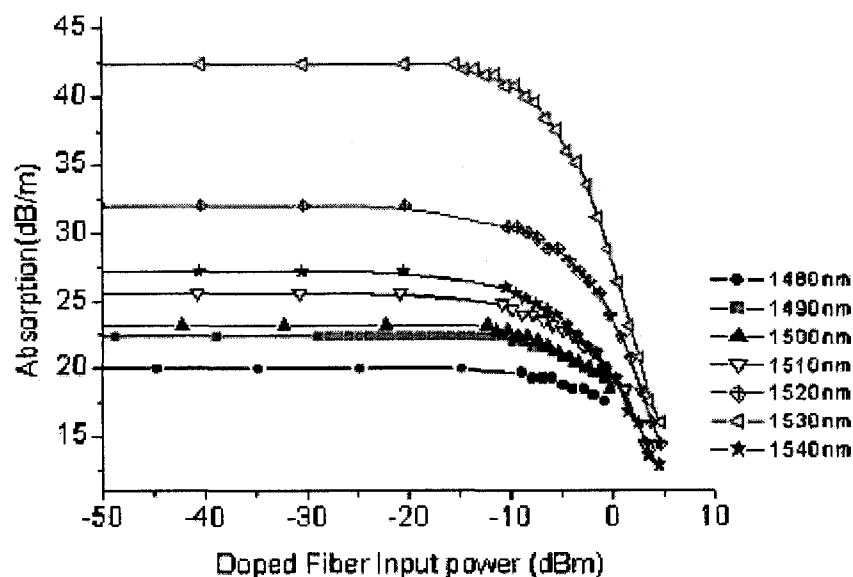


Figure 3-7 The net absorption of EDF measurement results

When input power is small, the fiber absorption is high and almost unchanged. The net absorption begins to decrease when the light power is increased above a certain threshold level. This is the effect of absorption bleaching. It is the result of part of the EDF absorption starting to be saturated. It can be seen in Fig 3-7 that the start of the bleaching point is around -15 dBm of input power. It is found that the unit length absorption bleaches drastically if the power is increased above this threshold. Other lengths of the same doped fiber were also measured with the same setup.

From this experimental result, we can conclude that in the whole absorption region, without the extra pump light, the EDF has net positive absorption. This absorption is wavelength dependent; the peak absorption wavelength is at  $\sim 1530$  nm, which is the best wavelength for the EDFA. The EDF is a saturable absorber. At any wavelength in the absorption region, a high power narrow line-width laser light can bleach the absorption of the EDF. The slope of this bleaching curve depends on the peak of the unpumped absorption and the pump wavelength.

### 3.3.2 Whole band absorption bleaching of the EDF

Considering the oscillating waves inside the external cavity might be multimode, when the EDF is pumped by a narrow line-width light, the effect on the absorption of an adjacent wavelength should be studied.

In the experiment the EDF absorption is measured with inband pumping and the setup is shown in figure 3-8. A pump laser is used in a counter-propagating direction to bleach the absorption, while the spectral insertion loss is measured in the forward direction using a low power tunable source. Data was recorded as a function of increasing pump power. The reflection from the pump light was found to be low enough so as not to affect the loss measurements.

One counter-propagating narrow line-width DFB laser light was coupled to the EDF; the pump power is strong enough to bleach the absorption of the piece of EDF used, so that probe light did not affect the ion population. An optical isolator was used at the output of probe source; in case of the pump source should affect the measurement at the probe wavelength. The isolator has more than 30 dB isolation, so that the changing of the pump light does not affect the probe light, and neither does the pump light reflect into the power meter. At the other end of the optical coupler, an index-matching gel was used to eliminate spurious reflections. The reflection from this end was 40 dB below the pump power. In order to ensure that the wavelength of the pump laser did not change, the power of the pump laser was decreased by changing an in-line attenuator, rather than changing the drive current.

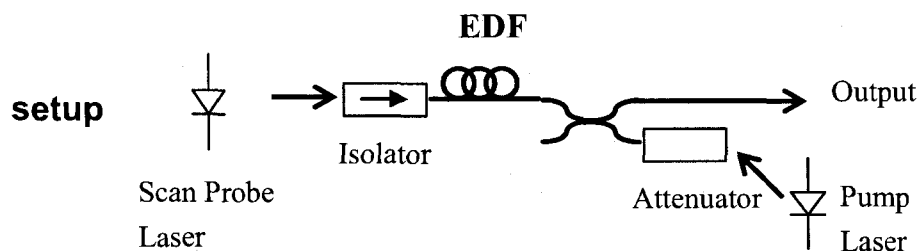


Figure 3-8 Experiment set up for inband pump absorption measurement

A 46cm long piece of EDF was used as the absorber. This EDF under test had the peak net absorption of about  $-21.6$  dB, at  $1528.7\text{nm}$  with  $47\text{dB/m}$ . A stable, narrow line-width source ( $\text{FWHM} < 3$  pm, amplitude fluctuation  $< 0.1\text{dBm}$ ) was used as a pump laser. A JDSU tunable laser in the  $1520\text{-}1570$  nm wavelength range was used to measure the absorption at each wavelength. The maximum power of the probe laser was kept deliberately very low ( $-30$  dB in comparison to the pump laser), so that the ion populations in the ground and upper states are not substantially altered by this probe laser. The resolutions of the measurement were  $\pm 1.5$  pm in wavelength and  $\pm 0.05$  dBm in power, respectively. The probe laser was scanned and the absorption spectrum measured across the whole band with and without the EDF. With the pump laser coupled to the same EDF, the absorption was re-measured at each wavelength within the absorption bandwidth of the EDF. The difference between pumped and unpumped absorption gives the bleached spectrum.

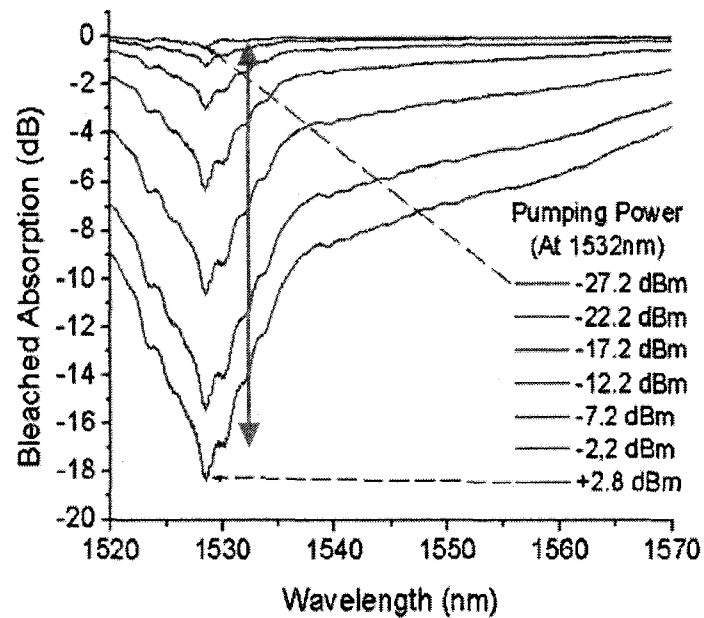


Figure 3-9 The bleaching spectrum of EDF with pumping at 1532 nm

When the pump laser wavelength at 1532 nm, where the net absorption of the EDF is  $\sim 36.5$  dB/m, the absorption is about 16.8 dB for this length of EDF. It was found that whole band (1520-1570) absorption spectrum was bleached by the narrow line-width pumping power, as shown in figure 3-9. When the pump power was changed by the attenuator, the absorption changed as well. When a 2.8 dBm power pump was used, the absorption was bleached by a maximum of about 19 dB at the absorption peak, at 1528.7 nm. Unlike an optical amplifier, bleaching also occurs at wavelengths shorter than the pump wavelength, which indicates that the ion populations are substantially affected by the pump photons.



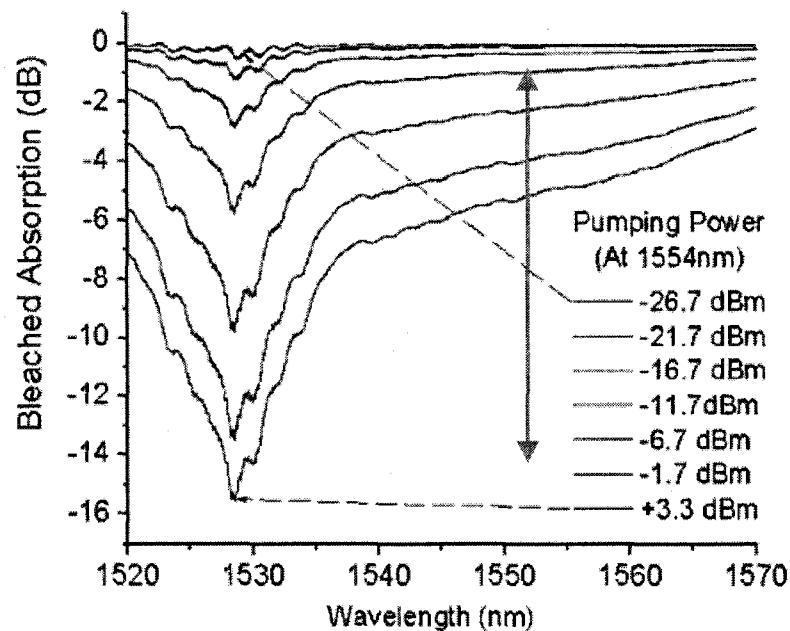


Figure 3-10: The bleaching spectrum of EDF with pumping at 1554nm

In the second experiment, the pump wavelength was moved to 1554nm, where the net unpumped absorption of the EDF was 14 dB/m; the absorption was about  $-6.4$  dB for this EDF. With a 3.3 dBm pump power, the absorption was bleached by about 16 dB at the absorption peak of 1528.7 nm. As shown in figure 3-10, compared to the case of the 1532 nm pump, the bleached absorption spectrum is similar in outline. Notice when the EDF was pumped at a wavelength with low net absorption (1554 nm), the largest change in absorption occurs at 1528.7 nm, where the unpumped absorption is highest. Since the EDF is considered to be spatially (axially) homogeneous, all pump photons have an equal probability to be absorbed [Desurvire, Zyskind, and Simpson 1990; Sulhoff, Srivastava, Wolf, Sun, and Zyskind 1997]. However, the absorption-rate is related to the difference between absorption and emission cross-sections at the pump wavelength. When an EDF is pumped with a narrow-line-width source, the absorption of photons is determined by the frequency dependence of absorption and emission rates at the pump wavelength. This causes less number of ions to be available for absorbing at other wavelengths outside of the pump wavelength resulting in a broadband saturable absorber.

A narrow line-width pump can only pump the erbium ions up to a very narrow energy band. Since the non radiative decay of ions between the adjacent sublevels is very low, no transfer takes place by ion diffusion. If the EDF is pumped with mW powers with a narrow-line-width source, there are more than enough photons to pump all the ions. This absorption bleaching occurs for all photons within the band, regardless of the wavelength. As none or only a small number of ions are left for other wavelength photons, the light can go through almost transparently. The results illustrate that the EDF is spatially homogeneous; all pump photons have the probability to be absorbed. The absorption-rate is related to the difference between the absorption and emission cross sections at the pump wavelength. Therefore, the photon absorption depends on its numbers and absorption-emission rate at a particular wavelength.

Pumping at other wavelengths within the absorption band was also tried; the results showed only minor differences. It is clear from the above experiments that by changing the inband pump power one can alter absorption to the all other wavelengths.

Although spectral hole burning is found in EDFA applications, we specifically did not see any evidence of spectral hole-burning close to the pump-wavelengths in our measurements. We tried to observe the occurrence of spectral hole-burning in our setup. In our experiments with a narrow line-width inband-pump the absorption of the EDF and the stimulated emission are at the same wavelength. The ions should be excited to a very narrow band of the upper level and almost no non-radiative (no scattering) transitions should occur within this band.

Studying the inband pumped absorption spectrum helps to find out the effect of the absorption in the vicinity of the pump spectrum, and can help to improve the performance of the external cavity laser. This is the modulation effect in the EDF absorption, which means the change of dominant wavelength light can change the whole band absorption, and thus change the output power at the other wavelength within the band. The wide-band nature of saturable absorption in doped fibers plays a significant

role in creating new devices such as single frequency lasers tunable over entire absorption spectrum of the doped fiber. The wave with the strongest intensity causes the ion population to change significantly. If the power is high enough, absorption bleaching suppress the absorption of other non dominant waves.

### 3.4 Doped fiber laser

Doped fiber laser is another main application for rare earth doped fiber. The biggest advantage of doped fiber lasers is that they are compatible with optical fiber systems and can be easily integrated with other fiber components, such as WDM couplers and fiber isolators. A doped fiber can be placed inside an external cavity, which is built between FBG or between FBG and laser diode [Kashyap, Armitage, Wyatt, Davey, and Williams 1990; Ball, G.A. and Morey, W.W. 1992; Mizrahi, DiGiovanni, Atkins, Grubb, Park, and Delavaux 1993; Guy, Taylor, and Kashyap 1995; Pan and Yuan Shi 1995; Loh, Laming, Zervas, Farries, and Koren 1995b; Timofeev and Kashyap 2003]. Doped fiber lasers can be structured as pumped oscillators, with the principals of rare earth doped fiber optical amplifiers and FP cavity lasers. An EDF laser with 300 mW power at a wavelength of 1537.5nm was reported [Kashyap, Armitage, Wyatt, Davey, and Williams 1990]. Since it is pumped as an optical amplifier, it can be made as a high power laser. Composite fiber grating with ring laser or loop mirror cavity are other possible configurations [Guy, Taylor, and Kashyap 1995; Pan and Yuan Shi 1995], and single frequency operation was demonstrated with an intracavity frequency selector. Tests performed on an externally modulated single frequency erbium doped laser have confirmed its robust stability for error free high speed application in transmission systems [Mizrahi, DiGiovanni, Atkins, Grubb, Park, and Delavaux 1993].

The waves oscillating inside the cavity should satisfy the phase condition, following the FP principle. The mode spacing is decided by  $c/(2nL)$ . If the bandwidth of the laser spectrum is greater than the mode spacing, more than one mode can oscillate in the

cavity. If the external mirror of fiber laser is a FBG, all the oscillating modes remain within the bandwidth of the FBG.

The simplest solution for fabricating a doped fiber grating laser is by a semiconductor laser diode and a narrow bandwidth FBG. The other end of the cavity is the rear facet of the semiconductor laser. This type of short cavity laser provides a very narrow line-width as well as a high degree of wavelength stability, and may be directly modulated [Loh, Laming, Zervas, Farries, and Koren 1995b; Timofeev and Kashyap 2003].

### 3.4.1 Doped Fiber External Cavity Laser (DFECL)

DFECL has similar structure as the FGECL. The difference is that there is a saturable absorber in the form of a piece of doped fiber inside the cavity. In this case, the semiconductor chip has an anti-reflection (AR) coating on the front facet, as shown in figure 3-11. The main cavity is formed between the rear facet of laser chip and the FBG. The oscillating wave is injected into the laser gain media. The lasing wavelength depends on the reflection wavelength of the FBG, as in the FGECL. The doped fiber works in the self-pumped regime; i.e. the doped fiber is pumped by the lasing wavelengths within the cavity.

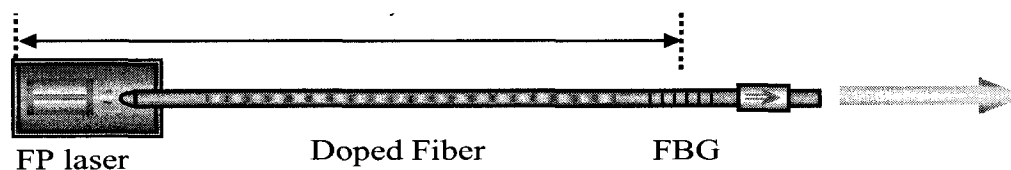


Figure 3-11 Schematic of the external cavity semiconductor laser

An erbium DFECL at 1535 nm was built with a 3 meter long cavity and it was reported to have a line-width of  $\sim 1$  kHz [Loh, Laming, Zervas, Farries, and Koren 1995b]. The DFECL can also be made as high power laser. High power stable operation of a DFECL was reported at 980 nm with an Ytterbium-doped fiber [Timofeev and Kashyap 2003].

In an optical amplifier, the doped fiber has traveling waves. The pumping wave and signal waves propagate through the doped fiber. The pumping power is always strong at the input end, and becomes weaker along the transmission direction through the doped fiber as the light is absorbed by the doped fiber. The remnant pump appears at the output. If the doped fiber absorption is not saturated, the signal waves can be absorbed by the doped fiber, and the gain is reduced. Therefore, to have large signal gain, one can increase the pump power with a longer piece of the doped fiber.

DFECL, on the other hand, works with standing wave in an external cavity. Spatial hole-burning has a strong effect on the laser's performance.

### 3.4.2 Spatial Hole Burning

Figure 3-12 shows a schematic of the DFECL with two counter propagating beams in the laser cavity. When two waves at the same frequency traveling in opposite directions are simultaneously present in a laser media, interference between these two waves produces both frequency beating and standing wave patterns in the optical intensity [Siegman, A.E. 1986].

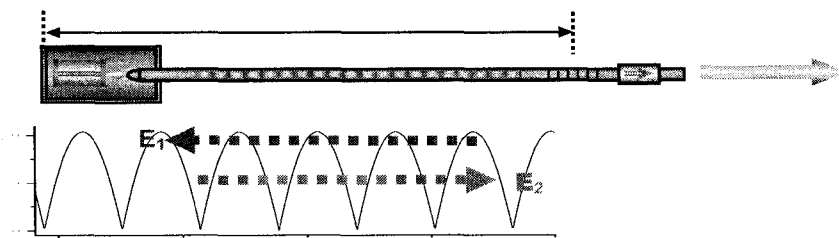


Figure 3-12 Schematic Waves in DFECL

These interference effects in turn may produce both temporal modulation and spatial variation in the amount of saturation in the laser media. The electric fields are described as:

$$E(z, t) = E_1(z, t) + E_2(z, t) = \text{Re}[\tilde{E}_1(z)e^{j(\omega_1 t - \beta_1 z)} + \tilde{E}_2(z)e^{j(\omega_2 t - \beta_2 z)}] \quad (3-5)$$

The optical intensity at any point  $z$  and any time  $t$  can be written

$$I(z, t) \propto |\tilde{E}(z, t)|^2 = |\tilde{E}_1(z, t)|^2 + |\tilde{E}_2(z, t)|^2 + 2\tilde{E}_1^*(z)\tilde{E}_2(z)e^{j[(\omega_1 - \omega_2)t - (\beta_1 - \beta_2)z]} + c.c. \quad (3-6)$$

as the standing wave pattern is in intensity, it induces spatial hole-burning, which can modify the saturation behavior of each wave independently, as well as induce a refractive or absorption grating. This absorption grating can couple the two initially independent waves to each other. The intensity distribution along the length of the cavity in the case of this type of interference is:

$$I(z) = I_1(z) + I_2(z) + 2\sqrt{I_1 I_2} \cos[(\beta_1 - \beta_2)z + \phi] \quad (3-7)$$

Where  $I_1$  and  $I_2$  are the intensities of the two waves, respectively, and sinusoidal standing wave portion has a spatial phase angle  $\phi$  related to the relative phases of the two E fields. In a homogeneously broadened saturable atomic media, the intensity pattern forms relative population saturation. It will presumably produce a spatially varying saturation of the form

$$\frac{\Delta N(z)}{\Delta N_0} = \frac{1}{1 + I(z)/I_{sat}} = \frac{1}{1 + [I_1 + I_2 + 2\sqrt{I_1 I_2} \cos(\Delta\beta z)]/I_{sat}} \quad (3-8)$$

Where,  $\Delta N(z)$  is the difference in the population of saturable absorbers in the longitudinal direction. For the gain media,  $\Delta N_0$  is an unsaturated population inversion value,  $I_{sat}$  is the saturation intensity. Therefore, the intensity distribution causes a refractive index change in the doped fiber. The periodical change in the population due to the standing wave modulates the ion-population and gives rise to spatial hole-burning and hence a spatially periodic modulation in the refractive index [Kostko and Kashyap 2004].

$$\Delta n_{12}(I) = \frac{c}{\pi} \frac{\alpha_H}{4f} (\Delta N_1 - \Delta N_2) \quad (3-9)$$

The population difference causes the refractive index change. Where,  $\alpha_H = \Delta n' / \Delta n''$  is the Henry factor [Henry 1982],  $c$  is the light velocity in free space and  $f$  is the wave frequency.  $\Delta N_1$  and  $\Delta N_2$  are population difference for different intensity saturation. This can be used to calculate difference between maximum and minimum saturation. The difference in population causes the refractive index change.

### 3.4.3 Dynamic Grating

In a laser with a doped fiber in the external cavity, high power at the resonant wavelength causes absorption bleaching in the doped fiber. As we have seen a narrow line-width pump can bleach the absorption over the whole band. When a standing wave is formed in a semiconductor external-cavity laser with a saturable absorber and external fiber grating mirror, the modulation in the ion-population gives rise to spatial hole-burning and hence a spatially periodic modulation in refractive index, causing a dynamic grating to form via the Kramers-Krönig effect. The reflectivity of this Bragg grating increases with the intra-cavity power that forms the longitudinal modulation of absorption. Since no obvious spectral hole-burning was found in the vicinity of the pump wavelength, the broadband absorption bleaching, and therefore spatial hole-burning is the key reason for line-width narrowing and stabilization of the wavelength of the DFECL.

For the saturable absorber, doped fiber absorption can be saturated by pumping with narrow line-width light and thus change the absorption of the entire band. The absorption change causes the refractive index change, but it is also related to the wavelength [Kostko and Kashyap 2004] of observation. In the external cavity, the power spatially distributes with the pattern of standing wave. As discussed before, the distribution in the standing wave power causes both spatial hole-burning and absorption

modulation, thus changing the refractive index locally. Therefore, a dynamic grating is formed with the same pattern as the standing waves. The coupling constant of an induced dynamic grating in the external cavity laser can be estimated from the refractive index change  $\Delta n$  in the doped fiber [Kostko and Kashyap 2004]:

$$\kappa = \frac{2\Delta n}{n\lambda} \quad (3-10)$$

Here  $\Delta n$  is the change in the refractive index of the doped fiber and  $\lambda$  is the central wavelength of the dynamic grating. The shape of the reflectivity spectrum of a dynamic grating is defined by the coupling factor and the length,  $L$  of the EDF. The maximum reflectivity of the grating may be calculated as [Kashyap, R. 1999]:

$$R = \tanh^2(\kappa L) \quad (3-11)$$

Therefore the reflectivity is related to the ratio of the standing wave intensity, and the length of the dynamic grating in the doped fiber.

When many waves are oscillating in the cavity, a dominant wave will have the strongest amplitude and be absorbed by the doped fiber, reaching saturation faster than the other modes. Thus, it causes the deepest refractive index modulation, and forms the strongest dynamic grating. The peak wavelength of the dynamic grating is determined by the dominant standing wave period. As the strongest dynamic grating is at the dominant wave, it will suppress the other waves. Also, as the doped fiber has inband bleaching characteristics, the absorption of other waves can be bleached by the dominant standing wave. The procedure continues to setup the dynamic grating until it reaches an equilibrium state, leading other modes suppression.

According to the energy level system, Erbium ions in the doped fiber have a very long lifetime in the upper level, mainly due to the slow radiative emission process. Therefore, the dynamic grating of doped fiber has a relatively long decay time. As soon as the dynamic grating is setup, any fast wavelength fluctuation cannot influence the



dynamic grating. This mechanism leads to the elimination of wavelength fluctuation and thus stabilizes the operating wavelength. As long as a dominant wave is strong enough to setup up the dynamic grating, the wavelength of operation can be anywhere within the bandwidth of the external FBG.

The setup time of dynamic grating is also related to the initial dominant ratio, which is considered as the ratio between the magnitude of the dominant mode and the first side mode. When the dominant wave is at the center of FBG bandwidth, the peak reflectivity would make the main mode wave much stronger than other side modes, thus it has greatest initial dominant ratio. This would allow the dominant wave to setup easily in a short time. If the dominant wave is at the edge wavelength of the FBG bandwidth, it is difficult to setup the dominant wave, or it may even not setup.

The refractive index change can be derived with the self-organized dynamic grating model [Kostko and Kashyap 2004]. From the previous measurement, we can extrapolate the spectra of absorption bleaching in order to calculate the spectrum of the change in refractive index due to pumping using the Kramers-Krönig relations. The spectra of the refractive index change at low-power ( $\sim -27$  dBm) and high-power ( $\sim 3$  dBm) pumping at 1532 nm and 1554 nm are shown in Figure 3-13. When the pump power is low ( $\sim -27$  dBm) and the EDF is pumped at 1532 nm, the refractive index change is  $\Delta n \sim 3 \times 10^{-8}$ , and  $\Delta n \sim 1.4 \times 10^{-8}$  at 1554 nm when the EDF is pumped at the same wavelength. When the EDF is pumped at 1554 nm, bleaching of absorption is still higher at the peak of the absorption spectrum (1528 nm), rather than at the wavelength of pumping.

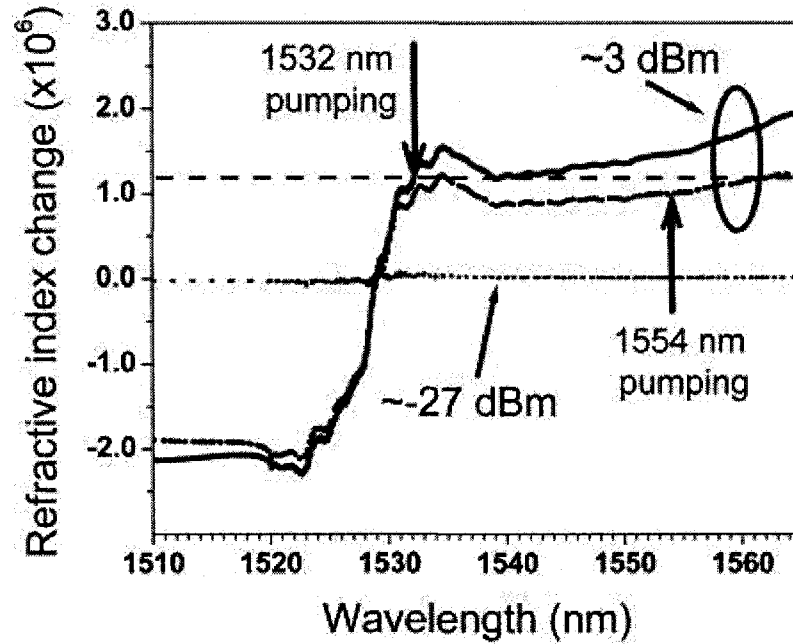


Figure 3-13. The spectra of refractive index change of the EDF at pump wavelengths of 1532 nm and 1554 nm at pump powers of 2.7 dBm and 3.3 dBm, respectively. Dotted line shows spectrum of the refractive index change at -27 dBm pump

When the fiber is pumped with +2.8 dBm of a narrow-line-width power at 1532 nm, the change in the refractive index at the same wavelength is almost two orders of magnitude larger,  $\Delta n \sim 1.2 \times 10^{-6}$ ; and  $\Delta n \sim 0.98 \times 10^{-6}$  when the EDF is pumped by 3.3 dBm at 1554 nm. For higher pump powers, e.g. 100 mW, the maximum possible change in absorption at 1532 nm may be an additional  $\sim 6$  dB/m, when the system is completely bleached and the population difference is saturated at high pump power. Thus the refractive index change may be estimated by multiplying its value at 2.8 dBm pump power by 1.16. Therefore, if the fiber is pumped with 100 mW at a wavelength of 1532 nm a maximum refractive index change of  $1.4 \times 10^{-6}$  may be expected at this wavelength.

The peak-to-trough pumped-unpumped change in refractive index is  $3.76 \times 10^{-6}$ , when pumped at 1532 nm and  $3.3 \times 10^{-6}$  when pumped at 1554 nm. This value is an

order of magnitude higher than that previously reported for the three-level system in EDF amplifier [Fleming and Whitley 1996]. Normalized to the peak absorption coefficient of 47 dB/m, this gives a general value relating the pumped-unpumped refractive index change to the pumped-unpumped change in transmission in the EDF of  $8.0 \times 10^{-8}$ , which is close to the value, obtained in [Fleming and Whitley 1996].

A coupling constant of an induced grating in the external cavity laser can be estimated from the refractive index change  $\Delta n$ , with a refractive index of the doped fiber ( $n \sim 1.45$ ). Hence, an EDF with an induced refractive index change of  $\Delta n \sim 1.4 \times 10^{-6}$  at  $\lambda = 1532$  nm has a dynamic grating with the coupling constant of  $\kappa \sim 1.26$ . A dynamic grating with a smaller coupling constant of  $\kappa \sim 0.887$  is formed at 1554 nm when an induced refractive index change is  $\Delta n \sim 1.0 \times 10^{-6}$ . Therefore, a coupling constant of a dynamic grating is higher at 1532 nm than at 1554 nm.

As the reflectivity of the grating depends on a product of  $\kappa L$  according to the equation 3-12, it can be maximized by increasing either the length or the coupling factor of the EDF. For example, a grating with  $\kappa \sim 1.26$  (at  $\lambda \sim 1532$  nm) and  $L = 0.50$  m has the same reflectivity  $R \sim 30\%$  as a grating with  $\kappa \sim 0.87$  ( $\lambda \sim 1554$  nm) and  $L \sim 0.73$  m. Therefore, by optimization of the pump wavelength, the doped fiber section of a laser may be designed shorter by 23 cm and have the same reflectivity as a grating with  $\kappa \sim 0.87$ . The peak of the refractive index change in Figure 3-11 gives the maximum coupling factor of the dynamic grating and thus is the optimal pump wavelength for the EDF. In a laser with a saturable absorber in the external cavity this is an optimal central wavelength of an external fiber Bragg grating of the laser.

### 3.5 Conclusion

In the case of the external cavity laser, the doped fiber function is distinctly different to that in an EDFA, as there is no extra pump light. The cavity oscillating waves can be considered as self pumping light or in-band light for the doped fiber.

The experiments studied in this chapter show the characteristics of the doped fiber in the case of self-pump and in-band pump. Although the doped fiber absorbs light within its absorption bandwidth, the result has shown that high power narrow line-width can cause a piece of doped fiber absorption to bleach. High power light can go through the doped fiber with very little power loss. The in-band pump experiment has shown that a narrow line-width pump can cause whole band absorption bleaching. Even if the pump wavelength is in the long wavelength region, where the absorption is relatively low, it bleaches the absorption at the peak absorption wavelength.

The characteristic indicates that any local optical intensity change modifies the absorption over whole bandwidth, and therefore changes the transmission of other wavelengths in the band. This is an extremely important feature for the application of the doped fiber in the external cavity laser. The wavelength with the highest intensity bleaches its own absorption and generating a standing wave in the external cavity.

A derivation also presented the possibility of refractive index change if this doped fiber is placed in a fiber external cavity laser. The refractive index change forms a dynamic grating in the doped fiber, and this is the mechanism which leads to an increased reflectivity and thus narrowing of the line-width and stabilises the wavelength in this laser. The next chapter discusses how this grating enhances the coherence, the stability, and tunability of the laser.

## CHAPTER 4      NARROW LINE-WIDTH AND STABILITY OF DFECL

### 4.1 Introduction

Narrow line-width and stable wavelength are important features for laser sources used for applications in wavelength division multiplexing (WDM), optical metrology, spectroscopy, and microwave photonics [Simonis and Purchase 1990; Campbell, Armitage, Sherlock, Williams, Payne, Robertson et al. 1996; Hashimoto, Takagi, Kato, Sasaki, Shigehara, Murashima et al. 2003; Wake and Beacham 2004]. In ROF applications, the transmission performance of direct modulation and optical microwave generation depend largely on the laser source, but good laser sources also benefit from external modulation.

Basically, a narrow line-width source has low phase noise, while a stable laser source provides low intensity and frequency noise. Several approaches can be used to have narrow line-width lasers. Extending the cavity length is one way to narrow the line-width. Early works showed that there was a benefit in line narrowing from the line-width enhancement factor of long external cavities [Henry and Kazarinov 1986; Kazarinov and Henry 1987; Olsson, Henry, Kazarinov, Lee, and Johnson 1987; Kashyap, Armitage, Wyatt, Davey, and Williams 1990; Bird, Armitage, Kashyap, Fatah, and Cameron 1991]. The laser line-width narrows approximately as the square of the length of the cavity [Kashyap, Armitage, Wyatt, Davey, and Williams 1990]. With the lengthening of the cavity, the oscillating mode spacing is also reduced. This has a strong influence and reduces the side mode suppression ratio.

As seen already, another way to narrow the line-width is to use a wavelength selective reflector. A Bragg grating is most commonly used element as the external reflector, because the reflectivity of the external grating is wavelength dependent and can be made arbitrarily small. The ideal situation is to have the reflection bandwidth

smaller than the mode spacing, and not in the coherence collapse state [Jones, Spencer, Lawrence, and Kane 2001; Timofeev and Kashyap 2003], so that only one mode can oscillate in the cavity.

Previous studies have shown that due to absorption modulation and absorption bleaching, a dynamic grating can be formed in a doped fiber within an external cavity. As the dynamic grating follows the pattern of the standing wave, a uniform grating has the same period as the standing wave. Also, a doped fiber can be made long with the consequence that the line-width of the dynamic grating is narrowed.

In this chapter, a new DFECL fabrication will be presented, which is operating at edge wavelength of the EDF's absorption bandwidth. The stability and line-width of these new lasers are demonstrated by experiments. The experimental results of the laser are also analyzed and compared with simulations of dynamic operation.

## 4.2 Doped Fiber External Cavity Laser

The structure of the DFECL is shown in Figure 4-1. The external cavity is formed by an FBG and a semiconductor laser with an anti-reflective front facet. A length of rare earth doped fiber is inside the external cavity. The cavity length is thus greater than 100 times larger than a semiconductor laser chip. As the EDF inside the cavity does not affect the FBG at the end of cavity, the DFECL initially works on the basis of FGECL.

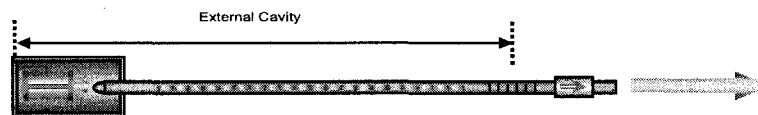


Figure 4-1 Schematic of the external cavity semiconductor laser

In the external cavity, the interference of waves from opposite directions forms a standing wave with the intensity spatially modulated along the fiber. Since the optical length of the laser diode gain material is much shorter than the optical length of the EDF,

and the laser diode is only at one end of the cavity, the length of the standing wave in the semiconductor chip is only a small fraction of the total length of the cavity.

The standing wave modulates the intensity distribution along the fiber. As a saturable absorber, the doped fiber absorption can be saturated by the intensity of all the lines (longitudinal modes) oscillating in the cavity, and thus change the absorption of the entire band. The absorption change modifies the refractive index via the Kramers-Krönig effect [Fleming and Whitley 1996; Kostko and Kashyap 2006], which forms several dynamic gratings. Because of the long lifetime of erbium ions in the up energy level, the dynamic gratings are also long lived. As the energy builds up in each mode within the cavity, a gain competition begins, and the energy is exchanged between the modes, suppressing all but the strongest modes. Finally, a dominant mode succeeds in suppressing all other oscillating modes. This slow response of the dynamic grating dampens fast fluctuations and stabilizes the laser.

In the external cavity, the power distributes spatially with the pattern of standing wave. Therefore, a dynamic grating is formed with same pattern as the standing waves. For analysis, the dynamic grating can be assumed as a uniform grating.

Therefore the reflectivity is related to the ratio of the standing wave intensity, and the length of the dynamic grating in the doped fiber.

The mode spacing between the modes oscillating in the cavity is defined as

$$\Delta\lambda_{MS} = \frac{\lambda^2}{2nL} \quad (4-1)$$

For a single mode laser, the bandwidth is exactly equal to the line-width of mode. Otherwise, the bandwidth of the laser light is related to the mode spacing, mode number  $N$  and the mode line-width  $\Delta\lambda_{mod}$ .

$$\Delta\lambda_{ECL} = (N - 1)\Delta\lambda_{MS} + \Delta\lambda_{mod} \quad (4-2)$$

Since the resonant modes inside the external cavity are selected by the FBG, for a short cavity laser, the FBG can easily remove the side modes with the mode spacing larger than the bandwidth of FBG. In order to reduce the line-width, the cavity length should not be very short. If the mode spacing is smaller than the bandwidth of the FBG, several modes may exist.

The bandwidth of an FBG depends on its length, and a long uniform FBG is not easy to fabricate. Generally, a FBG with a bandwidth of 5 pm at 1490 nm is possible only when the length of the grating is  $\sim 31$  cm. These gratings are too long to be written with the conventional fiber Bragg grating writing techniques and are cumbersome to use [Kashyap, R. 1999].

However, the dynamic grating has two aspects, a narrow bandwidth because it is long, and a peak reflectivity which is a function of  $\kappa L$ . The doped fiber dynamic grating is determined by the standing wave, so it is considered to be uniform, and it may be easily made longer than 10 cm, and therefore it is possible to induce a dynamic grating with a bandwidth of several picometers. The bandwidth of the dynamic grating can thus be much narrower than a short UV written FBG. Furthermore, with a longer doped fiber, the reflectivity of the dynamic grating increases, this may increase the finesse of the FP cavity, and thus narrow the line-width of the longitudinal mode. The wavelength of the maximum of the reflectivity spectrum of the refractive index dynamic grating corresponds to the maximum of the oscillating spectrum inside the cavity. As the dynamic grating has even narrower bandwidth than FBG, it provides extra gain to the oscillating waves inside the external cavity.

### **4.3 Design and Fabrication of New DFECL**

The first experimental report of doped fiber external cavity laser was in 1995 [Loh, Laming, Zervas, Farries, and Koren 1995a]. The DFECL was built at 1535 nm wavelength. The FBG had 80% reflectivity with 0.2 nm reflective bandwidth. About 3



meter long erbium doped fiber was used in the external cavity. The fiber with tapered lens couples directly to the laser diode. The measured full width half magnitude (FWHM) line-width was reported as about 1 kHz, although this was based on a self-heterodyne measurement technique. A DFECL was reported with high power, ultra-stable wavelength [Timofeev and Kashyap 2003] with ytterbium doped fiber in 2003. This DFECL operated at a wavelength of 980 nm. The length of doped fiber was 63 cm. The FBG for this laser had a reflectivity of 80% with a bandwidth of 0.2 nm. The output power of this DFECL was as high as 250 mW. The wavelength fluctuation was reported to be better than 0.05 nm over more than 2.5 hours.

The reported erbium DFECL operated at 1535 nm wavelength, which is the best wavelength for EDF absorption and emission. The reported ytterbium DFECL operated at 980nm wavelength; it is also the best wavelength for ytterbium doped fiber. As analyzed in chapter 3, at the absorption peak, the absorption modulation is at a maximum and so is the refractive index change, therefore, the dynamic grating is in its best operating point.

Currently the 1.5 micron wavelength region is the best window for fiber optic communication systems. It would useful if the DFECL were to operate within the whole bandwidth of this window, and perhaps even outside of this window (1530-1565nm). A new DFECL was chosen to work outside of the EDF peak absorption wavelength. The problem here is that at the edge of the absorption region, the absorption and emission rates of the EDF are much lower than they are at the peak. The advantage of this wavelength is that a high power semiconductor pump laser can be used.

The new DFECLs were designed to work at a wavelength of 1490 nm. The laser diode for DFECLs was a FP semiconductor laser with an anti-reflection coated front facet. The laser diode was a pump laser for an optical amplifier. The wavelength spectrum of the FP semiconductor lasers was very broad with a bandwidth of about 50 nm, wavelength from 1450 nm to 1500 nm. Its total output power was more than 20

dBm, but the peak power was only about -10dBm. At a wavelength of 1490 nm, the light intensity of the FP laser was less than -20 dBm.

The FBGs to form the external cavity mirror were fabricated in our lab and designed to have a narrow bandwidth. The peak wavelength was at ~1490 nm with the reflective bandwidth about 0.2 nm. The reflectivity of the FBG was chosen in the range of 75% to 80%.

A CorActive EDF used for DFECL has the absorption characteristics as Figure 4-2, which was measured with the method described in Chapter 3. Measurements were performed for this EDF with a narrow-line-width light pump at different power levels, and the spectra were recorded. The peak net absorption is at 1528nm wavelength. The maximum absorption at 1490 nm was ~ 16 dB/m (Figure. 4-2a) with small pump power (less than -20 dBm). When the pump power is increased to over -15dBm, the absorption begins to bleach. The absorption reduced to ~5dB/m with 5 dBm of input power, and the absorption may reduce to even lower values with a higher power. Pumping with narrow-line-width light bleaches the whole absorption bandwidth of the EDF. The maximum bleaching of absorption was 30dB/m, which is at the peak of the absorption spectrum at 1528 nm (Figure. 4-2b). This figure shows that the absorption may be bleached by ~ 15 dB/m at 1490 nm, when the pump power is ~ 6.7 dBm. From the Kramers-Krönig relations, the induced refractive index change at 1490 nm is calculated to be as  $\Delta n \sim 1.68 \times 10^{-6}$ . Assuming that the refractive index of the doped fiber is  $n \sim 1.45$ , we can derive the coupling factor of a dynamic grating in this doped fiber using Eq 4-1:  $\kappa \sim 1.55\text{m}^{-1}$ .

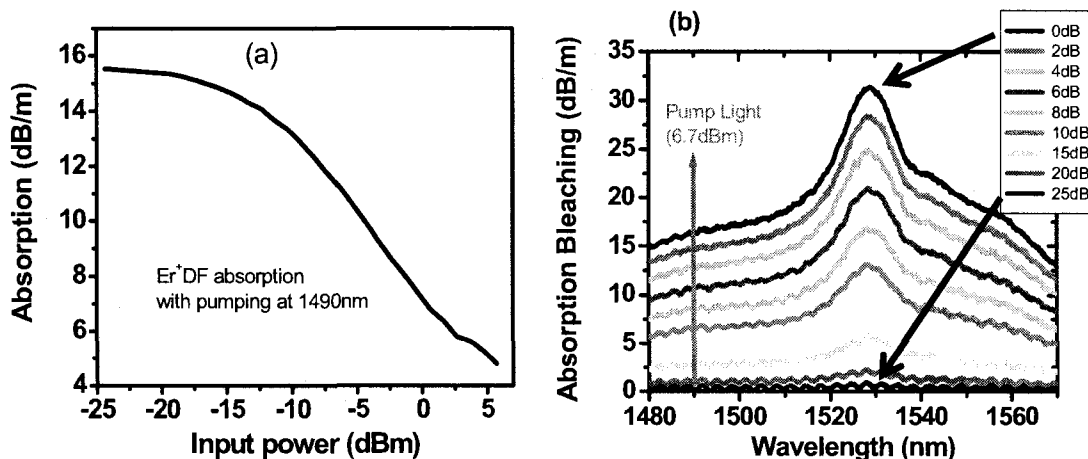


Figure 4-2 Absorption in erbium-doped fiber: (a) absorption at 1490 nm as a function of pump power; (b) bleaching of the whole absorption band when the erbium-doped fiber is pumped at 1490 nm (Pump power decreased by inline attenuation)

Two similar DFECLs operating at 1490 nm were built to study the effect of the EDF on the performance of the laser with the external cavity. DFECL-1 had a Fabry-Perot (FP) semiconductor diode laser, a piece of 28.5 cm EDF was in the external cavity, and the FBG had a  $\sim 0.2$  nm bandwidth and 7 dB maximum reflectivity. As the FP semiconductor laser already had a pigtailed fiber, and the FBG was made separately, the total external cavity length of DFECL-1 was  $\sim 95$  cm. The DFECL-2 had FP semiconductor laser with a piece of 28 cm EDF, and a FBG was  $\sim 0.2$  nm bandwidth and 6.5 dB of the reflectivity maximum. The length of the external cavity of DFECL-2 was  $\sim 67$  cm. Both FP lasers had very broad 1450-1500 nm lasing bandwidths. So the peaks output wavelength could be chosen to be at  $\sim 1490$  nm determined by the FBGs peak reflectivity wavelength.

#### 4.4 The stability of DFECL

The long term wavelength stability of the new made DFECL was measured. As shown in Figure 4-3. The semiconductor laser of the DFECL was located in the laser mount with temperature and current controls, the rest of the DFECL, such as doped fiber and FBG, were in the ambient room temperature. The wavelength was measured with the wavemeter, Burleigh WA1000, with resolution of  $\pm 0.7$  pm. The measurement was

made over a period of 7 hours. The result shows that the wavelength of the DFECL is mostly with the range of  $\pm 2.5$  pm for very long periods. Short time wavelength shift was about  $\pm 1$  pm.

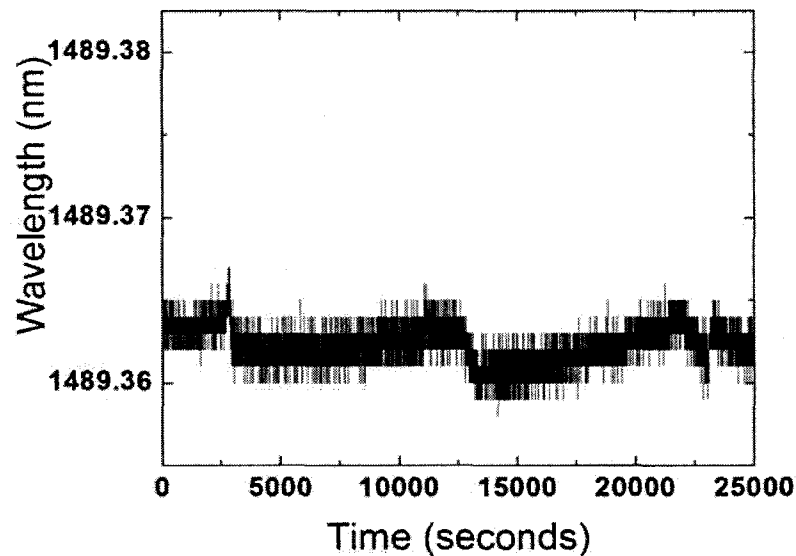


Figure 4-3 Long term stability of the DFECL

## 4.5 Simulations for DFECL

A time-domain transmission-line laser model was used to simulate the output spectrum of the DFECL. The algorithm for simulations of a DFECL along with the equations used in the time-domain model has been presented in Reference [Kostko and Kashyap 2004]. In this approach, the laser is described as a four-section device. The lengths of the sections (diode, fiber, doped fiber, FBG) in the cavity, the reflectivity, and the bandwidth of the FBG were assigned to match the parameters of the DFECL-2. The modeling parameters of the diode were adjusted using the measurements of the light-current and spectral characteristics. For time-domain simulation of the absorption changes and the evolution of the dynamic grating in the doped fiber section an experimental dependence of absorption on the input power, shown in Figure 4-4 [Kostko and Kashyap 2004; Liu, Kostko, Kashyap, Wu, and Kiiveri 2005], has been used.

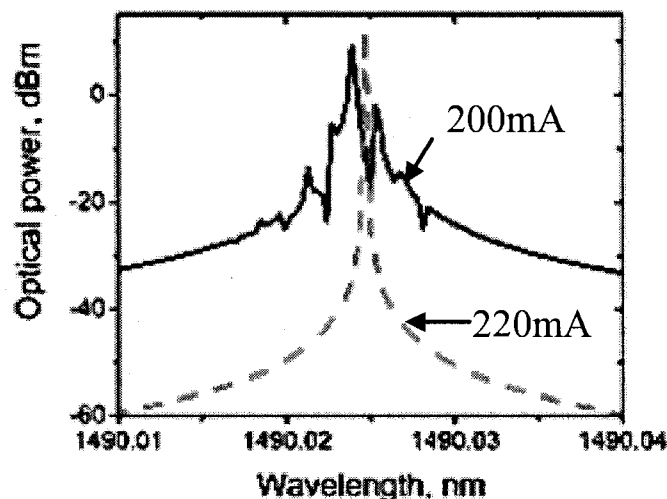


Figure 4-4 Simulated spectrum of DFECL-2: 200mA (solid) and 220 mA (dashed).

From the bandwidth of the FBG and the length of the cavity, we calculate that there should be more than 100 longitudinal modes oscillating in the cavity, if there is no influence from the dynamic grating.

In a DFECL with the doped fiber in the cavity, most of the side-modes are suppressed after approximately 500 ns of simulation time. In most cases, there are several modes oscillating at the same time [Liu, Kostko, Kashyap, Wu, and Kiiveri 2005]. These modes are the overlap of oscillating waves, because of the identical mode spacing. The spectra of these modes correspond to the bandwidth of the dynamic grating. In the simulations at a diode drive current of 200 mA, the laser had only 5 oscillating modes with the SMSR of less than 22 dB. The laser was able to achieve the single-mode regime when appropriate current was applied to the diode. The simulations indicated that the suppression of the side modes within the bandwidth of the dynamic grating depends on the power inside the cavity, which is defined by the diode drive current.

## 4.6 The Line-width Measurement of the DFECL

As discussed in chapter 2, there are two main reasons that cause the spectrum to broaden in a single longitudinal mode laser: these are phase noise and frequency chirp

[Henry 1982; Henry 1983; Agrawal, G.P. and Dutta, N.K. 1993; Kostko and Kashyap 2004]. Random phase noise is created with spontaneous emission in the laser cavity gain media, changing the phase of the free running laser frequency. This results in an increase in the laser line-width. Laser frequency chirp results in significant broadening when the laser injection current is modulated. The unwanted frequency modulation, or chirp, can broaden the laser spectrum well beyond the free running optical line-width.

The optical measurement technique is a direct way to measure the linewidth and is suitable for broad line-width measurement. The optical equipment should have enough measurement resolutions, as the light under measurement is compared to a reference light. The reference light should have even narrow line-width than the laser for measurement. Optical measurement is suitable to measure the line-width of normal semiconductor lasers. The major problem here is that the line-width of DFECL is much narrower than the reference sources in most optical equipments. As the line-width of a DFECL is most certainly below the resolution of the optical spectrum analyzer (OSA), another system must be employed.

By converting the optical light to the lower frequency, the line-width can be precisely measured using an entirely electrical approach. Two incoherent light waves can generate a microwave beat note frequency at the photodetector. The spectrum of beat note can be measured with the electrical spectrum analyzer (ESA), which has much higher resolution in frequency than the OSA. The heterodyne beating and homodyne beating methods are mostly used to measure lasers with very narrow line-width. The measured electrical line-width is approximately the sum of the line-widths of the two lasers. The heterodyne method uses the beating of the measured source with a reference source. If the reference laser's bandwidth is broader than the measured line-width, the measurement can not resolve the modes of the test laser.

The standard self-homodyne technique may be used to measure the narrow line-width light without any reference light source. In this case, the light is divided into two and

launched into the two paths of an interferometer. Coherence time is reduced by random events, such as spontaneous emission in the cavity, which alters the phase or frequency of the laser output field. In order to make the light at the output of the interferometer incoherent, an optical delay line is used in one of the paths. Thus the beat note at the photodetector is from two beams with the same line-width. As the beat frequency of self-homodyne light is centered at a frequency of 0 Hz, it can be difficult to obtain the line-width using a normal ESA if the line-width is less than 1 kHz. In the delayed self heterodyne technique a frequency offset is provided in one of the divided light paths, so the beat frequency is centered at the shifted frequency and the measurement result is identified easily.

The requirement for incoherent mixing sets a minimum delay requirement for the interferometer with respect to the laser's line-width [Ramos and Seeds 1990]:

$$\tau_0 \geq \frac{1}{\pi \Delta \nu} \quad (4-3)$$

Where  $\Delta \nu$  is the supposed line-width, in Hz, of the laser for measurement. If used with single mode fiber, with a refractive index of  $\sim 1.5$ , the minimum length of the delay line should be:

$$L = \frac{c \tau_0}{n} = \frac{c}{n \pi \Delta \nu} \approx \frac{3 \times 10^8}{1.5 \times \pi \Delta \nu} \quad (4-4)$$

To measure the spectrum with high resolution, heterodyne beating is the most used method [Loh, Laming, Zervas, Farries, and Koren 1995b; Derickson, D. 1998]. As an example, for a light with line-width of 10 MHz, as most single frequency semiconductor lasers have, the minimum required differential time delay will be about 30 ns, which is about 6.5 meters single mode fiber (SMF). As the doped fiber has the special effect of narrowing the line-width, the line-width should not be broader than an external cavity fiber laser. In the case of DFECL, in which the line-width is in the order of 1 kHz, the required delay line would be 65 km, which is difficult to implement in a delay line

interferometer. 25 km optical delay line was used for  $\sim 1$  kHz line-width DFECL measurement [Loh, Laming, Zervas, Farries, and Koren 1995b], which did not quite satisfy the minimum delay requirement [Derickson, D. 1998].

As discussed before, for long external cavity, the mode spacing is very small, therefore the side mode suppression becomes very difficult. If the side modes are not fully suppressed in the output of a long external-cavity laser, the longitudinal modes may beat with each other to generate the microwave beat-note signals, which are the superposition of the mode beat notes. Since the mode spacing is decided by the cavity length, all external-cavity modes can be considered to have same line-width with same mode spacing. The linewidth of beating note should be the overlap of all of the mode beating. The measured microwave signal line-width should be more than twice the line-width of a single EC mode. From analysis, the fabricated DFECL may have several modes remaining. The self-mode beating homodyne method was used for the line-width measurement.

## **4.7 Experiment of line-width measurement with self mode beat note**

The measurement setup is shown in figure 4-5. The semiconductor laser diode of the DFECL is placed on the laser mount (ILX 4890), which is controlled by ILX 3900 laser controller. The laser controller has temperature control resolution of  $0.1^\circ\text{C}$ , and drive current control resolution of  $0.1\text{ mA}$ . The output light the DFECL is connected to an optical coupler. One output port of the coupler is connected to an Optical Spectrum Analyzer (OSA) AD6317B for optical measurement; while the other port is coupled to a photodetector to measure the beat note for electrical spectrum analyzer (ESA) HP8563A. The equipments were connected to a computer for controlling and measuring.



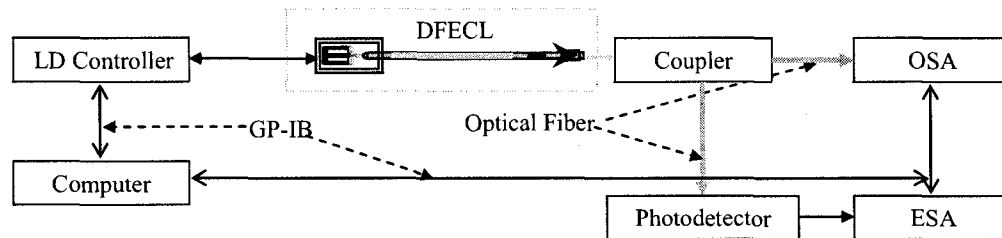


Figure 4-5 Setup of line-width measurement by self mode homodyne beating

The self-mode beating note spectrum of the DFECL measured by the ESA with a photodetector is shown in Figure 4-6. The line-width of the mode beat-note of the DFECL-1 at 1490 nm is approximately 12.5 kHz at the 20 dB level below the peak. Assuming that the spectrum has a Lorentzian profile, the FWHM of an external cavity mode is  $\sim 675$  Hz. With the same measurement, the FWHM for the DFECL-2 (67 cm cavity length) was calculated to be  $\sim 2$  kHz.

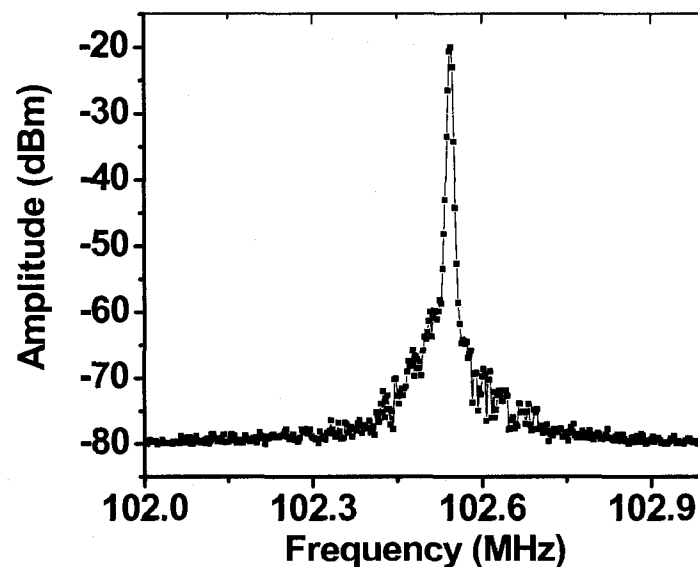


Figure 4-6 The beat spectrum of the DFECL-1 (EC 95-cm-long).

Comparing with the results reported in Reference [Loh, Laming, Zervas, Farries, and Koren 1995b] for the DFECL lasing at 1535 nm, where the line-width of a DFECL was measured by a delayed self-heterodyne beating method, our measurement result is

reasonable and satisfied to the analysis. In that experiment the line-width of less than 1 kHz at 1535 nm was obtained for a 3-meter-long DFECL, and the line-width of 8 kHz was measured when the cavity length was 0.43 m [Loh, Laming, Zervas, Farries, and Koren 1995b].

As it was assumed that the longitudinal side modes still exist, the SMSR of this DFECL has to be measured.

## 4.8 SMSR Measurement by self mode beating

The multi longitudinal modes of a laser beat with each other at the photodetector. Therefore, the detected spectrum from the square-law photodetector is due to self mode beating. The spectra will contain a superposition of all the mode beat products.

The self beat note of a long external cavity laser is shown in figure 4-7. As the mode number may be 100, the amplitudes of the adjacent modes might be at the same level. The microwave beat-signal therefore has a comb-like spectrum, which indicates that the side-mode suppression of the ECL is poor. The peak power is as high as -10 dBm.

On the other hand, the mode beat-notes of the DFECL, as shown in Figure 4-8, are much weaker than that of the ECL. The first longitudinal-mode beat-note of the DFECL has the peak power of approximately -40 dBm. The side modes in DFECL are suppressed and only 5 major spectral peaks have a power higher than -60 dBm level and that of the higher-order beat-notes is  $< -60$  dBm, which indicates that the spectrum envelope of the DFECL contains only a few modes. This measurement provides an estimate of the maximum number of the oscillating longitudinal modes in the spectrum, which is calculated using the number of the microwave frequencies with a power higher than the background noise ( $\sim < -60$  dBm).

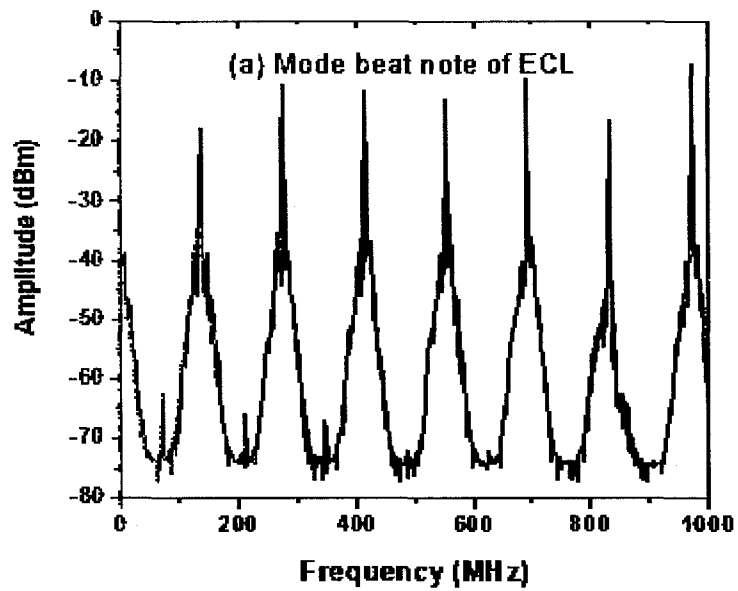


Figure 4-7 the mode beat note measurements of an ECL

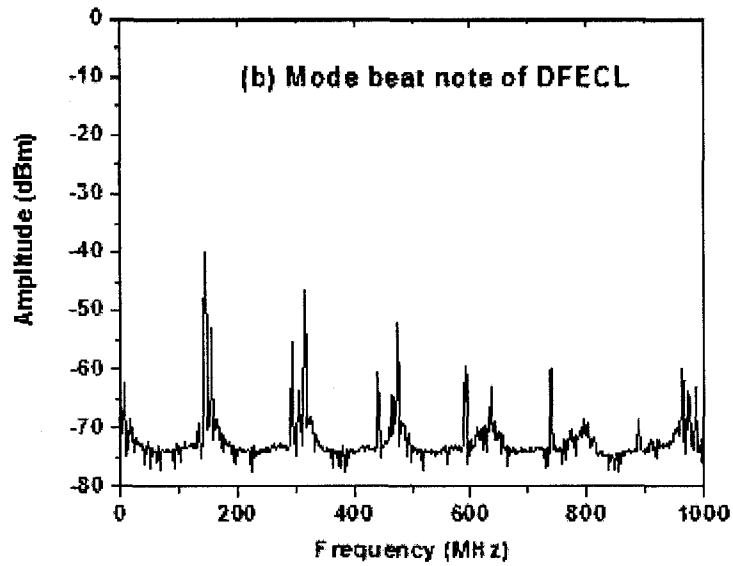


Figure 4-8 The mode beat note measurements of a DFECL

The SMSR and the amplitudes of the optical longitudinal modes may also be estimated analytically from Fig. 4-8, if a multimode optical field is described as:

$$E = \sum_i E_i f(\omega_i) \quad (4-5)$$

where  $E_i$ , and  $\omega_i$  are the electric field intensity, and frequency of the  $i^{th}$  optical longitudinal mode, respectively. In further analysis we assume that the optical spectrum is symmetrical ( $E_{-i} = E_i$ ) with only 9 modes  $E_{-4}, E_{-3} \dots E_4$  with the amplitude high enough to participate in the microwave signal generation, and the modes  $E_{-2}, E_{-1} \dots E_2$  are much stronger than the others.

The microwave self-beatnotes are generated at the mode spacing frequency and at its higher harmonics.

$$P^{RF} = \sum_j P_j^{RF} g(\omega_j) = kR \left( \sum_i E_i f(\omega_i) \right)^2 \quad (4-6)$$

Where  $\omega_j = \omega_i - \omega_{i-j}$ , is the frequency difference of two modes, and equals to the multiples of mode spacing.  $k$  is the conversion constant for normalising  $E$ , and  $R$  is the photo-detector's sensitivity.

The power of the first ( $P_1^{RF} = -38\text{dBm} = 10^{-3.8} \text{ mW}$ ), the second ( $P_2^{RF} = -45 \text{ dBm} = 10^{-4.5} \text{ mW}$ ), and the third ( $P_3^{RF} = -50\text{dBm} = 10^{-5} \text{ mW}$ ) beat-notes are defined as the overlap of the first-order, second-order, and the third-order adjacent modes of the optical spectrum, respectively. The first beat-note may be derived as:

$$P_1^{RF} = kR \sum_i E_i E_{i-1} f(\omega_i - \omega_{i-1}) \quad (4-7)$$

Substituting the value of the first beat-note for the DFECL and using the above assumptions on the symmetry of the spectrum, we get the following equation:

$$\begin{aligned} P_1^{RF} &= 10^{-3.8} \approx kR(E_{-2}E_{-1} + E_{-1}E_0 + E_0E_{+1} + E_1E_2) \\ &\approx kR(2E_0E_{+1} + 2E_1E_2) \end{aligned} \quad (4-8)$$

Assuming that  $E_0 > E_1 > E_2 > E_3$ , we derive:

$$E_1 \leq \frac{P_1^{RF}}{4E_0 kR} \quad (4-9)$$

The second beat-note may be written as:

$$P_2^{RF} = kR \sum_i E_i E_{i-2} f(\omega_i - \omega_{i-2}) \quad (4-10)$$

or

$$P_2^{RF} = 10^{-4.5} \approx kR(E_{-3}E_{-1} + E_{-2}E_0 + E_{-1}E_1 + E_0E_2 + E_1E_3) \quad (4-11)$$

Therefore, the second-order longitudinal mode depends on  $E_0$  and  $E_1$  as following:

$$E_2 \leq \frac{(P_2^{RF} / kR - E_1^2)}{4E_0} \quad (4-12)$$

Deriving the similar equations for the third- and the forth-order beat-notes, we get the following equations:

$$E_3 \approx \frac{(P_3^{RF} / kR - 2E_1E_2)}{4E_0} \quad (4-13)$$

$$E_4 \approx \frac{(P_4^{RF} / kR - E_2^2 - 2E_1E_3)}{4E_0} \quad (4-14)$$

Using equation (4-9), (4-12)-(4-14), we can calculate the amplitudes of the optical modes at various values of the dominant longitudinal mode magnitude  $E_0 = 10^{-5} \dots 1$ . The derived microwave beat-notes at different values of  $kR=0.2 \dots 1$  were then compared to the experiment. The optical modes, which satisfy the conditions for the microwave beat-notes in Fig. 4-8 and have the highest amplitudes, were estimated. We got:  $E_0 / E_1 = 57.4 = 17.5$  dB,  $E_0 / E_2 = 179.9 = 22.5$  dB,  $E_0 / E_3 = 3.4 \cdot 10^5 = 56.3$  dB,  $E_0 / E_4 = 1.3 \cdot 10^5 = 51.3$  dB. The analysis has shown that the suppression of the first-order longitudinal side-modes in the optical spectrum is at least 17 dB and the results do not depend on the

value of conversion constant  $kR$ . The measured spectrum has weaker power than in the simulations due to the optical losses resulting from the measurement set-up, therefore only the mode suppression may be compared.

As the optical modes  $E_0/E_3$  and  $E_0/E_4$  are suppressed by  $> 50$  dB at any value of  $k$ ,  $R$  and  $E_0$ , it is clear that the optical spectrum of the laser has maximum of 5 longitudinal modes. The results from the self mode beat measurement shows that the side mode suppression in a DFECL is more efficient than in an ECL and that the DFECL may have a maximum of 5 longitudinal modes in the optical spectrum.

## 4.9 SMSR measurement by heterodyne beating

The SMSR may also be measured by the heterodyne beating technique, by beating two similar independent lasers. As mentioned before, the design of both lasers used similar FP laser diodes and an external FBG, and their external cavity lengths were nominally the same. Both lasers operated at a similar temperature and diode driving current.

The setup of heterodyne beating is shown in Figure 4-9. The outputs of two DFECLs are coupled by an optical coupler, and converted to electrical signals by a photodetector and also monitored at the other output of the coupler. The signal from the photodetector was measured by an Electrical Spectrum Analyzer (ESA). The peak wavelengths of the sources were adjusted to  $\sim 1489.8$  nm and  $\sim 1489.9$  nm. Since the bandwidth of the photodetector used was 15 GHz, the beat signal was set at  $\sim 10$  GHz for measurement by an electrical spectrum analyzer after the photodetector.

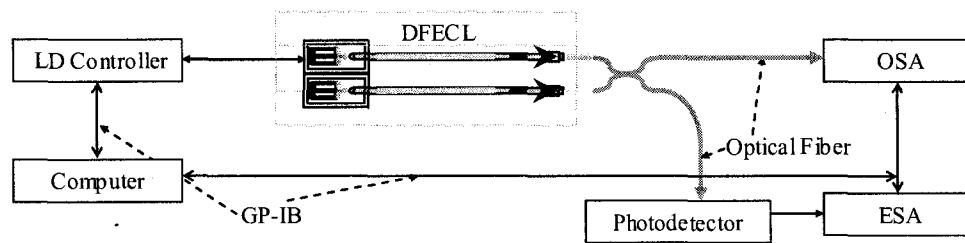


Figure 4-9 The setup for microwave generation by beating two DFECLs

Figure 4-10 shows the heterodyne beat-notes of two independent DFECL lights. The beat notes lie almost within the range of  $9 \pm 0.5$  GHz with the profile of the Gaussian function. The line-width measured with heterodyne beating is broader than that measured with a self-homodyne method due to the superposition of the beat notes in the heterodyne method and phase noise effects. Figure 4-11 shows the detailed view of the beat spectrum within the bandwidth of 3GHz. (7.5GHz- 10.5GHz). The dominant beat note has a maximum power of  $-3$  dBm and is the heterodyne beat note of the dominant longitudinal modes of the two DFECLs. The adjacent notes are the superposition of beating of the dominant modes with the other side modes. However, these beat-notes are  $\sim 15$  dB to 20 dB weaker than the peak note, which indicates that the side modes of each DFECL are suppressed by at least 15 dB.

The weaker side mode signals of the beat note are caused by beating of high-order side modes with the dominant modes and the side modes with the other side modes.

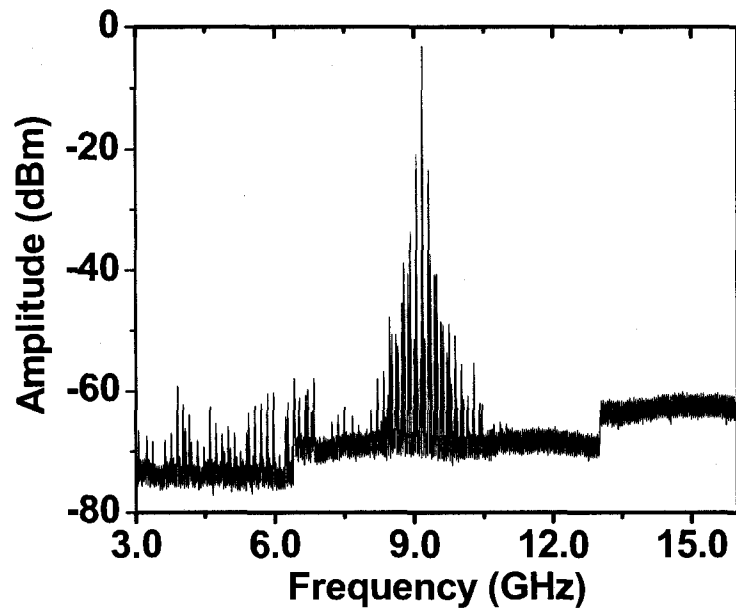


Figure 4-10, measurements of the heterodyne beat-note of the two DFECLs (BW=13GHz)

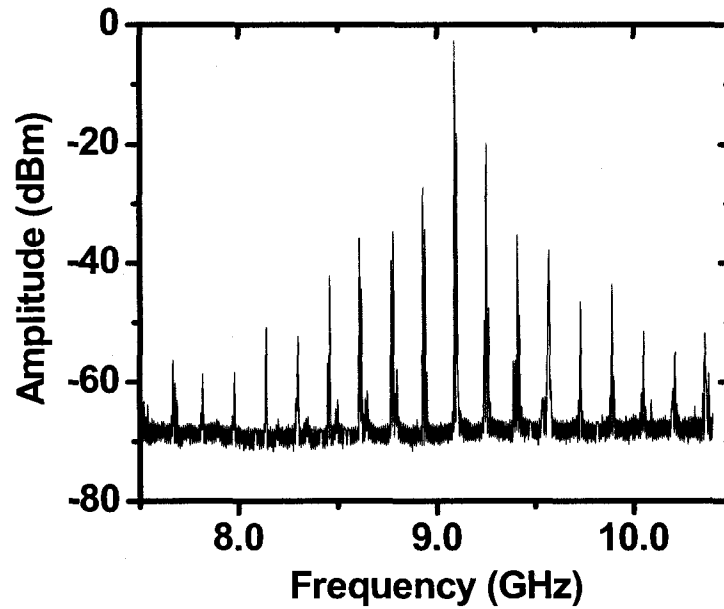


Figure 4-11 measurements of the heterodyne beat-note of the two DFECLs (BW=3GHz)

The SMSR may be estimated from the result of the heterodyne experiment, assuming that the spectra of two lasers are identical ( $E_{ai} = E_{bi}$ ). Since only 10 beat signals are suppressed by less than 50 dB, we consider only 11 modes in the oscillating spectra  $E_s$



... $E_5$ . Similar to the derived equations for self mode beating, the modes can be obtained in the microwave heterodyne measurement.

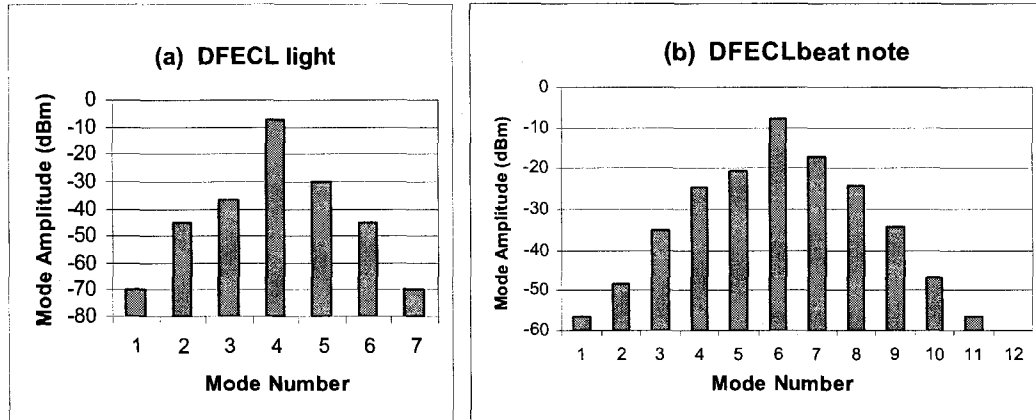


Figure 4-12 The derived light mode of DFECL from the experiment of DFECL heterodyne beat note

The results of the derivation are shown in figure 4-12. For the analysis, the assumed modes of DFECL are shown in figure 4-12a. With two similar sources, the beat notes as shown in figure 4-12b have a similar profile as from the heterodyne beat note experiment. From this derivation, we find that the side mode suppression of the DFECL can be as high as 20 dB.

Since the homodyne and heterodyne measurements were set up differently, the coupling loss, and inline attenuation were not the same in these experiments. Therefore in this particular case, in deriving optical amplitudes, we treated the results of two experiments separately. Combining the results of the self-mode beating and the heterodyne beating experiments, we may conclude that a DFECL has a SMSR of more than 17 dB.

From the Kramers-Krönig relations, the induced refractive index change is  $\Delta n \sim 1.68 \times 10^{-6}$ , and the refractive index of the doped fiber is  $n \sim 1.45$ . Using the equation (3-10), the coupling factor of the self-organized dynamic grating is  $\kappa \sim 1.55$ . The DFECL1 has 28 cm of doped fiber inside the 67-cm-long cavity. The mode spacing of the DFECL1 is

$\sim 150$  MHz, which gives  $\sim 175$  modes in the external cavity. However, with the self-organized dynamic grating in the doped fiber ( $R \sim 16.8\%$ ,  $\Delta\lambda \sim 5.52$  pm), the estimated number of modes is 5. For the DFECL2 with 28.5 cm of the doped fiber in the 95-cm long cavity, the mode spacing is  $\sim 103$  MHz. The dynamic grating in DFECL2 has  $R \sim 17.3\%$  and a bandwidth  $\Delta\lambda \sim 5.42$  pm. Due to the presence of the doped fiber the number of oscillating modes may be reduced from 194 to 6.

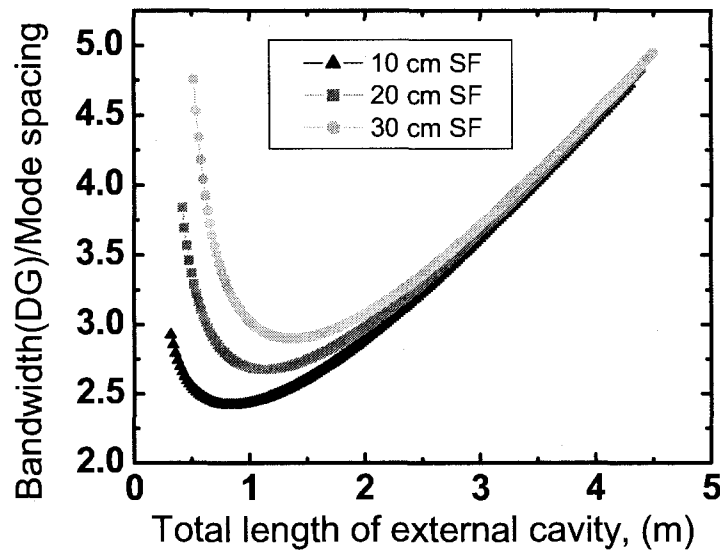


Figure 4-13 Calculation of the dynamic grating bandwidth divided by the spacing the in DFECL

Further calculation with the same FBG and doped fiber was also studied. As shown in figure 4-13. Three cases of the length of doped fiber in the external cavity are calculated. By calculating the bandwidth of dynamic grating and mode spacing ratio, it is found that the length of SMF in external cavity should be as short as possible. 10cm non-erbium doped fiber has fewer longitudinal modes than the cases with 20 cm or 30 cm non doped fiber. The optimized length of cavity is about 70 cm, with 10 cm non EDF, in the best situation,  $\sim 2$  modes remain, when the entire cavity is made with erbium doped fiber. Therefore, the dynamic grating can be as long as possible. It is difficult to suppress very closely spaced side modes, because the dynamic grating may not have a narrow enough reflective bandwidth.

High SMSR may be achieved by careful selection of its parameters, drive current and, most importantly, filling the whole external cavity with the doped fiber. A practical implementation of such a laser needs advanced splicing and coupling techniques.

## 4.10 Conclusion

In this chapter, the fabrication and experimental studies of DFECL are presented. A dynamic grating in the doped fiber can be formed by the absorption modulation from absorption bleaching caused by standing waves in the cavity. Due to the dynamic grating effect, the DFECL shows significant wavelength stability and line-width narrowing compared to a normal external cavity laser.

In order to study how the DFECL works in the whole absorption region of the doped fiber, new DFECL lasers were designed and fabricated. The new lasers operated at 1490 nm wavelength, at the edge of the absorption range of EDF.

Measurements have shown that the even at the 1490 nm wavelength, the DFECL has good performance as it is at the edge of the absorption wavelength. The new DFECL has long term and short term wavelength stability. The single mode line-width is very narrow, in the order of kilohertz. With self homodyne beating and heterodyne beating method, it has been shown that there are about 5-6 longitudinal modes that remain in the DFECL output spectrum, the side mode suppression ratio is between  $\sim 15$ -20 dB.

The experiments agreed with the theoretical analysis that there are only a few longitudinal modes inside the cavity of the DFECL instead of more than 100 modes in similar ECLs and have high SMSR; at some currents only one longitudinal mode oscillates. The analyses also indicate that a better DFECL may be realized by using only doped fiber for the entire length of the cavity, the FBG reflectivity and by carefully choosing the absorption of the doped fiber.

## CHAPTER 5 TUNING CHARACTERISTICS OF THE DFECL

### 5.1 Introduction

Tuneable lasers have many applications, such as in spectroscopy, sensor, radar and optical communications [Strzelecki, Cohen, and Coldren 1988; Betts, Tjugiarto, Xue, and Chu 1991; Mantz 1995; Bellemare, Lemieux, Tetu, and LaRochelle 1998; Delorme 1998]. In order to operate at a particular wavelength or frequency, a desirable tuneable source is useful. Wide tuning range lasers are extremely useful for WDM application. In the optical microwave generation applications [Simonis and Purchase 1990; Georges, Wu, Cutrer, Koren, Koch, and Lau 1995; Wake, Lima, and Davies 1995], a smaller tuning-range of the lasers is very attractive, because it allows the generation of tuneable microwave radiation by the photonics approach.

As we have seen in the preceding chapters, a doped fiber laser can be made to operate with a narrow line. It can also be made tuneable by using a variable coupler [Scrivener, Tarbox, and Maton 1989]. With this technique, the laser output obtained at 1.56  $\mu\text{m}$  wavelength can be varied by mechanical adjustment of the high power pump by a polished coupler component, enabling tuning of the laser in three discrete ranges within a 70 nm wavelength region. Discrete wavelength tuning ranges have also been observed in cavities without dispersive elements and have been attributed to the substantial Stark splitting of the energy levels [Barnes, Morkel, Reekie, and Payne 1989].

An external bulk grating tuning mechanism has been used to continuously tune an erbium fiber over 70 nm around 1550 nm [Wyatt 1989]. Efficient operation was obtained in this case by pumping the doped fiber with 980 nm radiation.

For external cavity lasers, the mechanism of laser tuning is realized by either tuning the length of the cavity or the peak reflectivity wavelength of the reflectors. FBG tuning is to change its Bragg period condition with either the temperature or mechanical stretching [Ball and Morey 1992; Kashyap, R. 1999] and is one of the most commonly

applied approaches for fiber laser wavelength tuning. The FBG tuning has a wide wavelength tuning range, usually in the order of tens of nanometers [Kashyap, R. 1999]. The tunability range for both, the FGECL and DFECL is similar, as their peak wavelength is related to the FBG reflection spectrum.

Of course as the DFECL has doped fiber inside the external cavity, it has been shown to be ultra stable, with a narrow line-width as well as high power [Loh, Laming, Zervas, Farries, and Koren 1995b; Timofeev and Kashyap 2003].

As the frequency of light is of the order of 200 THz and microwave or millimeter wave frequency range is in the range of GHz to tens-GHz, a small tuning range of the laser source can thus induce a large frequency change for ROF application. Therefore, a laser with a narrow tuning range and at a fixed wavelength becomes extremely useful for these applications.

## **5.2 Transient Response of DFECL**

The wavelength of DFECL is determined by the oscillation conditions of the external cavity, and mainly influenced by the peak reflectivity of effective grating and the differential absorption changes within the FBG bandwidth. With the doped fiber in the external cavity, the dynamic grating is formed by the standing wave. The change in standing wave changes the period of dynamic grating.

The lifetime of the erbium ions in the doped fiber is very long, of the order of 10 ms. Once the dynamic grating is setup, it dissipates very slowly. The slow response is the major reason that the DFECL with dynamic grating can eliminate fast wavelength fluctuation and stabilise the lasing output.

The procedure for the setup of the dynamic grating is relatively complicated. As discussed in the previous chapters, the long cavity DFECL has very narrow mode spacing, of the order of  $\sim 100$  MHz. The FBG used in the DFECL has a bandwidth of

about 0.2 nm, which is equivalent to 20 GHz. There are more than 100 longitudinal modes oscillating in the cavity. Even with the presence of the dynamic grating, there are around 5-6 longitudinal modes remaining, as shown in the experimental results in the previous chapter. As a result of the closeness of the modes, assuming a Gaussian spectrum, the adjacent mode amplitude varies only slowly across the band, especially for the modes in the center of the spectrum. The modes are competing to be the dominant mode. In the procedure, the mode which has a relatively strong intensity makes a relatively strong standing wave, and forms a strong dynamic grating. Since any grating has a peak reflectivity at its center of the band, the dynamic grating's peak reflectivity is at the wavelength at which it is formed, whilst the other waves have a relatively weak reflectivity, and therefore they are suppressed. This procedure would continue until the dynamic grating strength reaches its maximum, and this relates to the absorption bleaching characteristics of the fiber. In this way, the setup up time may be long. If several modes in the center spectrum have approximately the same intensity, any of them may become the dominant mode. The one that has the fastest growth forms the dominant dynamic grating.

Because of the long setup and dissipation times of the dynamic grating, the response is slow. Dynamic grating in doped fiber cannot follow the fast wavelength fluctuation in the laser diode. This is mechanism which leads to the elimination of wavelength fluctuation. Thus, the dynamic grating can stabilise the wavelength of the DFECL.

The dynamic grating setup procedure can be experimentally verified by measuring the transient response of the DFECL. To carry out the measurement, the experimental setup shown in figure 5-1 was used. The semiconductor laser was fixed on a temperature controlled mount while all other parts of the DFECL were at room temperature ( $\sim 21^\circ\text{C}$ ). Only the semiconductor laser diode of the DFECL was controlled by an ILX LDC-3900 laser diode controller, with a drive current resolution of 0.1 mA and temperature resolution of 0.1  $^\circ\text{C}$ . The resolution of reading data from the LDC-3900 for temperature and driving current were 0.01 degree and 0.01 mA, respectively. The laser output was

connected to optical couplers and then to the measurement instruments (power meter, OSA and wave meter). The peak wavelength was measured with a Burleigh WA-1000 wave meter, with the resolution of  $\pm 0.7$  pm. The output power was measured with an HP optical multimeter, with the resolution of 0.05 dBm. An Ando AQ-6317B OSA was also used to monitor the line shape of the laser, and measure the peak and mean power. The equipment was connected to a computer with GPIB cables, and the measurement was controlled by a computer.

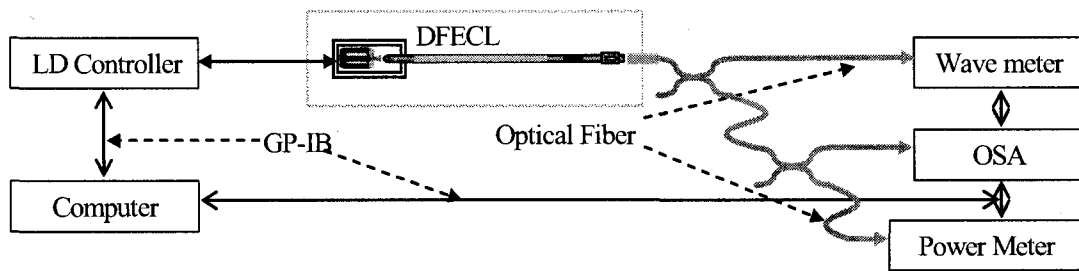


Figure 5-1 Setup for output of DFECL measurement

The result of the long-term peak wavelength and power intensity measurement is shown in figure 5-2. During the measurement, the laser current was switched on and off. The laser diode was operating at  $21^{\circ}\text{C}$  and the drive current was set at 100 mA. It is clear from the Figure 5-2 that the wavelength and the intensity of the dominant longitudinal mode become stable a few seconds after the laser was switched on. The wavelength of the laser could become stable at 1489.36 nm with only  $\pm 1$  pm fluctuation and the variation in the intensity was within  $\pm 0.05$  dBm, almost limited by the resolution of the measurement system.

The final stable-wavelength and power were different each time after switch on, although, the wavelength and power could remain stable for long periods of time. However for the same drive current and temperature, the final stable operating wavelength varied randomly within the range of  $\sim \pm 2.5$  pm each time after it was switched on. It took few seconds for the laser to go the stable states.

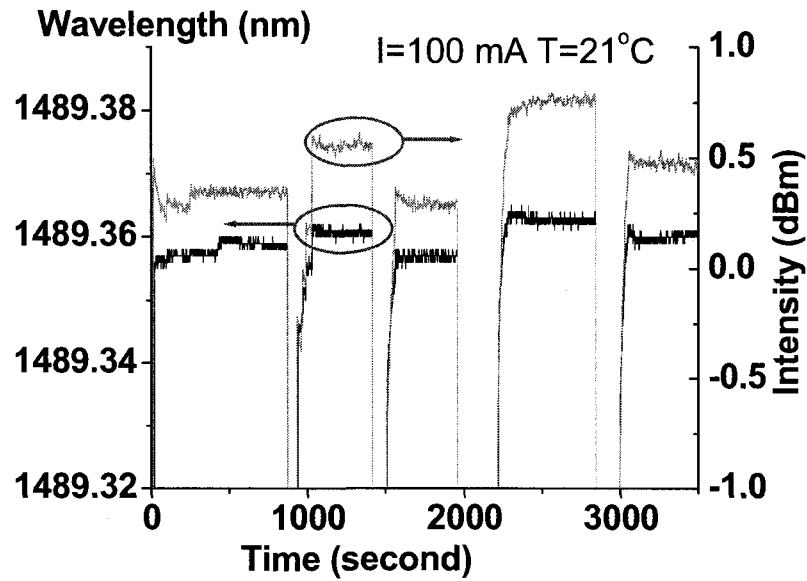


Figure 5-2 Switch on/off experiment for measuring the dynamic grating setup characteristics

The same experiment was also done for a drive current of 120 mA, as shown in figure 5-3. The switch-on performance of the operating wavelength was similar to the experiment with a drive current of 100 mA. The difference is in the final stable wavelength range which moved to  $1489.37 \text{ nm} \pm 2.5 \text{ pm}$ .

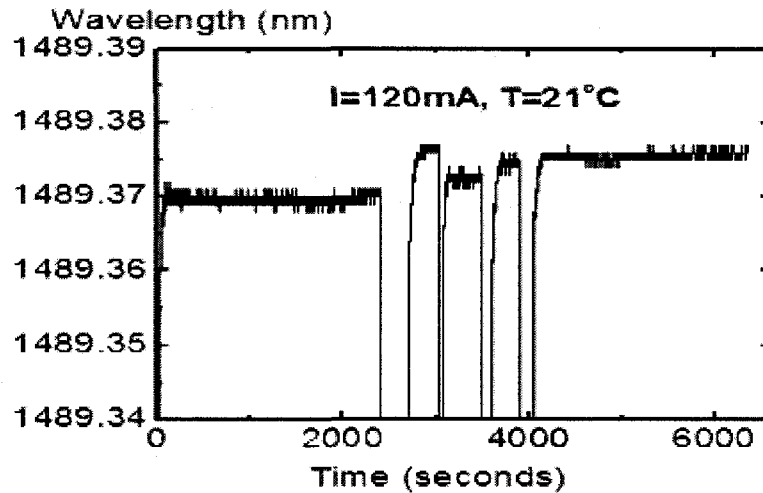


Figure 5-3 Wavelength stability of DFECL with switch on/off at  $I = 120 \text{ m}$

The experimental results showed that even under the same drive current and temperature the stable wavelength ( $\pm 1 \text{ pm}$  fluctuation) would sit within a range of  $\sim$



$\pm 2.5$  pm. This result implies that immediately after the current is applied to the laser, several modes might have same intensity and compete to be the dominant mode. All of them have the same probability to become the dominant one. As soon as the dynamic grating is formed by one dominant mode, it starts to suppress the other modes. Fast wavelength fluctuations do not disturb the ion distribution and the dynamic grating. This characteristic of the dynamic grating in the EDF helps to dampen out fast changes in the emission wavelength and stabilize the wavelength as well as the power.

The laser may become more stable if two main factors affecting the stability of the DFECL are improved: the environmental temperature and the stability of the laser diode current. The possible solutions may be to package the whole DFECL and to improve the resolution of diode temperature and current controller. However, it is remarkable that such a long cavity laser may operate with such a narrow line-width and stability with such a simple configuration.

### **5.3 Tuning the DFECL**

The DFECL can be tuned by either the FBG or by the dynamic grating. Similar to the ECL or FGECL, a wide wavelength tuning range can be realized by the tuning of FBG. Since the FBG tuning of a DFECL is exactly the same as the tuning of ECL, the tuning performance the DFECL discussed here is only about the tuning of the dynamic grating.

The tuning of the dynamic grating works on a different principal from FBG tuning. As the erbium ions in the doped fiber have a long lifetime, fast fluctuations in the FBG or the temperature of the external cavity are damped by the slow response of the dynamic grating. The possible tuning of dynamic grating is by slowly and continuously changing the standing wave. The changes in the semiconductor laser would change the whole oscillating condition of the DFECL. For a semiconductor laser, the change of either drive current and temperature of the laser diode cause a wavelength shift (through the Henry-factor) as well as power intensity change.

This analysis can be verified by experiment. The experimental setup was the same as shown in figure 5-1. The tuning of the DFECL was realized by tuning the semiconductor laser with the laser diode controller. Considering the long setup time of the dynamic grating, the semiconductor laser tuning was set with 1 second delay so that the transient response could be neglected.

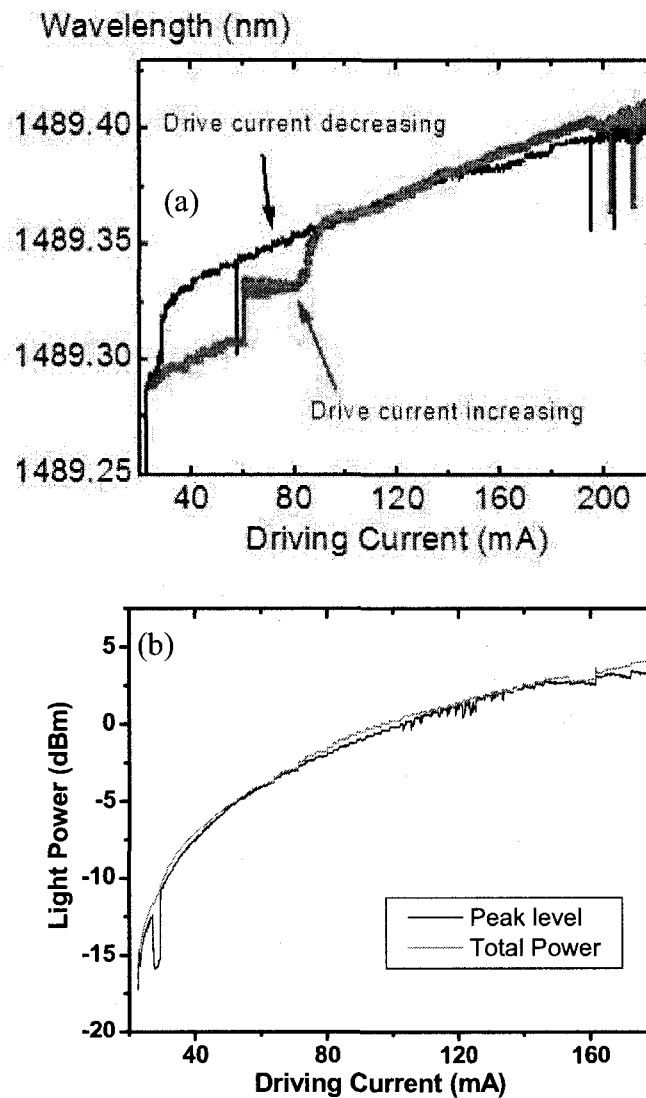


Figure 5-4 (a) Wavelength and (b) power tuning by changing the driving current laser diode

The experimental result of wavelength tuning by changing the drive current of semiconductor laser diode is shown in Figure 5-4a. The output power of the light-

current relation is shown in Figure 5-4b. The temperature was kept constant at 21°C. The current was changed in 2000 steps over the full wavelength tuning range. In the situation when the driving current was increasing, the lasing threshold was about 30 mA. At that time, the power in the EDF was low; it could not bleach the absorption. Only when the current was more than 90 mA, the external cavity mode was locked to its dominant mode. Thereafter, the wavelength shift is almost linear and mode-hop-free within the range up to 190 mA. For tuning with the current decreasing, the smooth and mode-hop-free tuning can be down to as low as 30mA. Only one indecisive point at a current of 60 mA was measured and attributed to the inability of the wave-meter to determine the dominant mode. It is believed that this sudden but momentary change in the wavelength cannot be considered as a mode-hop rather than an indication that the spectrum is not single-mode immediately after the mode-hop and that it may take the laser longer than 1 second to become single-mode again after the change of current. The driving tuning range was as much as 160 mA (30-190mA). The wavelength tuning can be more than 0.06 nm, which is equivalent to ~8 GHz. The tuning rate is 0.375 pm/mA, which is equivalent to 50 MHz/mA. Figure 5-4 shows that for practical implementation in ROF systems the best current range was between 90 mA and 190 mA with a wavelength tuning range of 45 pm. This is a large range for mode-hop free operation.

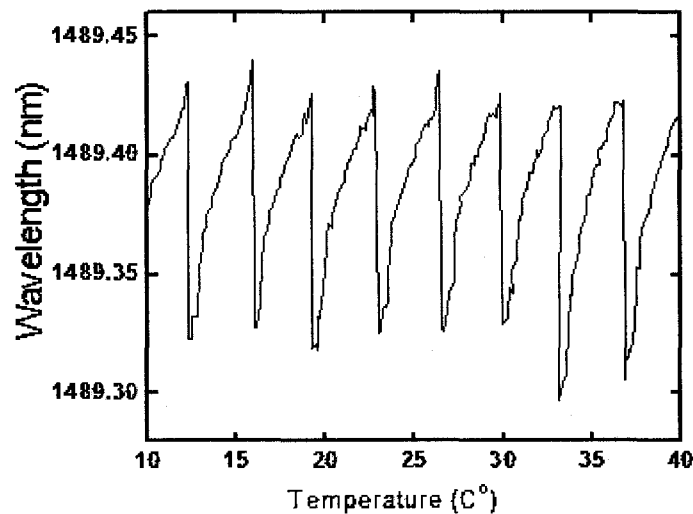


Figure 5-5 The Wavelength tuning by changing the temperature of the laser diode

The wavelength temperature tuning is shown in figure 5-5. The wavelength was tuned continuously within  $\sim 0.1$  nm. This was within the bandwidth of the external FBG, because the FBG performance is not affected by the laser diode temperature or current changes. The wavelength tuning is periodic with a mode hop at every  $\sim 7^\circ\text{C}$ . The wavelength tuning with temperature was rapid, because the semiconductor laser is temperature sensitive. The precise wavelength tuning may not be available with the temperature tuning, as the temperature controller usually does not have enough control resolution.

As the dynamic grating is induced by the external FBG, the tuning range of the dynamic grating is not altered by the drive current and temperature of laser diode. In order to have the required output with a certain power, temperature tuning can be used along with drive current tuning. The wavelength shift with temperature of the DFECL at different diode drive currents is shown in Figure 5-6. It demonstrates that we can set the DFECL output wavelength at different drive currents by choosing the appropriate operating temperature within a range of  $7^\circ\text{C}$ . The tuning range of 100 pm is primarily defined by the bandwidth of the FBG (0.2nm).

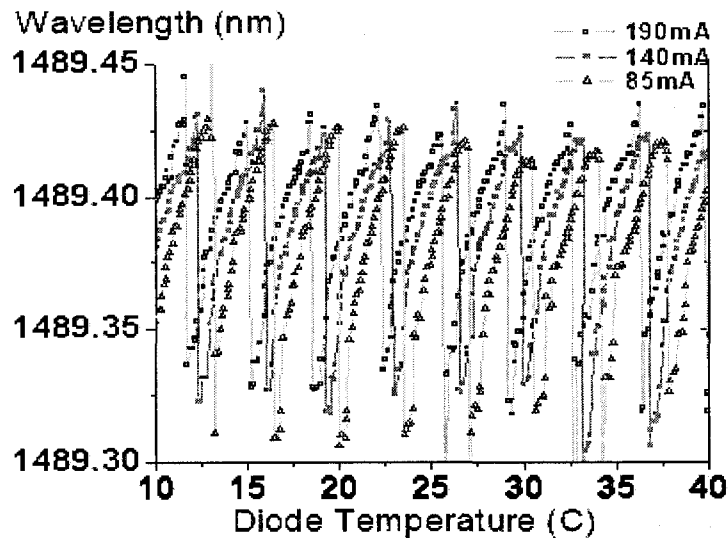


Figure 5-6 The wavelength tuning of DFECL as a function of drive current and temperature

The experimental results indicate that the output wavelength of DFECL depends on the peak reflectivity of dynamic grating as well as that of the FBG. As the oscillating wave is originally coupled from the semiconductor laser, the wavelength of the semiconductor laser shifts to longer wavelength when its driving current or temperature is increased. With a slow and continuous increase in the amplitude of one side mode by tuning of semiconductor laser's drive current or temperature, the adjacent mode can have the amplitude larger than the original one. Continuous tuning is the result of the competition of the closely-spaced external-cavity modes ( $\sim 1$  pm) to form a dominant dynamic grating. The continuous tuning is defined by both fine-tuning of the external-cavity mode and intermediate mode-hops: when the external-cavity side-mode is stronger than the dominant mode and can form the dynamic grating, an intermediate mode-hop occurs. Therefore, the peak wavelength moves to this wavelength. Both driving current and temperature control of semiconductor laser can change the dominant standing wave and thus the dominant dynamic grating. Since the semiconductor laser is more sensitive to operating temperature, the wavelength tuning is much faster than the tuning caused by the driving current.

## 5.4 Conclusion

The results demonstrate that the wavelength of the DFECL is precisely controllable by tuning the semiconductor laser's pump wavelength. The wavelength may be tuned smoothly and continuously over 60 pm when the drive current is ramped by 160 mA. Meanwhile, by changing the laser diode operating temperature the wavelength can be tuned by over 100 pm with a slope of 25 pm/ $^{\circ}$ C (or 3 GHz/ $^{\circ}$ C). The slope of the laser frequency change vs. current is equivalent to 50 MHz/mA. The optical wavelength resolution is 5MHz, with the current controller resolution of 0.1 mA. Since microwave photonic generation usually works from a few GHz to a few tens of GHz, this experiment shows that the direct optical tuning approach of DFECL can provide a simple and inexpensive way for optically tuning the microwave frequency. For both current and temperature control, the tuning bandwidth is narrower than the FBG

bandwidth. As the reflectivity decreases significantly at the edges of the FBG bandwidth, it becomes more difficult to lock to a dominant external-cavity mode. As a comparison, a DFB laser usually has tuning coefficient of ( $\sim 1$  GHz/mA) and a temperature coefficient of  $23.74$  GHz/ $^{\circ}\text{C}$ , making it extremely sensitive to small changes. The lower sensitivity of the DFECL will also benefit in controlling fixed single frequency operation as it lowers the feedback loop control frequency of the electronics necessary for this operation.

## CHAPTER 6      DFECL FOR ROF APPLICATIONS

### 6.1 Introduction

High power, low noise, and high stability and large modulation bandwidth are the key features of laser sources for ROF transmission. However, the line-width of laser is broadened due to phase noise, and it remains a major problem for communication applications.

Compact semiconductor lasers have been developed successfully for optical communication, but the line-width and its stability are not always as desired. A normal FP semiconductor laser has a very broad line-width (in  $\sim$ nm). With integrated distributed feedback, a free running DFB laser has a line-width of  $\sim$ 10MHz ( $\sim$ 0.1pm). Line-width reduction has been studied to lower chirp for optical communication [Henry 1982; Olsson, Henry, Kazarinov, Lee, and Johnson 1987]. Optical feedback locking has greatly benefited the line-width and wavelength stability of lasers [Ramos and Seeds 1990]. An external cavity is used to enhance the performance by narrowing the line-width, and the peak power of a semiconductor laser is also increased [Olsson, Henry, Kazarinov, Lee, and Johnson 1987]. An ECL can have a line-width as low as  $\sim$ 50 KHz. With a saturable rare-earth doped fiber [Kostko and Kashyap 2006], the DFECL presents very good performance in line-width, as well as stable wavelength and high power, making them useful for ROF applications. Unfortunately, the direct modulation bandwidth may seem to be a drawback for DFECL applications.

In this chapter, a study of direct modulation performance of an ultra long DFECL is presented. Even though the resonant frequency of the long DFECL is very low; it can be modulated at the multiples of its round-trip resonant frequency. Our experimental results show that this DFECL can be directly modulated at more than the 22<sup>nd</sup> multiple of its cavity round trip resonance frequency. Narrow bandwidth signals can be directly modulated and transmitted with very little spectral distortion. High quality orthogonal

frequency domain modulation (OFDM) signal transmission by directly modulating the DFECL has verified that it can be used for ROF communications.

## 6.2 Resonance enhanced direct modulation

Directly modulating the drive current of a semiconductor laser is a simple and low cost way to transmit microwave signals over optical fiber networks. Since the laser light output is proportional to the drive current over a large current range, the output light intensity can be easily modulated. One problem of direct modulation is that the modulated drive current can modulate the temperature slightly, and then modulate the wavelength of the laser. Although there is temperature control available for most lasers, any change in the driving current can still cause temperature changes due to thermal lag. Direct modulation of the semiconductor laser by its drive current can cause frequency as well as amplitude modulation of the emitted laser radiation [Paoli and Ripper 1970]. This is one of the main reasons why direct modulation cannot be used in high performance transmission applications without other compensating techniques.

Another reason which limits direct modulation is the low modulation bandwidth. Direct modulation bandwidth is limited by either photon relaxation frequency, or cavity resonant frequency [Paoli and Ripper 1970; Lau and Yariv 1985; Nagarajan, Levy, and Bowers 1994]. In most cases, the semiconductor laser can be made very short with the result that the cavity resonance frequency is high, up to 150 GHz; the modulation bandwidth of a semiconductor laser is mainly limited by the photon relaxation oscillation frequency, which is due to the photon lifetime in the gain medium [Paoli and Ripper 1970]. When the cavity length is not very short, the cavity round trip resonant frequency may become lower than the photon relaxation frequency. The direct modulation of these long cavity lasers can easily reach the cavity resonance frequency. The direct modulation bandwidth is then limited by the laser cavity round-trip resonance frequency, and leads to mode locking [Haus 1981; Haus and Mecozzi 1993]. Normally, the direct modulation response of a FP semiconductor laser has a peak at the resonance



frequency; beyond this frequency, the modulation response decrease rapidly [Paoli and Ripper 1970].

The theoretical analysis and the modeling of the modulation frequency has been extensively studied in the literature [Agrawal 1984b; Dods, Ogura, and Watanabe 1993] for a low modulation frequency. When the modulation frequency is much higher than the cavity resonance frequency, it is found that the situation becomes quite different; the transmission response may be sharply increased at a multiple of the resonance frequency. Both active and passive mode-locking analysis are used to describe this phenomenon [Lau 1990; Georges, Cutrer, Solgaard, and Lau 1995; Doerr 1996]. The standard treatment of active mode-locking assumes gain modulation, and passive mode-locking describes it in the time domain. A narrow bandwidth RF modulation signal can thus be transmitted at the multiples of resonant frequency. The direct modulation transmission bandwidth is then extended to multiples of the resonant frequency. Higher modulation efficiency is achieved within the pass-bandwidth [Georges, Cutrer, Solgaard, and Lau 1995].

In some cases, the microwave signal for transmission is with narrowband sub-carriers. Narrow bandwidth signals are modulated onto a microwave or millimetre wave carrier, and then applied to the optical wave. Hence, the resonantly enhanced direct modulation can be used for modulated microwave transmission.

A direct modulation of a GaAlAs semiconductor laser diode has been demonstrated at a frequency up to 18 GHz, while the conventional -3dB direct modulation bandwidth of this semiconductor laser is less than 10 GHz [Lau and Yariv 1985]. The example of the 300 MHz narrowband windows is enhanced for microwave signal transmission at the multiples of round trip resonant frequency [Georges, Cutrer, Solgaard, and Lau 1995]. The experimentally demonstration of 40 GHz modulation was reported in Reference [Nagarajan, Levy, and Bowers 1994]. A short cavity semiconductor laser can be directly modulated beyond 100 GHz [Lau 1990]. Direct modulation of 3 channels

digital signal at 1.24 Gb/s for a ~4 cm long cavity semiconductor laser has been reported [Doerr 1996]. Because electrical parasitics were difficult to overcome effectively for a frequency higher than 40GHz, the modulation of the semiconductor laser could not be achieved at very high frequencies and therefore, the direct modulation frequency was only at 2~3 multiples of round trip resonant frequency as reported in References [Lau 1990; Georges, Cutrer, Solgaard, and Lau 1995]. This resonantly enhanced direct modulation can be used to increase the modulation bandwidth with a low intrinsic modulation bandwidth laser, by extending the laser with an external cavity. Resonance enhancement of directly modulated semiconductor laser with an external cavity [Nagarajan, Levy, and Bowers 1994] of more than 30 dB at multiples of the resonance frequency has been demonstrated. Although the relative intensive noise (RIN) is also enhanced, carrier to noise ratio can still reach 90dB/Hz. By properly coupling the semiconductor laser to an external cavity, a semiconductor laser diode with 5 GHz modulation bandwidth can transmit a 700 MHz narrow-band signal at 35GHz. A 40 MB/s BPSK signal was transmitted at 35 GHz, and the bit error rate was better than  $10^{-9}$  [Nagarajan, Levy, and Bowers 1994].

Optically, this resonance enhanced modulated light wave can be considered as multimode light. The light is composed of a central mode with two side modes which are away from the optical carrier mode at the modulation frequency. If the modulation side modes are located in any multiple of the round trip resonance frequency, they fit the phase condition of the cavity resonance.

### **6.3 Direct Modulation of DFECL**

A doped fiber is a saturable absorber. It performs a similar function as the gain media in the laser cavity. The resonance enhanced direct modulation may also be available for the DFECL. The extended modulation bandwidth may be useful for its application in fiber optic communications.

The DFECL for this experiment was built by using a JDS 3400 laser diode, CorActive EDF, and a FBG. The commercial laser diode was a high power FP semiconductor pump laser, working as a multi longitudinal mode light source with a very broad bandwidth (1450 – 1500 nm). The antireflection-coated front facet had a reflectivity of  $<1\%$ . The FBG had a full bandwidth of  $\sim 0.2$  nm and a peak reflectivity of 6 dB (75%) at its center wavelength ( $\sim 1489.4$  nm). The absorption of this EDF was  $\sim 16$  dB/m at wavelength of 1490 nm, for low pump powers (at -20 dBm). When the pump power reaches 6.7 dBm at 1489 nm, the absorption drops to 1 dB/m, resulting in 15 dB/m of bleaching. A 30cm long EDF was used. Since the laser diode, EDF, and FBG are connected with single mode fiber, the total length of the external cavity between one end of laser diode and FBG was  $\sim 95$  cm. The round trip time of the external cavity was measured to be  $\sim 9.2$  ns; the equivalent resonance frequency was  $\sim 109$  MHz.

During the experiment, only the semiconductor laser diode of the DFECL was placed on a temperature controlled ILX LDM4980RF laser diode mount (with modulation bandwidth  $>2.5$ GHz), the other parts of the DFECL were at ambient room temperature. The DFECL was controlled by an ILX LDC-3900 laser diode controller. The RF wave was directly applied to the laser diode via the ILX laser diode mount.

The experimental setup for direct modulation of the DFECL is shown in Figure 6-1. With the temperature of the external cavity uncontrolled, it was noted that the wavelength stability of this laser was better than  $\pm 1$  pm and the peak power stability was better than  $\pm 0.1$  dBm. The DFECL under measurement was fixed to a temperature of  $19.1^\circ\text{C}$  and with a drive current of 159.7 mA, so that the wavelength and cavity resonance frequency would not change. The laser's center wavelength was at 1489.89nm. As the output light power could be more than 10 dBm, for safety consideration, inline attenuation was applied. A tunable single frequency microwave signal from an HP83712B synthesized tunable CW generator (range of 10MHz-20GHz) was applied to the DFECL as direct modulation. The modulated light was then transmitted through a fiber system to a photo-receiver. The demodulated microwave

spectrum from the photo-receiver was then observed on an Agilent E4446A spectrum analyzer. All of the instruments for control and measurement were connected to a computer with a GPIB cable, and the measurements were automatic and controlled by a Labview program. The tuning step for the modulation frequency was 2MHz with about a 1 second delay in order to accommodate the response of the spectrum analyzer.

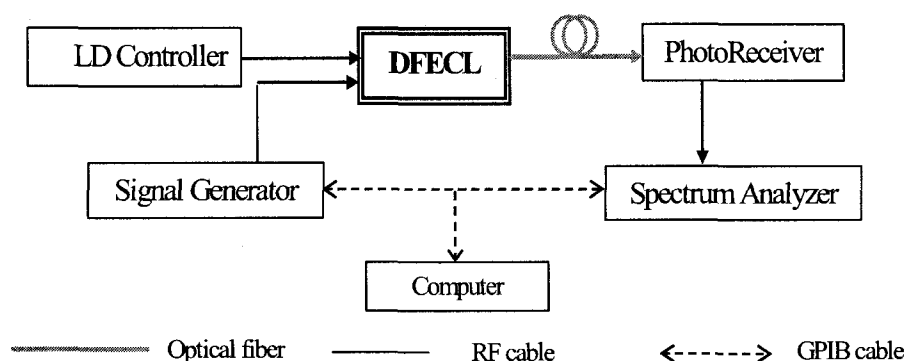


Figure 6-1 Setup for DFECCL direct modulation

From the experiment of single frequency direct modulation transmission response, it was observed that near the first resonance frequency, the direct modulation characteristics were as expected as in direct modulation of normal semiconductor lasers, exhibiting the resonance peak due to standard relaxation oscillation. As the modulation frequency increased much higher than the resonance frequency, the transmission response of DFECCL became periodic. The periodic spacing is exactly equal to the resonant frequency. As shown in figure 6-2, in the range of 1.8 – 2.8 GHz (similar behaviour was observed up to 4GHz), the peaks and dips differ by more than 25 dB. At around 2.8 GHz, even higher enhanced resonance direct modulation transmission is observed than that at low frequencies. At each enhanced peak, the 3dB bandwidth is about 10MHz. The peaks of transmission begin to decrease for a modulation frequency higher than 2.8 GHz.

The result gives more than a 25 dB difference in transmission response between peak and the dip due to the detuning from the multiples of the resonance frequency. In this

experiment, as the RF laser diode mount in the experiment has the modulation bandwidth of  $>2.5\text{GHz}$ , the envelope of the extended transmission response was limited by the setup of the transmission system rather than the DFECL direct modulation response itself. It should be noted that the semiconductor chip is a pump laser in a low frequency package; it is not intended to be modulated at high frequencies.

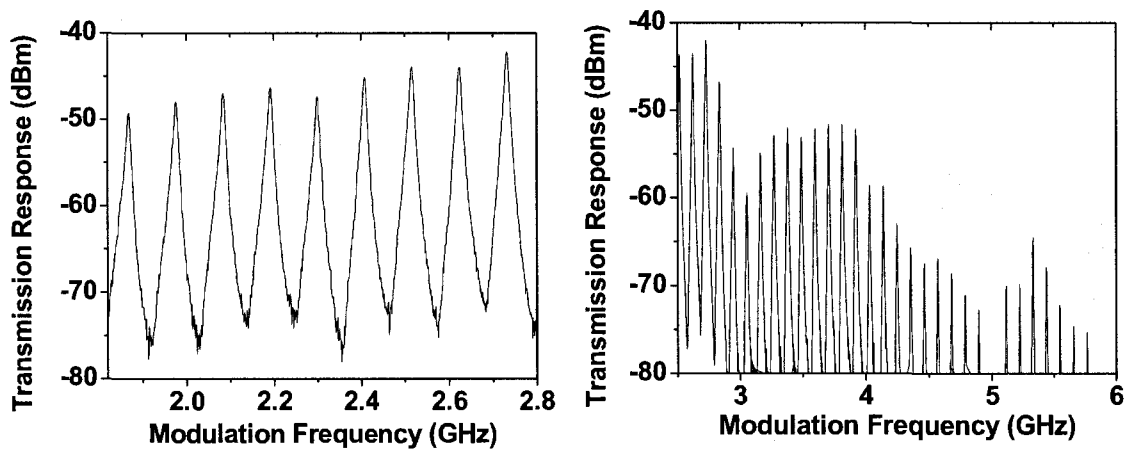


Figure 6-2 Transmission response of direct modulation of long DFECL

Mode-locking with the saturable absorber in the external cavity can be observed in the transmission response. The transmission response of DFECL is enhanced discontinuously at only the multiples of cavity resonant frequency, and the modulation transmission bandwidth is therefore also extended. This makes it possible to modulate a narrowband microwave signal on a carrier at each transmission peak and with a very good narrowband filter response.

Theoretically, since the light wave oscillating inside the external cavity should be within the reflection bandwidth of the FBG, the optical spectrum of the direct modulation frequency of DFECL should be limited by the FBG's bandwidth. The transmitted modulated RF frequency must be less than the half bandwidth of the FBG. In our case, the FBG has the bandwidth of  $0.2\text{nm}$ , which is equivalent to  $\sim 30\text{GHz}$ , so that the bandwidth could not be larger than  $15\text{GHz}$ , even if all other conditions were met.

## 6.4 Narrow Band Microwave Transmission

As there was an  $\sim 10\text{MHz}$  bandwidth of each peak for resonance enhanced direct modulation of the DFECL, it is possible to transmit a narrow bandwidth wireless signal, at one peak transmission frequency of this DFECL.

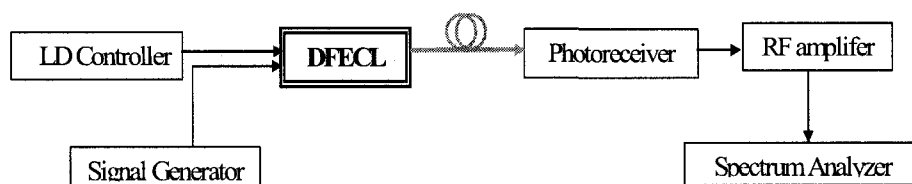


Figure 6-3 The setup for microwave transmission by DFECL

A following experiment was made to transmit a modulated microwave signal by this long DFECL. The center frequency was chosen at one peak of the transmission ( $\sim 2.4\text{GHz}$ ), and the microwave signal was amplitude modulated by a  $500\text{ kHz}$  signal from Marconi 2031 signal generator. The signal spectrum was within the bandwidth of  $10\text{MHz}$ , as shown in figure 6-4a. As the light wave to the optical receiver was attenuated by optical components in this experiment, a broadband ( $100\text{ kHz}$ - $3\text{ GHz}$ ) RF amplifier HP8347A was used after the photo-receiver, as shown in figure 6-3. The received signal was observed by an ESA, as shown in figure 6-4b. There is no obvious difference of the spectrum for the  $10\text{MHz}$  bandwidth. From figure 6-5, in the spectral range of  $0$ - $2.5\text{ GHz}$ , the received microwave signal can be clearly identified. All the harmonic frequencies and resonant frequencies were  $50\text{dB}$  lower than the received signal.

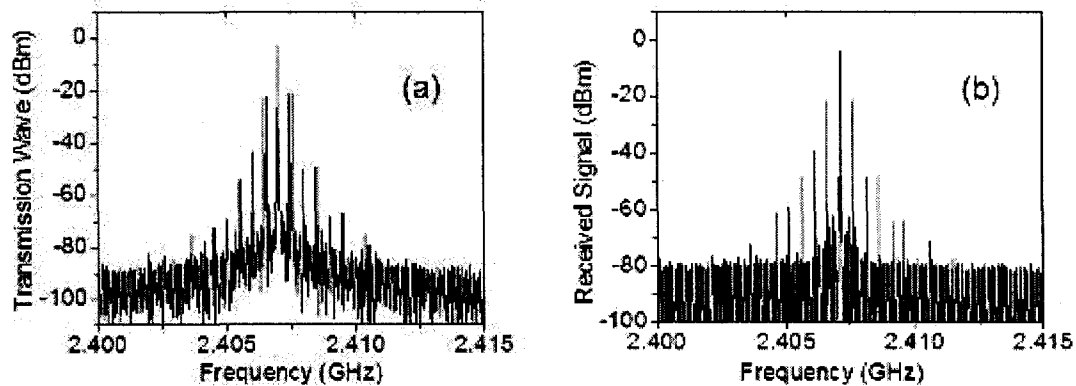


Figure 6-4 The narrow bandwidth signal transmission with direct modulating a DFECL

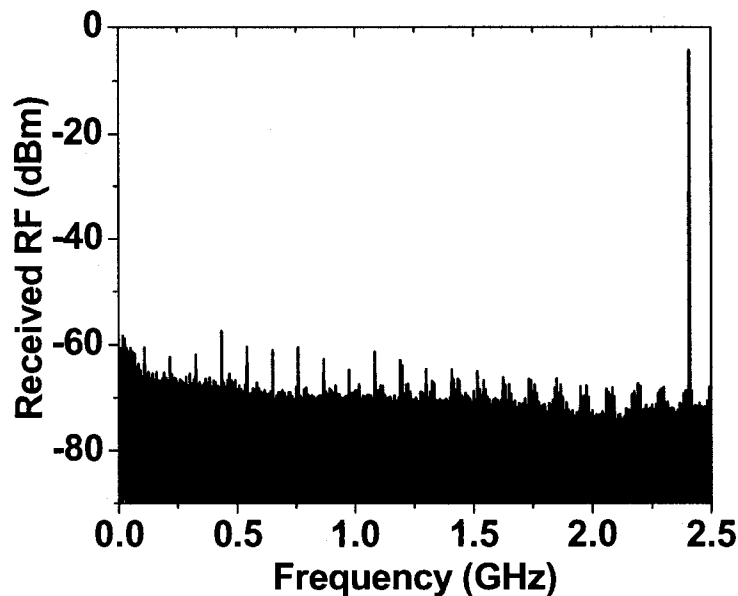


Figure 6-5 The received spectrum from DFECL direct modulation

Frequency modulation (FM) signals from the generator were then applied to the DFECL direct modulation. The transmitted signal spectrum was within the bandwidth of 10MHz, as shown in figure 6-6a. The received signal spectrum distortion is not obvious within this bandwidth region, as in figure 6-6b. When the bandwidth of frequency modulation microwave is increased to 20MHz, as shown in figure 6-7a, the signal spectrum distortion can be observed in figure 6-7b, but is still less than 6 dB.

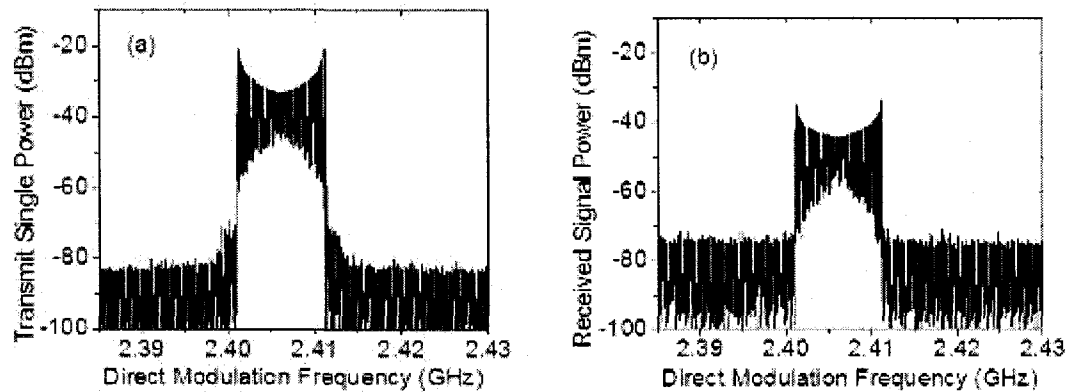


Figure 6-6 The transmission of 10 MHz bandwidth FM wave from DFECL direct modulation

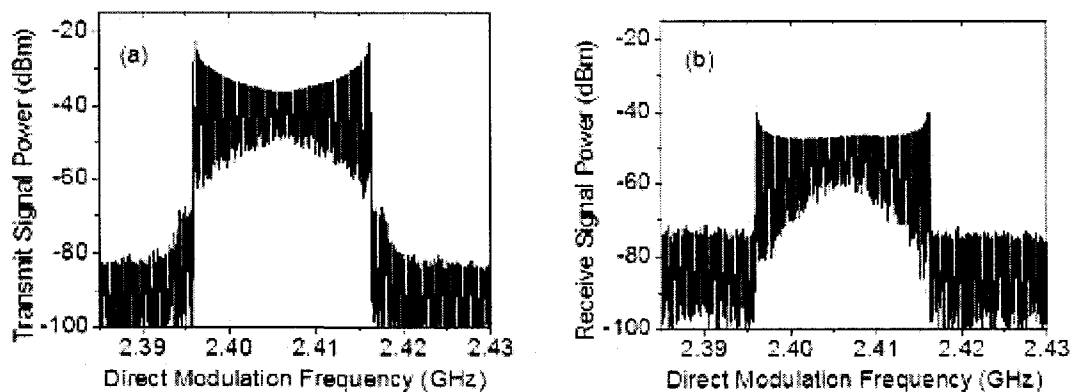


Figure 6-7 The transmission of 20MHz bandwidth FM wave from DFECL direct modulation

## 6.5 Transmission from DFECL to an antenna

The microwave transmission experiment was also set for wireless transmission. The received FM microwave signal was sent to a broadband antenna. The spectrum measurements were set at different points, respectively. The setup is shown in figure 6-8. The measurement point A is direct from the signal generator (Marconi 2031). The measurement point B is from the antenna with the signal directly transmitted from the signal generator. The measurement point C is from the RF amplifier. The point D is after the antenna with the wireless signal transmission from point C. Point E is from the Photo-receiver.



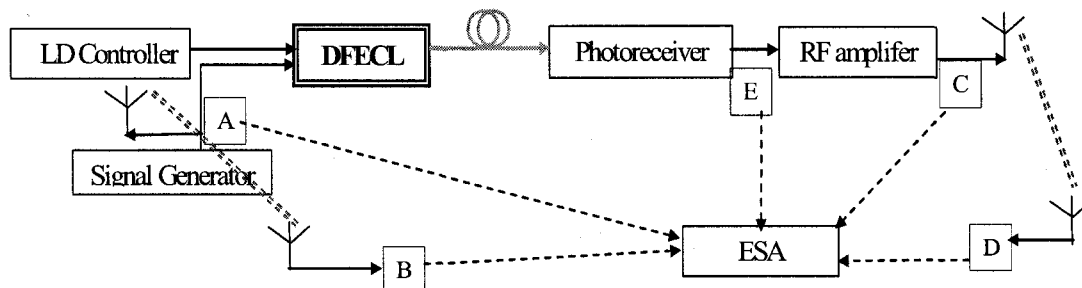


Figure 6-8 Set-up for directly modulating a DFECL with various measuring points

The measurement results are shown in figure 6-9. In these measurements, the transmitted signal has a 20 MHz FM bandwidth. The RF carrier was at  $\sim 2.41$  GHz. From these results, we can see that the spectrum outline distortion was from the optical transmission. The maximum distortion within the 20 MHz bandwidth is about 6 dB,

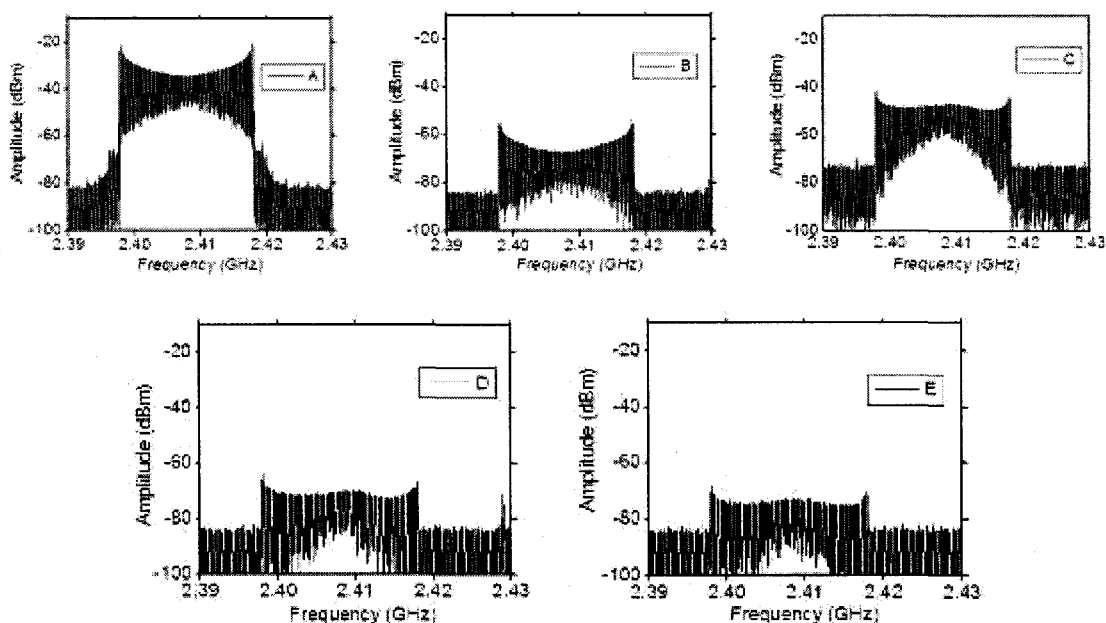


Figure 6-9 Direct Modulation of DFECL with 20MHz bandwidth FM signal at 0 dBm RF carrier, (A): Spectrum of RF source, (B): the spectrum with only antenna transmission, (C): received spectrum at photo-detector after directly modulating the DFECL, and RF amplifier, (D), the spectrum from the photo-detector after directly modulating the DFECL and RF amplifier and antenna transmission. (E), received spectrum photo-detector after directly modulating the DFECL

One can notice that the antenna does have transmission loss, but the spectrum distortion is mainly from resonance enhancement. These experimental results have verified that narrow bandwidth 2.4GHz FM signal can directly modulate the DFECL, and a signal is available for transmission at the antenna.

## **6.6 OFDM signal transmission with DFECL**

Orthogonal Frequency-Division Multiplexing (OFDM) is a modulation technique for transmitting large amounts of digital data over a radio wave [Cimini 1985; May, Rohling, and Engels 1998; Rohling, May, Brueninghaus, and Gruenheid 1999]. OFDM works by splitting the radio signal into multiple smaller sub-signals that are then transmitted simultaneously at different frequencies to the receiver. OFDM uses a large number of closely-spaced orthogonal sub-carriers for communication. Quadrature amplitude modulation (QAM) used for each sub-carrier is modulated at a low symbol rate, maintaining data rates similar to conventional single-carrier modulation schemes in the same bandwidth. The primary advantage of OFDM over single-carrier schemes is its ability to cope with severe channel conditions. OFDM has developed into a popular scheme for wideband digital communication systems, such as Wi-Fi (IEEE 802.11a/g) Wireless LANs. OFDM scheme has been successfully developed and applied to wireless communication.

The IEEE 802.11 signals are based on OFDM modulation with 20 MHz or 40 MHz bandwidth around the RF carrier frequency of 2.5 or 5 GHz. The bandwidth is divided to 52 sub-carriers with 48 data tones that can be modulated by multi-level QAM. The IEEE 802.11a maximum transmission rate, 54Mb/s, is achievable using a dense 64-QAM constellation, which is very sensitive to link noise and distortion. The OFDM modulation signal is a good example for ROF transmission. Properly chosen, the bias point of the external modulator would have very good transmission performance with ROF external modulation [Sisto, LaRochelle, and Rusch 2006].

A DFECL for this experiment was built by using a JDS 3400 semiconductor laser diode, a length of EDF, and a FBG. The FBG had a full bandwidth of  $\sim 0.2$  nm and a peak reflectivity of 6 dB at its center wavelength. A 30cm long EDF was used. The whole cavity was  $\sim 93$  cm long. The round trip time of the external cavity was  $\sim 9.2$  ns equivalent to a resonant frequency of  $\sim 112$  MHz.

In the experiment (figure 6-10), the 64-QAM OFDM signal was generated by an Agilent E4438C ESG vector signal generator (VSG). The received signal from the photo-receiver was then observed on an Agilent E4440A PSA vector spectrum analyzer (VSA). During the experiment, the laser chip of the DFECL had 207.6 mA drive current and a 17.6 C temperature. The other parts of the DFECL were at normal room temperature. The optical power applied to the photo-receiver was about 3 dBm, at the wavelength of 1489.6 nm.

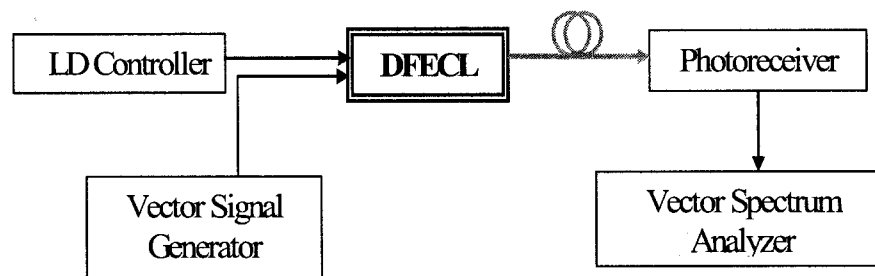


Figure 6-10 The setup of OFDM direct modulation

From the previous experiment, it was found that the 20 MHz bandwidth transmission has about 6 dB distortion, and even though it was not as good as the 10 MHz bandwidth transmission, it might be acceptable in our application. Following the standard of IEEE 802.11a/g, the 64-QAM IEEE 802.11a with a maximum rate of 54 Mb/s from the E4438C was set with a 20MHz bandwidth, and the RF carrier was carefully tuned to 2.4668 GHz, to get best transmission response. The VSA RF intensity was set to 0dBm, 5 dBm, 7.5dBm, and 10 dBm, respectively.

The received signal spectrum is shown in figure 6-11. The received OFDM signal spectrum is very clear with about 35 - 45 dB above the noise level. Up to 10 dBm RF

power has been applied to DFECL as direct modulation. The highest RF input signal gave the best signal to noise ratio. It should be noted that the semiconductor chip is a pump laser within a low frequency package. Meanwhile, the laser was driven at more than 200 mA with a relatively small RF signal which is why the detected RF signals are lower than -30 dBm. We believe that this could be improved by designing a laser chip with the appropriate high frequency RF package.

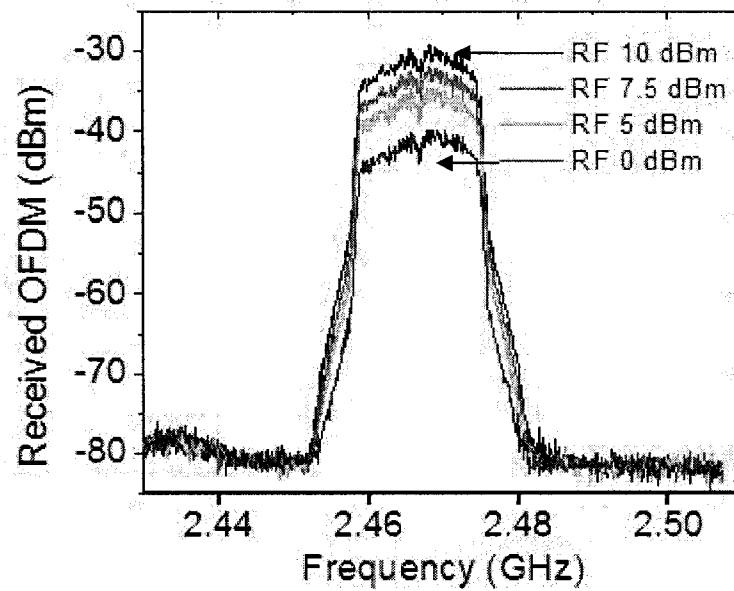


Figure 6-11 The receive OFDM spectrum transmitted from direct modulating a DFECL

Error Vector Magnitude (EVM) - the transmitter modulation accuracy test, is calculated by comparing the actual measured signal with an ideal reference signal to determine the error vector. EVM is one of key measurements of 802.11a/g OFDM transmit signals can be made. The EVM value is the root mean square (RMS) value of the error vector over time at the instants of the symbol (or chip) clock transitions. The dominant contributors to poor EVM performance are phase and amplitude mismatches, phase noise, and non-linearity of the transmitter.

$$EVM_{dB} = 10 \log_{10} \left( \frac{\sum_n |r_n - z_n|^2}{\sum_n |r_n|^2} \right) \quad (6-1)$$

$$EVM_{\%} = \left( \sqrt{\frac{(\sum_n |r_n - z_n|^2)}{\sum_n |r_n|^2}} \right) \times 100\% \quad (6-2)$$

where  $r$  represents the transmitted 64-QAM symbols and  $z$  are the received ones.

The signals are composed of frames with a synchronization symbol, a channel-response training symbol, and a payload of 16 OFDM-symbols. After detection, the 64-QAM symbols are extracted to measure the EVM. The EVM and detected RF power measurements were performed by VSA as a function of the RF powers injected to the DFECL. IEEE 802.11a protocol specifies -25 dB or 8.75% as the maximum allowable EVM value for error free transmission. Most wireless products EVM can reach -33 dB (2%).

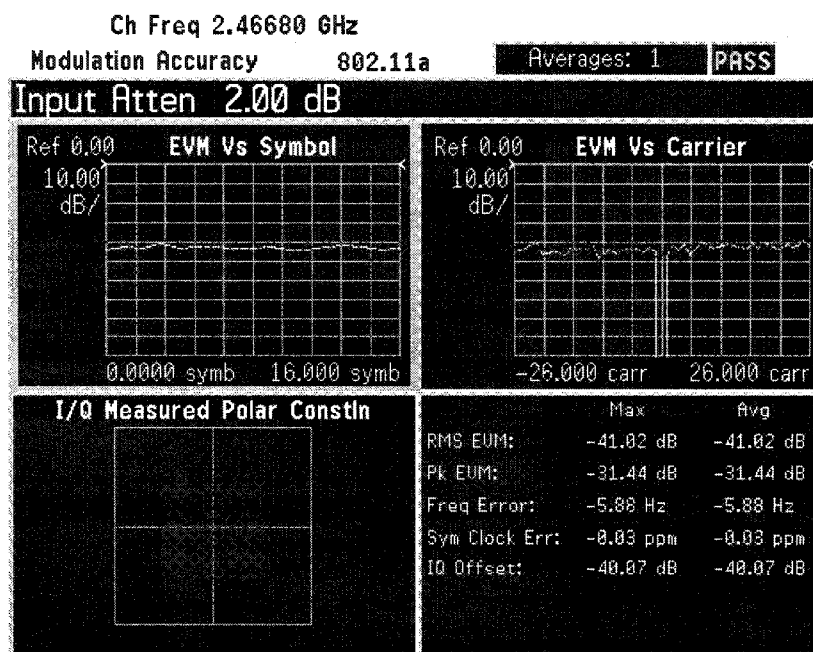


Figure 6-12 The receive EVM from direct modulating a DFECL

One shot of OFDM EVM measurement result of the received signal for directly modulating the long DFECL is shown in figure 6-12. The best RMS EVM can be better than -41dB, with the frequency error of 5.88 Hz, synchronize clock error of 0.03 ppm,

and IQ (In-phase component / quadrature component) offset of - 40 dB. The benefit from the frequency stability and phase noise of the DFECL is obvious.

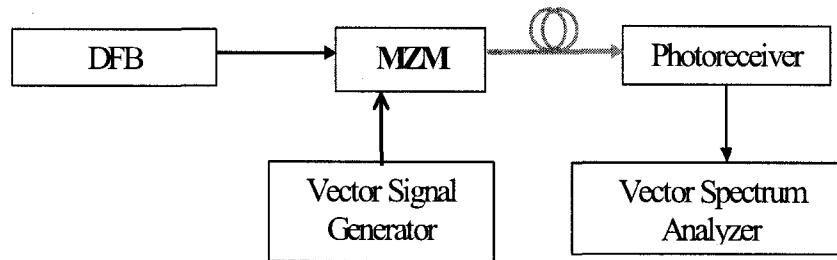


Figure 6-13 The external OFDM modulation setup

For comparison, a measurement was done with an externally-modulated source consisting of a DFB laser (with 5 dBm optical power) and Mach-Zehnder modulator (MZM) (figure 6-13). In this case the MZM bias was set at the quadrature point to suppress second harmonic distortion and increase the modulation efficiency. The detected optical powers on the photo-detector were +3 dBm for direct modulation and - 3.5 dBm for external modulation. There was a 6.5 dB difference because of the losses introduced by the external modulator. Figure 6-14 presents the EVM measurement results for the two setups and the electrical back-to-back EVM measurement with the VSG directly connected to the VSA.

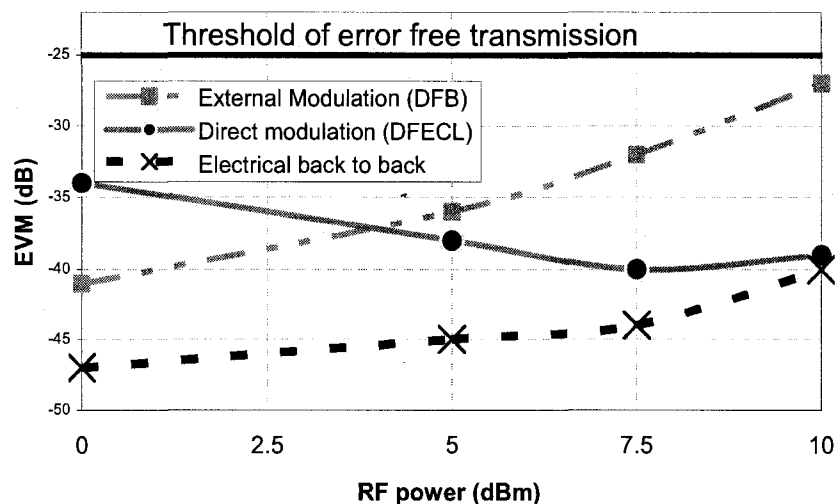


Figure 6-14 EVM measurements for DFECL direct modulation and DFB external modulation

The EVM degradation with increasing RF power for externally-modulated link is expected and is caused by MZ third-order distortion as reported in [Horvath and Frigyes 2005]. Meanwhile, the EVM decreased with RF power for direct modulating DFECL. This is because the RF power to the DFECL was still small relative to the high power pump laser. It is believed that the RF power could go even higher for direct modulation.

In contrast to the external modulation scheme, direct modulation is simple as it does not need an external modulator or an optical amplifier. It can provide high optical power. A pronounced improvement in signal quality is noted, for high RF power levels with EVM levelling off to the electrical back-to-back value at 10 dBm of input RF power. It is evident that the DFECL transmission has higher quality than the externally-modulated link for the ROF region of interest.

## 6.7 Conclusion

As a fundamental approach to microwave optical transmission, the direct modulation of a laser usually has high noise, and is limited by its modulation bandwidth. With mode-locking in a saturable absorber, the transmission response of direct modulation can be enhanced to the resonance frequency. Therefore, it is possible to directly modulate a laser with a narrow bandwidth radio frequency signal at a multiple of the cavity resonance frequency. The ultra long DFECL has very low noise but with a low resonance frequency, its modulation bandwidth is very small. With a doped fiber in the external cavity, it can have a good resonantly enhanced modulation frequency. The direct modulation transmission bandwidth of the DFECL can be extended to multiples of the round-trip resonance frequency of the external cavity.

We have experimentally verified that the DFECL can be applied with resonance enhancement by direct modulation. The  $\sim 2.4$  GHz RF signal transmission has been demonstrated with the DFECL at its 22<sup>nd</sup> multiple of the cavity round-trip resonance

frequency. The enhanced modulation bandwidth can be even higher, with better RF interface circuits and optimized cavity length and FBG bandwidth.

At the receiver, the transmitted microwave by directly modulating the DFECL was clearly observed and can be easily identified. No spectral distortion was observed over a 10 MHz bandwidth FM signal transmission with a  $\sim 2.4$  GHz RF carrier. There is not much spectrum distortion for 20 MHz bandwidth FM transmission. A high quality 64-QAM IEEE 802.11a signal was also transmitted by directly modulating this DFECL. The measured OFDM EVM was better than -41 dB.

The high quality 64-QAM IEEE 802.11a signal transmission experiment verified that the resonantly enhanced direct modulation is available for ROF applications. A benefit of the narrow line-width and stable wavelength the OFDM signal transmission by direct modulation of the DFECL shows very good EVM performance as has been demonstrated. It may be even better than external modulation in some operating conditions and always a lower cost solution in comparison. We conclude that this ultra-long DFECL can be used for narrowband wireless communication by simple direct modulation.

As there is a 25 dB (>300) peak to dip suppression, the DFECL may find possible application in multi-channel ROF transmission. By proper design of the cavity length and the reflectivity of the FBG, the transmission peaks can be made to match the specific frequencies of the transmission channels.



## **CHAPTER 7     FULLY DOPED FIBER DFECLS**

### **7.1 Introduction**

For a DFECL, the dynamic grating in doped fiber is one of the key factors to narrow the line-width and stabilise the wavelength. As discussed in chapter 3, a long dynamic grating has better effect for line-width narrowing. Meanwhile, due to the long cavity length, the mode spacing is very close, and high side mode suppression is difficult to realize. The previous study (in chapter 4) has shown that a long cavity DFECL has very small mode spacing, it is very difficult to suppress the nearest side modes, there are still a few side modes that remain.

In this chapter, a new improvement of the DFECL study is presented. A new DFECL was designed and built with almost 100% EDF in the external cavity of the DFECL.

### **7.2 Design of a fully EDF external cavity laser**

In order to decrease the mode number, the dynamic grating should occupy the entire cavity length. Theoretical analysis has indicated that occupying the external cavity with doped fiber can improve the SMSR. With very short SMF ( $< 5$  mm) in the external cavity, the calculation indicated that the optimized cavity length is in 0.1 – 0.3 m range, (as shown in figure 7-1). The shorter the length of un-doped fiber in the cavity, the better it is for reducing the number of oscillating modes. The existing external cavity mode number can be close to 2 as the bandwidth of dynamic grating is only a little bit wider than the mode spacing of the external cavity. It is possible to achieve single longitudinal mode operation with the appropriate tuning of the wavelength of the FBG to be at the centre of the bandwidth of the dynamic grating. Practically, since the FBG is not in EDF, the realized non-EDF length is about 5 mm long; the length of EDF for DFECL was selected with the range of 20 - 30 cm. A normal external cavity laser with the same cavity length and FBG will have a mode number of more than 50.

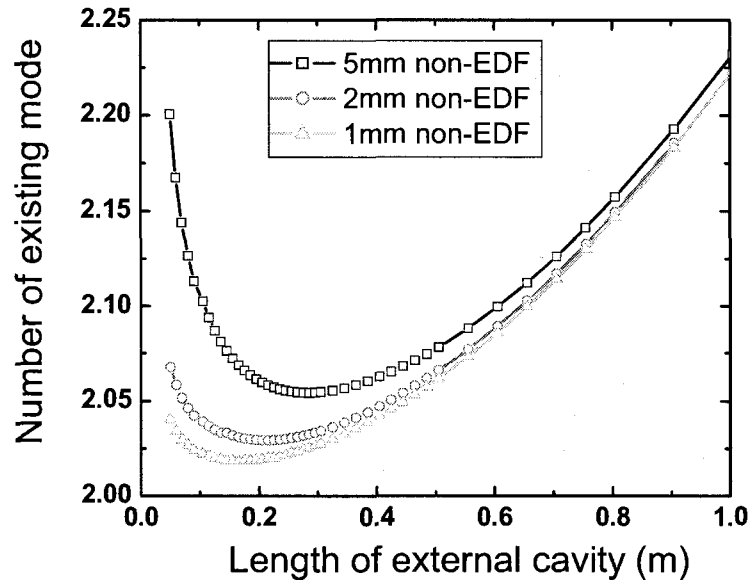


Figure 7-1 Calculation of the dynamic grating divided by the mode spacing in the DFECL

In order to realize a fully EDF occupied external cavity, technically, two problems need to be solved; light coupling between laser chip and the EDF has to be good, and so should the coupling between EDF and spliced external FBG, unless the FBG is written directly into the EDF. As the EDF was not very photosensitive, an external FBG was spliced to it, although ideally, an FBG in the EDF would have been preferable. The coupling between the laser chip and EDF can be realized by making a lens directly on EDF. Studies have shown that the fiber lens shape greatly influences the light coupling coefficient [Presby and Edwards 1992; Sambanthan and Rahman 2005; Sambanthan and Rahman 2005]. Although 100% coupling to a fiber using a hyperbolic lens is theoretically possible [Presby and Edwards 1992], a tapered hemispherically lens is a suitable alternative which may be realized in the lab, with a coupling efficiency ~50% [Sambanthan and Rahman 2005] or even more.

A standard optical fiber allows two orthogonal polarization modes of slightly different effective indexes. This polarization mode dispersion (PMD) becomes important when the line-width of the laser light is extremely narrow. Polarization

maintaining (PM) fiber is used to control the polarization and thus eliminates one polarized mode.

A schematic of the designed DFECL is shown in figure 7-2. The DFECL is almost 100% EDF in the external cavity. An angled facet chip is used as the semiconductor laser so that the reflection between the chip and EDF is very low.

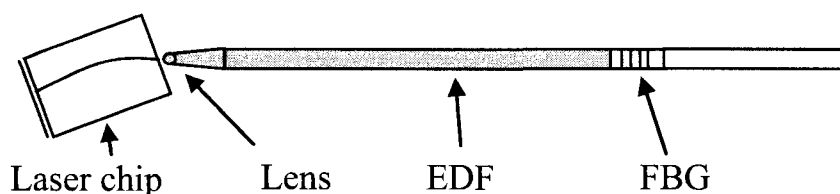


Figure 7-2 Schematic structure of fully EDF external cavity laser

### 7.3 Experiment and results

A fully EDF external cavity laser was built for this study. The high power semiconductor laser for this DFECL has angled facet gain chip. With 300 mA drive current, the total output power was 60 mW. The effective reflectivity of the output facet was less than 0.01%, and the rear facet had a reflectivity of about 90%.

The EDF used for the external cavity was from CorActive. The absorption of this EDF is  $\sim 30$  dB/m at  $\sim 1530$  nm wavelength. The absorption of this EDF can be bleached with high power narrow line-width laser. According to the calculation and also due to the strong absorption of this EDF, about 26 cm EDF was used for making the external cavity. This EDF is also polarization maintaining and the birefringence is greater than  $1.4 \times 10^{-4}$ . The fiber was oriented such that the polarization axes were aligned to the lasers polarization axes. A taper lens was made direct on this doped fiber for the coupling between the EDF and the laser chip and is shown in figure 6-16. The lens made on this EDF has focal length of about 45 microns. The focal length of this lens was deliberately made large so that it would not interfere with the alignment to an angled facet laser chip



Figure 7-3 Doped fiber lens for the DFECL

The FBG for this DFECL was centered at  $\sim 1528$  nm wavelength, with 0.2 nm reflective bandwidth, and the peak reflectivity was  $\sim 9$  dB. The FBG was located approximately 5 mm from the EDF end. Thus the external cavity could be considered to be comprised almost entirely of EDF.

The laser chip and fiber lens for DFECL under experiment were located on two Melles Griot six-axis Parallel Flexure Position Stages for precise position alignment. The laser was driven by ILX laser diode controller. The drive current was set to 300mA and temperature to 20 °C. With the best coupling alignment, this DFECL lased at  $\sim 1527.6$  nm. The maximum total power was measured to be more than 10 dBm. The light spectrum of the DFECL measured with optical spectrum analyzer (OSA) is shown in figure 7-4. The line-width of this laser is better than the OSA resolution (0.01 nm). The optical SMSR was better than 50 dB. As the length of the external cavity is around 26 cm, the external mode spacing is less than 400MHz. The external side mode could not be measured with this optical approach. Observed with an electrical spectrum analyzer (ESA), the beat notes of the oscillating modes on a photodetector are shown in figure 7-5. All of the self mode-beat notes were very low ( $< 70$  dBm), indicating the existence of only a single mode in the cavity.

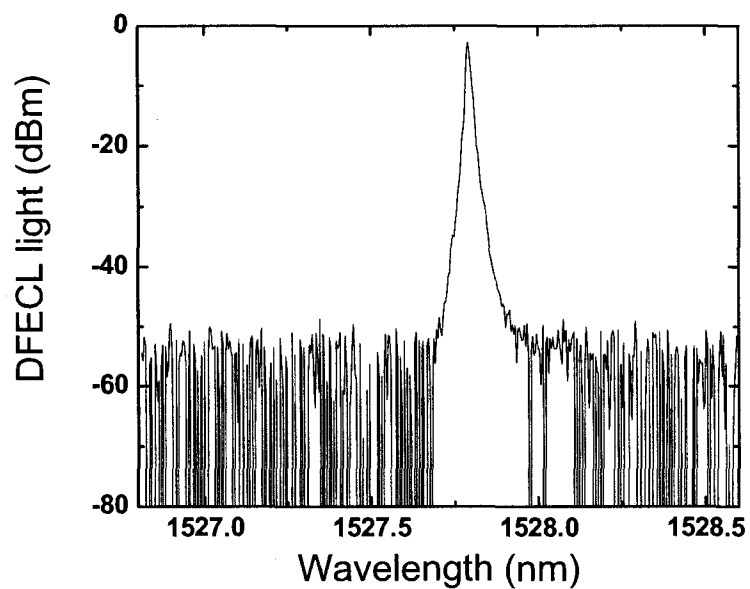


Figure 7-4 Optical spectrum of fully EDF external cavity laser

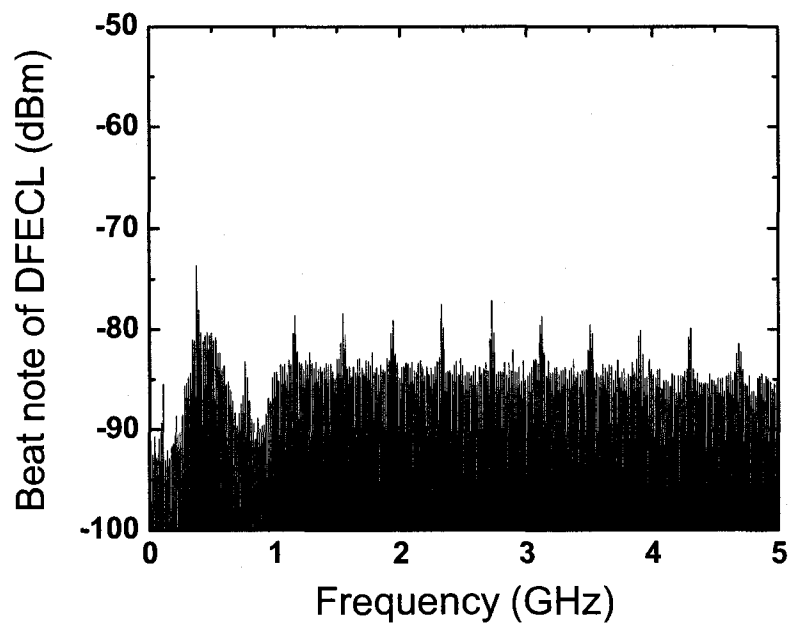


Figure 7-5 Self mode beat note of the fully EDF external laser

The external cavity SMSR of this DFECL was then measured by heterodyne beating with another single mode laser. An Anritsu MG9638a tuneable single mode laser was

used for this experiment. This tuneable laser has a line-width of  $\sim 700$  kHz, and its wavelength stability is better than 100MHz. The RF heterodyne beat note is shown in figure 7-6. As the tuneable laser is a single mode laser, the side modes in the beat notes are from the beating of the DFECL side modes with the tuneable laser. The mode spacing and the SMSR is equal to that of the DFECL. From the figure, it is noticed that the mode spacing is about 390 MHz, which is equivalent to the external cavity resonant frequency. The external cavity SMSR is more than 45 dB. The line-width of DFECL was measured by self mode-beating. As shown in figure 7-7, the -20 dB line-width of the beat note is about 7 kHz. If the light spectrum has a Lorentzian profile [Loh, Laming, Zervas, Farries, and Koren 1995b], the FWHM line-width is expected to be 350Hz.

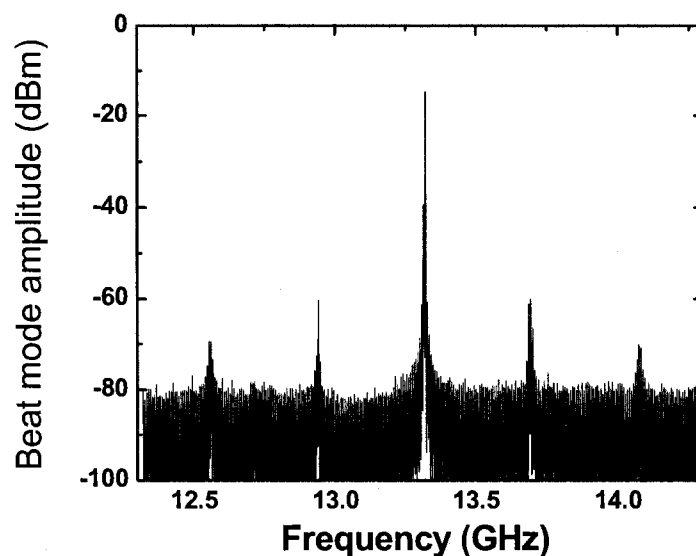


Figure 7-6 Spectrum of Beating the DFECL with a single mode tuneable laser

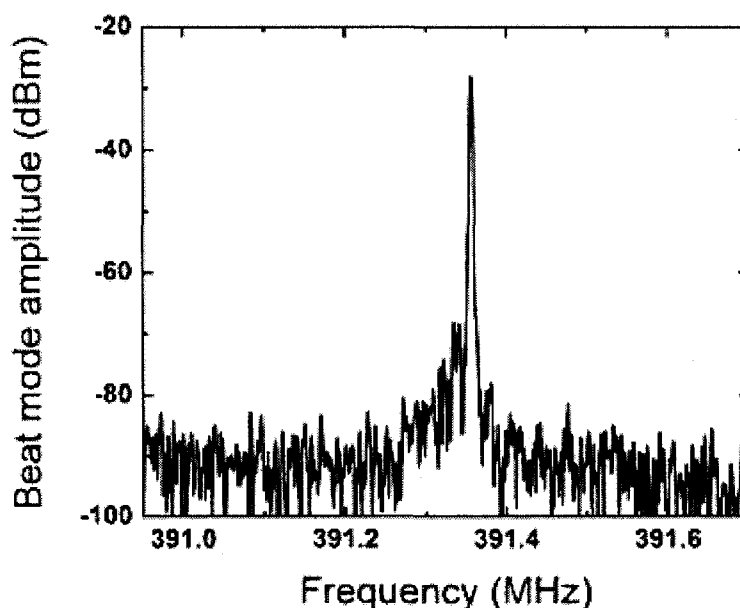


Figure 7-7 The line-width of DFECL measured with self beat note

During the experiment, it was also noticed that the mechanical stability of the coupling affects the operation of the laser output and its mode selection. Any perturbation destroys the dominant oscillating mode. With the best mechanical isolation, the RF heterodyne beat note of the DFECL and tuneable laser was found to be very stable, with less than 200 MHz frequency drift observed over tens of minutes. We believe that a complete EDF external cavity and a fully packaged laser would make it highly stable.

Compared with the DFECL in chapter 4, our new DFECL has an almost 100% EDF external cavity. With equal length of EDF, the external mode spacing is larger in our new laser. Thus, for the dynamic grating formed in EDF, it is easier to suppress the side mode and reach single mode operation. The experimental results have shown that this new almost fully EDF external cavity laser has better wavelength stability and side mode suppression performance.

## 7.4 Conclusion

The nearly fully doped fibre DFECL was built by making the lens directly on the EDF, and splicing an FBG very close to the EDF's other end. With properly designed parameters, the DFECL operated at  $\sim 1528$  nm wavelength. The DFECL demonstrated high power, stable wave length and narrow line-width. The great improvement of this DFECL is in the SMSR. Even though the external cavity mode spacing is less than 390 MHz, the measured SMSR is better than 45 dB, demonstrating the laser is capable of lasing in a single longitudinal mode, confirming the theoretical prediction.



## CHAPTER 8 CONCLUSION

### 8.1 Thesis overview

This thesis has focused on the analysis, design and demonstration of an ultra long doped fiber external cavity laser (DFECL), for the purposes of radio over fiber communication and fiber optic communication applications. The characteristics of the DFECL have been deeply studied after analysis and careful design and fabrication. Novel DFECLs were built at  $\sim 1490$  nm and  $\sim 1530$  nm wavelength for this study. The newly discovered features of the DFECL, such as side mode suppression, the tuneable wavelength, and resonantly enhanced direct modulation, are extremely important for the applications of this stable and narrow line-width laser.

Before this study, the studies of doped fiber were mainly focused on the application in fiber amplifier. As a saturable absorber, a doped fiber has also been used for fiber lasers. In the external cavity laser, doped fiber works on the different principle compared to the doped fiber amplifier, because there is no extra pump light. The doped fiber can be considered as self-pumped by the waves oscillating in the cavity.

The experiments studied in this project presented the different characteristics of the doped fiber in the case of self-pumped and inband pumped situations. Although the doped fiber has an absorption band, the result has shown that narrow line-width high power light can cause of the doped fiber absorption to bleach. High power light can propagate through the doped fiber with little power loss. The in-band pump experiment has shown that a high power narrow line-width light can cause whole band absorption bleaching. Even with the pump wavelength in the longer wavelength region, where the absorption is relative low; it can cause the absorption bleaching at the much shorter peak absorption wavelength. This characteristic indicates that an intensity change of a strong beam would change the whole bandwidth absorption, and therefore change the

transmission of other wavelengths within the band. This is an extremely important feature for the application of the doped fiber in the external cavity laser.

A derivation also presented the possible refractive index change if this doped fiber is applied to the DFECL. The refractive index change forms a dynamic grating in the doped fiber, and this is the mechanism for narrowing the line-width and stabilising the wavelength for DFECL.

The detailed fabrication of new DFECLs and the fundamental characteristics of the DFECL were presented. The DFECL has a long external cavity, with wavelength selective reflectors, and a saturable absorber in the cavity. The analysis presented that with the doped fiber absorption bleaching and thus absorption modulation, spatial hole burning in doped fiber can form a dynamic grating. The dynamic grating has an extra influence on the oscillating wave in the cavity, narrowing the line-width and stabilizing the wavelength.

In order to find out if the DFECL can work in the whole absorption region of the doped fiber, new DFECL lasers were designed and made. The new lasers worked at 1490 nm wavelength, at the edge of EDF absorption range. Measurements have shown that even at the 1490 nm wavelength, the DFECL also has good performances. The new DFECL has long term wavelength stability better than 5 pm and short term wavelength stability better than 1 pm. The line-width was very narrow, in the order of kilohertz. With self homodyne and heterodyne beating methods, it was shown that there are about 5-6 longitudinal modes remaining in the DFECL output spectrum, with the side mode suppression ratio of ~15-20 dB. The microwave optical generation was also demonstrated in experiments with the DFECL heterodyne beating.

Our experiments agreed with the theoretical analysis: there are only a few longitudinal modes inside the cavity of the DFECL instead of more than 100 modes in a similar ECL. The analysis also indicated that better DFECL could be realized by 100% doped fiber occupation of the external cavity with a suitable cavity length.

The study of DFECL wavelength tuneable performance was also presented. The long lifetime of erbium ions the doped fiber has a distinct advantage in slowing the response of the dynamic grating and for smoothing out environmentally induced fast frequency fluctuations. Meanwhile, the mode spacing of the long external cavity is very close, competing to be the dominant mode. The DFECL wavelength can be tuned slowly and constantly. The DFECL can be either tuned by the fiber Bragg grating over a wide range, or fine tuned with the dynamic grating. The wavelength tuning by the dynamic grating is realized by changing the dominant standing wave in the cavity.

The wavelength tuning performance by changing the driving current was measured by fixing the laser temperature. At 21°C, the lasing threshold is ~30 mA, and the mode-hop free range was approximately linear for about 60 pm with 160 mA drive current tuning. The slope of the laser frequency change vs. current is approximately 50MHz/mA. The DFECL wavelength tuning can also be realized with the control of temperature. The wavelength of DFECL can be tuned within the bandwidth of the external FBG (~100 pm), which is about 13 GHz, by tuning the semiconductor laser's temperature. Although temperature tuning does not have sufficient tuning resolution, in order to have high output power, it is possible to tune the wavelength of the DFECL by combined tuning of both the temperature and driving current. Since microwave photonic generation usually works from a few GHz to a few tens of GHz, this result shows that the direct optical tuning approach can provide a simple and inexpensive way for optically tuning the microwave frequency. It will also benefit in controlling fixed single frequency operation as it reduces the feedback loop control frequency of the electronics necessary for this operation.

Direct modulation was supposed to be a drawback of the DFECL, because of the ultra long cavity. The low round-trip resonance frequency of the DFECL limits the direct modulation bandwidth by normal approaches. Resonance enhanced direct modulation is an approach used to modulate a laser diode at a high frequency. With a saturable absorber and mode-locking, the highly enhanced transmission response of

direct modulation is extended to multiples of the resonant frequency. A narrow band radio frequency signal can be transmitted with direct modulation at a multiple of the external cavity resonant frequency. For long DFECL, with a doped fiber in the external cavity, it can have a good resonantly enhanced modulation performance. The transmission frequency of direct modulation of the DFECL is thus extended.

In experiments, we have verified that the DFECL can be used in the resonance enhanced direct modulation mode. The transmitted RF carrier was at the 22<sup>nd</sup> multiple of the cavity resonance frequency. At the receiver, the transmitted microwave was clear and could be easily identified. There is no spectral distortion for a 10 MHz bandwidth FM microwave transmission. There is only a little spectrum distortion with 20 MHz bandwidth FM transmission by directly modulating the DFECL. 64-QAM OFDM modulation signal was also transmitted by directly modulating this DFECL. The measured OFDM EVM was measured to be better than -41 dB, which is even better than most the microwave optical transmission systems with external modulation.

Finally, a new DFECL was presented with almost fully doped fiber in its external cavity. This DFECL has demonstrated with more than 45 dB SMSR. Its wavelength stability and line-width are also improved from our previous DFECL. This result has proved our theoretical analysis in the previous chapter. This is the first demo of a fully EDF laser.

## **8.2 Direction for future work**

The work presented in this thesis consisted of the comprehensive investigations into the characteristics of doped fiber, the analysis, design and implementation of a new DFECL.

The DFECL with fully doped fiber inside the external cavity presents better performance, and verifies the effect of dynamic grating. The experiment, analysis and

simulation have indicated that there are possible approaches to achieve narrow line-width single mode operation with good SMSR.

As the fully EDF laser's external cavity was assembled with mechanical coupling, it is found the stability is not very satisfactory. Better implementation is also needed to build this new DFECL. With a good packaging technique, the new DFECL would improve the characteristics. Drive current and operation temperature are two other factors affect the DFECL operation. The better stabilities of the power supplier and temperature might benefit the laser.

There should be more unique features of the DFECL and more future applications expected, for example in sensing and instrumentation. The results of direct modulating the DFECL at multiples of its cavity resonant frequency indicate that this DFECL can be used as high quality OFDM signal transmission at high frequency. In the aspect of direct modulation of DFECL, several works may be studied. Different data modulation schemes can be applied to this laser for characterizing the transmission. Making a better microwave interface circuit might be another worthwhile exercise, as the laser mount for the DFECL in this thesis has the modulation bandwidth limited to 2.5 GHz. Real 802.11a/g signal needs to be transmitted at 2.4 GHz and 5.8 GHz. If the drive circuit has a response more than 5.8 GHz, it will be possible to perform real 802.11a/g transmission experiments.

External modulation of the DFECL may also be a possible avenue of study. High power is one advantage of the DFECL, so that long distance fiber optic transmission without optical amplifiers could have a great benefit in lowering cost. The narrow line-width light would have a low dispersion penalty over long distance transmission.

Other optical approaches for narrowing the line-width and stabilising the laser, such as optical phase-locked loop (OPLL), may also be applied to this DFECL. As the OPLL has been reported to be a good way to stabilise the wavelength and the narrow line-width, the OPLL would also benefit the DFECL. Finally, the slow dynamic grating of DFECL

would help the OPLL as the bandwidth for the control loop would be much lower than for beat frequency sources using simple FGLs.

## REFERENCES

- AGRAWAL, G.P. 1984a. "Line narrowing in a single-mode injection laser due to external optical feedback". *IEEE Journal of Quantum Electronics*. QE-20:5. 468-71.
- AGRAWAL, G.P. 1984b. "Generalized rate equations and modulation characteristics of external-cavity semiconductor lasers". *Journal of Applied Physics*. 56:11. 3110-15.
- AGRAWAL, G.P. 1987. "Four-wave mixing and phase conjugation in semiconductor laser media". *Optics Letters*. 12: 4. 260-2.
- AGRAWAL, G.P. 2002. "Fiber-optic communication systems". *Wiley Interscience*. 3rd edition :
- AGRAWAL, G.P., DUTTA, N.K. 1993. "Semiconductor lasers". *Van Nostrand Reinhold*. 2nd edition :
- AGRAWAL, G.P., HENRY, C.H. 1988-. "Modulation performance of a semiconductor laser coupled to an external high Q resonator". *IEEE Journal of Quantum Electronics*. 24:2. 134-42.
- BALL, G.A., GLENN, W.H. 1992. "Design of a single-mode linear-cavity erbium fiber laser utilizing Bragg reflectors". *Journal of Lightwave Technology*. 10:10. 1338-43.
- BALL, G.A., MOREY, W.W. 1992. "Narrow linewidth fiber laser with integrated master oscillator power amplifier". *Proc. OFC 92*. OFC 92 : 97.
- BALL, G.A., MOREY, W.W. 1992. "Continuously tunable single-mode erbium fiber laser". *Optics Letters*. 17:6. 420-2.
- BARNES, W.L., MORKEL, P.R., REEKIE, L., PAYNE, D.N. 1989. "High-quantum-efficiency  $\text{Er}^{3+}$  fiber lasers pumped at 980 nm". *Optics Letters*. 14:18. 1002-4.
- BELLEMARE, A., LEMIEUX, J.-F., TETU, M., LAROCHELLE, S. 1998. "100 GHz step-tunable single-frequency erbium-doped fiber lasers [and application as frequency references for DWDM transmitters]". 3416, P. 220-8.
- BETTS, R.A., TJUGIARTO, T., XUE, Y.L., CHU, P.L. 1991. "Nonlinear refractive

- index in erbium doped optical fiber: Theory and experiment". *IEEE Journal of Quantum Electronics*. 27:4. 908-13.
- BIRD, D.M., ARMITAGE, J.R., KASHYAP, R., FATAH, R.M.A., CAMERON, K.H. 1991. "Narrow line semiconductor laser using fibre grating". *Electronics Letters*. 27:13. 1115-16.
- BISWAS, B.N., BHATTACHARYA, A. 2001. "Optical generation of microwave signal through heterodyne optical PLL". P. 207-17.
- BOLSHTYANSKY, M. 2003. "Spectral hole burning in erbium-doped fiber amplifiers". *Journal of Lightwave Technology*. 21:4. 1032-8.
- BORDONALLI, A.C., WALTON, C., SEEDS, A.J. 1996. "High-performance homodyne optical injection phase-lock loop using wide-linewidth semiconductor lasers". *IEEE Photonics Technology Letters*. 8:9. 1217-19.
- BORDONALLI, A.C., WALTON, C., SEEDS, A.J. 1999. "High-performance phase locking of wide linewidth semiconductor lasers by combined use of optical injection locking and optical phase-lock loop". *Journal of Lightwave Technology*. 17:2. 328-42.
- BOUYER, P., GUSTAVSON, T.L., HARITOS, K.G., KASEVICH, M.A. 1996. "Microwave signal generation with optical injection locking". *Optics Letters*. 21:18. 1502-4.
- BRINKMEYER, E., BRENNECKE, W., ZUERN, M., ULRICH, R. 1986. "FIBRE BRAGG REFLECTOR FOR MODE SELECTION AND LINE-NARROWING OF INJECTION LASER.". *Electronics Letters*. 22:3. 134-135.
- CAMPBELL, R.J., ARMITAGE, J.R., SHERLOCK, G., WILLIAMS, D.L., PAYNE, R., ROBERTSON, M. et al. 1996. "Wavelength stable uncooled fibre grating semiconductor laser for use in an all optical WDM access network". *Electronics Letters*. 32:2. 119-20.
- CHEN, D., FETTERMAN, H.R., CHEN, A., STEIER, W.H., DALTON, L.R., WANG, W. et al. 1997. "Demonstration of 110 GHz electro-optic polymer modulators". *Applied Physics Letters*. 70:25. 3335-3337.
- CHIBA, A.1., FUJIWARA, H.1., HOTTA, J.1., TAKEUCHI, S.1., SASAKI, K.1. 2003. "Fine frequency tuning of a microspherical cavity by temperature control". P. 690.
- CIMINI, L.J.Jr. 1985. "Analysis and simulation of a digital mobile channel using orthogonal frequency division multiplexing". *IEEE Transactions on Communications*. CM-33:7. 665-75.



- COOPER, A.J. 1990. "'Fibre/radio' for the provision of cordless/mobile telephony services in the access network". *Electronics Letters*. 26:24. 2054-6.
- COQUIN, G.A., CHEUNG, K.W. 1988. "Electronically tunable external-cavity semiconductor laser". *Electronics Letters*. 24:10. 599-600.
- COX, C.H.I., BETTS, G.E., JOHNSON, L.M. 1990. "An analytic and experimental comparison of direct and external modulation in analog fiber-optic links". *IEEE Transactions on Microwave Theory and Techniques*. 38:5. 501-9.
- DANDRIDGE, A., GOLDBERG, L. 1982. "CURRENT-INDUCED FREQUENCY MODULATION IN DIODE LASERS.". *Electronics Letters*. 18:7. 302-304.
- DELORME, F. 1998. "Widely tunable 1.55 $\mu$ m lasers for wavelength-division-multiplexed optical fiber communications". *IEEE Journal of Quantum Electronics*. 34:9. 1706-16.
- DERICKSON, D. 1998. "Fiber optic test and measurement". *Prentice Hall PRT*.
- DESURVIRE, E. 1990. "Study of the complex atomic susceptibility of erbium-doped fiber amplifiers". *Journal of Lightwave Technology*. 8:10. 1517-27.
- DESURVIRE, E. 1991. "Erbium-doped fiber amplifiers: basic physics and theoretical modeling". *International Journal of High Speed Electronics*. 2:1-2. 89-114.
- DESURVIRE, E. 2002. "Erbium doped fiber amplifiers: principles and applications". *Wiley Interscience*.
- DESURVIRE, E., SIMPSON, J.R. 1990. "Evaluation of  $^4I_{15/2}$  and  $^4I_{13/2}$  Stark-level energies in erbium-doped aluminosilicate glass fibers". *Optics Letters*. 15:10. 547-9.
- DESURVIRE, E., SIMPSON, J.R., BECKER, P.C. 1987. "High-gain erbium-doped traveling-wave fiber amplifier". *Optics Letters*. 12:11. 888-90.
- DESURVIRE, E., ZYSKIND, J.L., SIMPSON, J.R. 1990. "Spectral gain hole-burning at 1.53  $\mu$ m in erbium-doped fiber amplifiers". *IEEE Photonics Technology Letters*. 2:4. 246-8.
- DESURVIRE, E.1., GILES, C.R.1., SIMPSON, J.R. 1989. "Gain saturation effects in high-speed, multichannel erbium-doped fiber amplifiers at  $\lambda=1.53 \mu$ m". *Journal of Lightwave Technology*. 7:12. 2095-104.
- DIGONNET, M.J.F., GAETA, C.J. 1985. "Theoretical analysis of optical fiber laser

- amplifiers and oscillators". *Applied Optics*. 24:3. 333-42.
- DODS, S.R.A., OGURA, M., WATANABE, M. 1993. "Small-signal analysis of semiconductor lasers modulated at frequencies on the order of the beat frequency". *IEEE Journal of Quantum Electronics*. 29:10. 2631-8.
- DOERR, C.R. 1996. "Direct modulation of long-cavity semiconductor lasers". *Journal of Lightwave Technology*. 14:9. 2052-61.
- ENLOE, J.H., RODDA, J.L. 1965. "Laser phase locked loop". *Proceedings of the IEEE*. 53:2. 165-166.
- FISCHER, B., ZYSKIND, J.I., SULHOFF, J.W., DIGIOVANNI, D.J. 1993. "Nonlinear wave mixing and induced gratings in erbium-doped fiber amplifiers". *Optics Letters*. 18:24. 2108-10.
- FLEMING, M.W., MOORADIAN, A. 1981. "Spectral characteristics of external-cavity controlled semiconductor lasers". *IEEE Journal of Quantum Electronics*. QE-17:1. 44-59.
- FLEMING, S.C., WHITLEY, T.J. 1996. "Measurement and analysis of pump-dependent refractive index and dispersion effects in erbium-doped fiber amplifiers". *IEEE Journal of Quantum Electronics*. 32:7. 1113-21.
- FLETCHER, C.S.1., CLOSE, J.D.1. 2004-. "Extended temperature tuning of an external cavity diode laser". *Applied Physics B (Lasers and Optics)*. B78:3-4. 305-13.
- FRISKEN, S.J. 1992. "Transient Bragg reflection gratings in erbium-doped fiber amplifiers". *Optics Letters*. 17:24. 1776-8.
- GEORGES, J.B., WU, T.C., CUTRER, D.M., KOREN, U., KOCH, T.L., LAU, K.Y. 1995. "Millimeter-wave optical transmitter at 45 GHz by resonant modulation of a monolithic tunable DBR laser". P. 337-8.
- GEORGES, J.B., CUTRER, D.M., SOLGAARD, O., LAU, K.Y. 1995. "Optical transmission of narrowband millimeter-wave signals". *IEEE Transactions on Microwave Theory and Techniques*. 43:9/2. 2229-2240.
- GILES, C.R., DESURVIRE, E. 1991. "Modeling erbium-doped fiber amplifiers". *Journal of Lightwave Technology*. 9:2. 271-83.
- GODARD, A., PAULIAT, G., ROOSEN, G., DUCLOUX, E. 2004. "Modal competition via four-wave mixing in single-mode extended-cavity semiconductor lasers". *IEEE Journal of Quantum Electronics*. 40: 8. 970-81.

- GOLDBERG, L., TAYLOR, H.F., WELLER, J.F., BLOOM, D.M. 1983. "Microwave signal generation with injection-locked laser diodes". *Electronics Letters*. 19:13. 491-3.
- GOLDBERG, L., YUREK, A.M., TAYLOR, H.F., WELLER, J.F. 1985. "35 GHz microwave signal generation with an injection-locked laser diode". *Electronics Letters*. 21:18. 814-15.
- GRANT, M.A., MICHIE, W.C., FLETCHER, M.J. 1987. "The performance of optical phase-locked loops in the presence of nonnegligible loop propagation delay". *Journal of Lightwave Technology*. T-5: 4. 592-7.
- GUOHUA QI, JIANPING YAO, SEREGELYI, J., PAQUET, S., BELISLE, C., XIUPU ZHANG et al. 2006. "Phase-noise analysis of optically generated millimeter-wave signals with external optical modulation techniques". *Journal of Lightwave Technology*. 24:12. 4861-75.
- GUY, M.J., TAYLOR, J.R., KASHYAP, R. 1995. "Single-frequency erbium fibre ring laser with intracavity phase-shifted fibre Bragg grating narrowband filter". *Electronics Letters*. 31:22. 1924-1925.
- HANSMANN, S., WALTER, H., HILLMER, H., BURKHARD, H. 1994. "Static and dynamic properties of InGaAsP-InP distributed feedback lasers-a detailed comparison between experiment and theory". *IEEE Journal of Quantum Electronics*. 30:11. 2477-84.
- HASHIMOTO, J.I., TAKAGI, T., KATO, T., SASAKI, G., SHIGEHARA, M., MURASHIMA, K. et al. 2003. "Fiber-Bragg-grating external cavity semiconductor laser (FGL) module for DWDM transmission". *Journal of Lightwave Technology*. 21:9. 2002-9.
- HAUS, H.A.1. 1981. "Modelocking of semiconductor laser diodes". *Japanese Journal of Applied Physics*. 20:6. 1007-20.
- HAUS, H.A.1., MECOZZI, A.1. 1993. "Noise of mode-locked lasers". *IEEE Journal of Quantum Electronics*. 29:3. 983-96.
- HAYASHI, I., PANISH, M.B., FOY, P.W. 1969. "A low-threshold room-temperature injection laser". *IEEE Journal of Quantum Electronics*. QE-5:5. 211-2.
- HAYASHI, I., PANISH, M.B., FOY, P.W., SUMSKI, S. 1970. "Junction lasers which operate continuously at room temperature". *Applied Physics Letters*. 17:3. 109-11.
- HENRY, C.H. 1982. "Theory of the linewidth of semiconductor lasers". *IEEE Journal of Quantum Electronics*. QE-18:2. 259-64.

- HENRY, C.H. 1983. "Theory of the phase noise and power spectrum of a single mode injection laser". *IEEE Journal of Quantum Electronics*. QE-19:9. 1391-7.
- HENRY, C.H. 1986. "Phase noise in semiconductor lasers". *Journal of Lightwave Technology*. T-4:3. 298-311.
- HENRY, C.H., KAZARINOV, R.F. 1986. "Instability of semiconductor lasers due to optical feedback from distant reflectors". *IEEE Journal of Quantum Electronics*. QE-22:2 . 294-301.
- HORVATH, N., FRIGYES, I. 2005. "Effects of the nonlinearity of a Mach-Zehnder modulator on OFDM radio-over-fiber transmission". *IEEE Communications Letters*. 9:10. 921-3.
- HUI, R., D'OTTAVI, A., MECOZZI, A., SPANO, P. 1991. "Injection locking in distributed feedback semiconductor lasers". *IEEE Journal of Quantum Electronics*. 27:6. 1688-95.
- IKEGAMI, T., SUEMATSU, Y. 1968. "Carrier lifetime measurement of a junction laser using direct modulation". *IEEE Journal of Quantum Electronics*. QE-4:4. 148-151.
- JANOS, M., MINASIAN, R.A. 1997. "Measurement of pump-induced refractive index changes in erbium-doped optical fibre". *Electronics Letters*. 33:1. 78-80.
- JANOS, M., GUY, S.C. 1998. "Signal-induced refractive index changes in erbium-doped fiber amplifiers". *Journal of Lightwave Technology*. 16:4. 542-548.
- JAVAN, A., BENNETT, W.R.Jr., HERRIOTT, D.R. 1961. "Population inversion and continuous optical maser oscillation in a gas discharge containing A He-Ne mixture". *Physical Review Letters*. 6:3. 106-110.
- JOHANSSON, L.A., SEEDS, A.J. 2001. "Multi-octave photonic RF synthesiser based on two DFB lasers". P. 97-9.
- JOINDOT, I. 1992. "Measurements of relative intensity noise (RIN) in semiconductor lasers". *Journal de Physique III (Applied Physics, Materials Science, Fluids, Plasma and Instrumentation)*. 2:9. 1591-603.
- JONES, R.J.1., SPENCER, P.S.1., LAWRENCE, J., KANE, D.M. 2001. "Influence of external cavity length on the coherence collapse regime in laser diodes subject to optical feedback". *IEE Proceedings-Optoelectronics*. 148:1. 7-12.
- JUN WANG, FEI ZENG, JIANPING YAO 2005. "All-optical microwave bandpass filter with negative coefficients based on PM-IM conversion". *IEEE Photonics*

- Technology Letters*. 17:10. 2176-8.
- JUN WANG, JIANPING YAO 2006. "A tunable photonic microwave notch filter based on all-optical mixing". *IEEE Photonics Technology Letters*. 18:2. 382-4.
- KASHYAP, R. 1999. "Fiber Bragg Grating". *Academic Press*.
- KASHYAP, R., ARMITAGE, J.R., WYATT, R., DAVEY, S.T., WILLIAMS, D.L. 1990. "All-fibre narrowband reflection gratings at 1500 nm". *Electronics Letters*. 26:11. 730-2.
- KASHYAP, R., PAYNE, R.A., WHITLEY, T.J., SHERLOCK, G. 1994. "Wavelength-uncommitted lasers". *Electronics Letters*. 30:13. 1065-7.
- KAZARINOV, R.F., HENRY, C.H. 1987. "The relation of line narrowing and chirp reduction resulting from the coupling of a semiconductor laser to passive resonator". *IEEE Journal of Quantum Electronics*. QE-23:9. 1401-9.
- KAZARINOV, R.F., HENRY, C.H., LOGAN, R.A. 1982. "Longitudinal mode self-stabilization in semiconductor lasers". *Journal of Applied Physics*. 53:7. 4631-44.
- KAZOVSKY, L.G., JENSEN, B. 1990. "Experimental relative frequency stabilization of a set of lasers using optical phase-locked loops". *IEEE Photonics Technology Letters*. 2:7. 516-18.
- KNODL, T.1., HANKE, C.1., SARAVANAN, B.K.1., PESCHKE, M.1., MACALUSO, R.1., STEGMULLER, B.1. 2004. "40 GHz monolithic integrated 1.3  $\mu\text{m}$  InGaAlAs-InP laser-modulator with double-stack MQW layer structure". Vol.2, P. 675-6.
- KOSTKO, I.A., KASHYAP, R. 2004. "Modeling of self-organized coherence-collapsed and enhanced regime semiconductor fibre grating reflector lasers". SPIE 5579, P. 367-74.
- KOSTKO, I.A., KASHYAP, R. 2006. "Dynamics of ultimate spectral narrowing in a semiconductor fiber-grating laser with an intra-cavity saturable absorber". *Optics Express*. 14:7.
- KOSTKO, I.A., KASHYAP, R. 2006. "Dynamics of ultimate spectral narrowing in a semiconductor fiber-grating laser with an intracavity saturable absorber". *Optics Express*. 14:7. 2706-2714.
- LAMING, R.I., POOLE, S.B., TARBOX, E.J. 1988. "Pump excited-state absorption in erbium-doped fibers". *Optics Letters*. 13:12. 1084-6.

- LAMING, R.I., REEKIE, L., MORKEL, P.R., PAYNE, D.N. 1989. "Multichannel crosstalk and pump noise characterisation of Er<sup>3+</sup>-doped fibre amplifier pumped at 980 nm". *Electronics Letters*. 25:7. 455-456.
- LAPERLE, C., SVILANS, M., POIRIER, M., TETU, M. 1999. "Frequency multiplication of microwave signals by sideband optical injection locking using a monolithic dual-wavelength DFB laser device". *IEEE Transactions on Microwave Theory and Techniques*. 47:7. 1219-24.
- LAU, K.Y. 1990. "Narrow-band modulation of semiconductor lasers at millimeter wave frequencies (100 GHz) by mode locking". *IEEE Journal of Quantum Electronics*. 26:2. 250-61.
- LAU, K.Y., YARIV, A. 1985. "Direct modulation and active mode locking of ultrahigh speed GaAlAs lasers at frequencies up to 18 GHz". *Applied Physics Letters*. 46:4. 326-8.
- LAX, M., LOUISELL, W.H. 1967. "Quantum noise IX: Quantum Fokker-Planck solution for laser noise". *IEEE Journal of Quantum Electronics*. QE-3:2. 47-58.
- LIDOYNE, O., GALLION, P., CHABRAN, C., DEBARGE, G. 1990. "Locking range, phase noise and power spectrum of an injection-locked semiconductor laser". *IEE Proceedings J (Optoelectronics)*. 137:3. 147-54.
- LIU, R.N., KOSTKO, I.A., KASHYAP, R., WU, K., KIIVERI, P. 2005. "Inband-pumped, broadband bleaching of absorption and refractive index changes in erbium-doped fiber". *Optics Communications*. 255:1-3. 65-71.
- LOH, W.H., LAMING, R.I., ZERVAS, M.N., FARRIES, M.C., KOREN, U. 1995a. "Novel hybrid single frequency semiconductor laser with erbium fibre-based external cavity". 1, P. 135-138.
- LOH, W.H., LAMING, R.I., ZERVAS, M.N., FARRIES, M.C., KOREN, U. 1995b. "Single frequency erbium fiber external cavity semiconductor laser". *Applied Physics Letters*. 66:25. 3422-4.
- MADHUMITA BHATTACHARYA, ANUJ KUMAR SAW, TARAPRASAD CHATTOPADHYAY 2003. "Optical generation of mm-wave signal through optoelectronic phase-locked loop". 23, P. 391-2.
- MAIMAN, T.H. 1960. "Optical maser action in ruby". *British Communications and Electronics*. 7:9. 674-675.
- MANTZ, A.W. 1995. "A review of spectroscopic applications of tunable semiconductor lasers". *Spectrochimica Acta, Part A (Molecular Spectroscopy)*. 51A:13. 2211-36.

- MAY, Th., ROHLING, H., ENGELS, V. 1998. "Performance analysis of Viterbi decoding for 64-DAPSK and 64-QAM modulated OFDM signals". *IEEE Transactions on Communications*. 46:2. 182-190.
- MERRETT, R.P., COOPER, A.J., SYMINGTON, I.C. 1991. "A cordless access system using radio-over-fibre techniques". P. 921-4.
- MINISCALCO, W.J. 1991. "Erbium-doped glasses for fiber amplifiers at 1500 nm". *Journal of Lightwave Technology*. 9:2. 234-250.
- MITA, Y., YOSHIDA, T., YAGAMI, T., SHIONOYA, S. 1992. "Luminescence and relaxation processes in  $\text{Er}^{3+}$ -doped glass fibers". *Journal of Applied Physics*. 71:2. 938-41.
- MIZRAHI, V., DIGIOVANNI, D.J., ATKINS, R.M., GRUBB, S.G., YONG-KWAN PARK, DELAVALUX, J.-M.P. 1993. "Stable single-mode erbium fiber-grating laser for digital communication". *Journal of Lightwave Technology*. 11:12. 2021-5.
- MIZRAHI, V., DIGIOVANNI, D.J., ATKINS, R.M., GRUBB, S.G., PARK, Y.-K., DELAVALUX, J.-M.P. 1993. "Stable single-mode erbium fiber-grating laser for digital communication". *Journal of Lightwave Technology*. 11:12. 2021-2025.
- MORKEL, P.R., LAMING, R.I. 1989. "Theoretical modeling of erbium-doped fiber amplifiers with excited-state absorption". *Optics Letters*. 14:19. 1062-4.
- MOSES, E.I., TURNER, J.J., TANG, C.L. 1976. "Mode-locking of laser oscillators by injection-locking". 18, P. 23-4.
- NAGARAJAN, R., LEVY, S., BOWERS, J.E. 1994. "Millimeter wave narrowband optical fiber links using external cavity semiconductor lasers". *Journal of Lightwave Technology*. 12:1. 127-36.
- NOGUCHI, K., MITOMI, O., MIYAZAWA, H. 1998. "Millimeter-wave  $\text{Ti:LiNbO}_3$  optical modulators". *Journal of Lightwave Technology*. 16:4. 615-19.
- O'REILLY, J.J., LANE, P.M., HEIDEMANN, R., HOFSTETTER, R. 1992. "Optical generation of very narrow linewidth millimetre wave signals". *Electronics Letters*. 28:25. 2309-2311.
- OGAWA, H., POLIFKO, D., BANBA, S. 1992. "Millimeter-wave fiber optics systems for personal radio communication". *IEEE Transactions on Microwave Theory and Techniques*. 40:12. 2285-93.
- OLESEN, H., JACOBSEN, G. 1982. "A theoretical and experimental analysis of modulated laser fields and power spectra". *IEEE Journal of Quantum Electronics*.

QE-18:12. 2069-80.

OLSSON, N.A., HENRY, C.H., KAZARINOV, R.F., LEE, H.J., JOHNSON, B.H. 1987. "Relation between chirp and linewidth reduction in external Bragg reflector semiconductor lasers". *Applied Physics Letters*. 51:2. 92-3.

PAN, J.J., YUAN SHI 1995. "Tunable  $\text{Er}^{3+}$ -doped fibre ring laser using fibre grating incorporated by optical circulator or fibre coupler". *Electronics Letters*. 31:14. 1164-5.

PAOLI, T.L., RIPPER, J.E. 1970. "Direct modulation of semiconductor lasers". *Proceedings of the IEEE*. 58:10. 1457-65.

PARK, C.A., ROWE, C.J., BUUS, J., REID, D.C.J., CARTER, A., BENNION, I. 1986. "SINGLE-MODE BEHAVIOUR OF A MULTIMODE 1.55  $\mu\text{m}$  LASER WITH A FIBRE GRATING EXTERNAL CAVITY.". *Electronics Letters*. 22:21. 1132-1134.

PRESBY, H.M., EDWARDS, C.A. 1992. "Near 100% efficient fibre microlenses". *Electronics Letters*. 28:6. 582-584.

RAMOS, R.T., SEEDS, A.J. 1990. "Delay, linewidth and bandwidth limitations in optical phase-locked loop design". *Electronics Letters*. 26:6. 389-91.

RAMOS, R.T., SEEDS, A.J. 1992. "Fast heterodyne optical phase-lock loop using double quantum well laser diodes". *Electronics Letters*. 28:1. 82-3.

RICHARDS, D.H., JACKEL, J.L., ALI, M.A. 1998. "Multichannel EDFA chain control: A comparison of two all-optical approaches". *IEEE Photonics Technology Letters*. 10:1. 156-158.

ROHLING, H., MAY, T., BRUENINGHAUS, K., GRUENHEID, R. 1999. "Broad-band OFDM radio transmission for multimedia applications". *Proceedings of the IEEE*. 87:10. 1778-1789.

ROUSSELL, H.I., HELKEY, R.I., BETTS, G.I., COX, C.I. 1997. "Effect of optical feedback on high-dynamic-range Fabry-Perot laser optical links". *IEEE Photonics Technology Letters*. 9:1. 106-8.

RUDKEVICH, E., BANEY, D.M., STIMPLE, J., DERICKSON, D., WANG, G. 1999. "Nonresonant spectral-hole burning in erbium-doped fiber amplifiers". *IEEE Photonics Technology Letters*. 11:5. 542-4.

SAKAMOTO, S.R., SPICKERMANN, R., DAGLI, N. 1995. "Narrow gap coplanar slow wave electrode for travelling wave electro-optic modulators". *Electronics Letters*. 31:14. 1183-5.



- SALEH, B.E.A., TEICH, M.C. 1991. "Fundamentals of Photonics". New York: Wiley-Interscience.
- SAMBANTHAN, K., RAHMAN, F.A. 2005. "Method to improve the coupling efficiency of a hemispherically lensed asymmetric tapered-core fiber". *Optics Communications*. 254:1-3. 112-118.
- SARKER, B.C., YOSHINO, T., MAJUMDER, S.P. 2004. "Bit error rate performance of an optical IM-DD transmission system with wavelength converter". *Journal of Optical Communications*. 25:1. 14-19.
- SCHREMER, A.T., TANG, C.L. 1990. "External-cavity semiconductor laser with 1000 GHz continuous piezoelectric tuning range". *IEEE Photonics Technology Letters*. 2:1. 3-5.
- SCRIVENER, P.L., TARBOX, E.J., MATON, P.D. 1989. "Narrow linewidth tunable operation of  $\text{Er}^{3+}$ -doped single-mode fibre laser". *Electronics Letters*. 25:8. 549-50.
- SEEDS, A.J. 2002. "Microwave photonics". *IEEE Transactions on Microwave Theory and Techniques*. 50:3. 877-87.
- SHIMIZU, M., YAMADA, M., HORIGUCHI, M., TAKESHITA, T., OKAYASU, M. 1990. "Erbium-doped fibre amplifiers with an extremely high gain coefficient of 11.0 dB/mW". *Electronics Letters*. 26:20. 1641-3.
- SIEGMAN, A.E. 1986. "Lasers". University science books.
- SIMONIS, G.J., PURCHASE, K.G. 1990. "Optical generation, distribution, and control of microwaves using laser heterodyne". *IEEE Transactions on Microwave Theory and Techniques*. 38:5. 667-9.
- SIMONS, R. 1990. "Optical Control of Microwave Device". Norwood, Artch House.
- SISTO, M.M., LAROCHELLE, S., RUSCH, L.A. 2006. "Gain optimization by modulator-bias control in radio-over-fiber links". *Journal of Lightwave Technology*. 24:12. 4974-82.
- SORIN, W.V., NEWTON, S.A. 1988. "Single-frequency output from a broadband-tunable external fiber-cavity laser". *Optics Letters*. 13:9. 731-3.
- SPANO, P., PIAZZOLLA, S., TAMBURRINI, M. 1985. "Measurements of the injection-locking influence on the frequency noise spectrum of single-mode

- semiconductor lasers". *Optics Letters*. 10:11. 556-8.
- SRIVASTAVA, A.K.1., ZYSKIND, J.L.1., SULHOFF, J.W.1., EVANKOW, J.D.Jr.1., MILLS, M.A.1. 1996. "Room temperature spectral hole-burning in erbium-doped fiber amplifiers". P. 33-4.
- STATZ, H., TANG, C.L., LAVINE, J.M. 1964. "Spectral output of semiconductor lasers". *Journal of Applied Physics*. 35:9. 2581-2585.
- STEELE, R.C. 1983. "Optical phase-locked loop using semiconductor laser diodes". *Electronics Letters*. 19:2. 69-71.
- STEPHENS, W.E., JOSEPH, T.R., CHEN, B.U. 1984. "Analog microwave fiber optic communications links". P. 533-4.
- STRZELECKI, E.M., COHEN, D.A., COLDREN, L.A. 1988. "Investigation of tunable single frequency diode lasers for sensor applications". 6, P. 1610-18.
- SULHOFF, J.W., SRIVASTAVA, A.K., WOLF, C., SUN, Y., ZYSKIND, J.L. 1997. "Spectral-hole burning in erbium-doped silica and fluoride fibers". *IEEE Photonics Technology Letters*. 9:12. 1578-9.
- THIRSTRUP, C., SHI, Y., PALSDOTTIR, B. 1996. "Pump-induced refractive index modulation and dispersions in  $\text{Er}^{3+}$ -doped fibers". *Journal of Lightwave Technology*. 14:5. 732-738.
- TIMOFEEV, F.N., BAYVEL, P., MIDWINTER, J.E., WYATT, R., KASHYAP, R., ROBERTSON, M. 1997. "2.6 Gbit/s dense WDM transmission in standard fibre using directly-modulated fibre grating lasers". *Electronics Letters*. 33:19. 1632-3.
- TIMOFEEV, F.N., BAYVEL, P., MIKHAILOV, V., LAVROVA, O.A., WYATT, R., KASHYAP, R. et al. 1997. "2.5 Gbit/s directly-modulated fibre grating laser for WDM networks". *Electronics Letters*. 33:16. 1406-7.
- TIMOFEEV, F.N., BAYVEL, P., WYATT, R., KASHYAP, R., LEALMAN, I.F., MAXWELL, G.D. 1998. "10 Gbit/s directly-modulated, high temperature-stability, external fibre grating laser for dense WDM networks". 2, P. 360-361.
- TIMOFEEV, F.N., KASHYAP, R. 2003. "High-power, ultra-stable, single-frequency operation of a long, doped-fiber external-cavity, grating-semiconductor laser". *Optics Express*. 11:6.
- TIMOFEEV, F.N., KOSTKO, I.A., BAYVEL, P., BERGER, O., WYATT, R., KASHYAP, R. et al. 1999. "10 Gbit/s directly modulated, high temperature-stability external fibre grating laser for dense WDM networks". *Electronics Letters*.

35:20. 1737-1739.

TIMOFEEV, F.N., SIMIN, G.S., SHATALOV, M.S., GUREVICH, S.A., BAYVEL, P., WYATT, R. et al. 2000a. "Experimental and theoretical study of high temperature-stability and low-chirp 1.55  $\mu\text{m}$  semiconductor laser with an external fiber grating". *Fiber and Integrated Optics*. 19:4. 327-53.

VAHALA, K., PASLASKI, J., YARIV, A. 1985. "Observation of modulation speed enhancement, frequency modulation suppression, and phase noise reduction by detuned loading in a coupled-cavity semiconductor laser". *Applied Physics Letters*. 46:11. 1025-7.

VENGSAKAR, A.M. 1997. "Long-period fiber gratings". P. 12-15.

WAKE, D., BEACHAM, K. 2004. "Radio-over-fiber networks for mobile communications". 5466, P. 1-12.

WAKE, D., LIMA, C.R., DAVIES, P.A. 1995. "Optical generation of millimeter-wave signals for fiber-radio systems using a dual-mode DFB semiconductor laser". *IEEE Transactions on Microwave Theory and Techniques*. 43:9. 2270-6.

WEI-CHUAN SHIH, CHEE WEI WONG, YONG BAE JEON, SANG-GOOK KIM, BARBASTATHIS, G.I. 2002. "Electrostatic and piezoelectric analog tunable diffractive gratings". vol.1, P. 75-6.

WEISSER, S., RALSTON, J.D., EISELE, K., SAH, R.E., HORNING, J., LARKINS, E.C. et al. 1994. "Dry-etched short-cavity ridge waveguide MQW lasers suitable for monolithic integration with direct modulation bandwidth up to 33 GHz at low drive currents". vol.2, P. 973-6.

WYATT, R. 1989. "High-power broadly tunable erbium-doped silica fibre laser". *Electronics Letters*. 25:22. 1498-9.

WYATT, R., DEVLIN, W.J. 1983. "10 kHz linewidth 1.5  $\mu\text{m}$  InGaAsP external cavity laser with 55 nm tuning range". *Electronics Letters*. 19:3. 110-12.

WYATT, R.I., HODGKINSON, T.G.I., SMITH, D.W.I. 1983. "1.52  $\mu\text{m}$  PSK heterodyne experiment featuring an external cavity diode laser local oscillator". *Electronics Letters*. 19:14. 550-2.

WYATT, R.I., SMITH, D.W.I., CAMERON, K.H.I. 1982. "Megahertz linewidth from a 1.5  $\mu\text{m}$  semiconductor laser with HeNe laser injection". *Electronics Letters*. 18:7. 292-3.

YADLOWSKY, M.J. 1999. "Pump wavelength-dependent spectral-hole burning in

- EDFAs". *Journal of Lightwave Technology*. 17:9. 1643-8.
- YAMADA, M., SUEMATSU, Y. 1979. "A condition of single longitudinal mode operation in injection lasers with index-guiding structure". *IEEE Journal of Quantum Electronics*. QE-15:8. 743-9.
- YARIV, A. 1991. "Optical electronic in Modern Communications". *Oxford University Press*. 4th Editions :
- YI LUO, BING XIONG, JIAN WANG, PENGFEI CAI, CHANGZHENG SUN 2006  
"40 GHz AlGaInAs multiple-quantum-well integrated electroabsorption modulator/distributed feedback laser based on identical epitaxial layer sche". *Japanese Journal of Applied Physics, Part 2 (Letters)*. 45:37-41. 1071-3.